EFFECT OF NANOSCALE ZERO VALENT IRON TOWARD BACTERIA AND THEIR RESPONSE

Miss Panaya Kotchaplai

A Dissertation Submitted in Partial Fulfillment of the Requirements
for the Degree of Doctor of Philosophy Program in Environmental Management
(Interdisciplinary Program)
Graduate School
Chulalongkorn University
Academic Year 2016

ผลของอนุภาคเหล็กขนาดนาโนต่อแบคทีเรียและการตอบสนองของเซลล์

นางสาวปณยา คชพลาย

วิทยานิพนธ์นี้เป็นส่วนหนึ่งของการศึกษาตามหลักสูตรปริญญาวิทยาศาสตรดุษฎีบัณฑิต
สาขาวิชาการจัดการสิ่งแวดล้อม (สหสาขาวิชา)
บัณฑิตวิทยาลัย จุฬาลงกรณ์มหาวิทยาลัย
ปีการศึกษา 2559

Thesis Title	EFFECT OF NANOSCALE ZERO VALENT IRON TOWARD BACTERIA AND THEIR RESPONSE
By	Miss Panaya Kotchaplai
Field of Study	Environmental Management
Thesis Advisor	Associate Professor Alisa Vangnai, Ph.D.
Thesis Co-Advisor	Professor Eakalak Khan, Ph.D.

Accepted by the Graduate School, Chulalongkorn University in Partial Fulfillment of the Requirements for the Doctoral Degree

.....Dean of the Graduate School
(Associate Professor Sunait Chutintaranond, Ph.D.)

THESIS COMMITTEE

.....Chairman
(Associate Professor Ekawan Luepromchai, Ph.D.)

.....Thesis Advisor
(Associate Professor Alisa Vangnai, Ph.D.)

.....Thesis Co-Advisor
(Professor Eakalak Khan, Ph.D.)

.....Examiner
(Associate Professor Tawan Limpiyakorn, Ph.D.)

.....Examiner
(Associate Professor Rungaroon Waditee-Sirisattha, Ph.D.)

.....External Examiner
(Assistant Professor Tanapon Phenrat, Ph.D.)

ปณยา คชพลาย : ผลของอนุภาคเหล็กขนาดนาโนต่อแบคทีเรียและการตอบสนองของเซลล์ (EFFECT OF NANOSCALE ZERO VALENT IRON TOWARD BACTERIA AND THEIR RESPONSE) อ.ที่ปรึกษาวิทยานิพนธ์หลัก: รศ. ดร. อลิสา วังใน, อ.ที่ปรึกษาวิทยานิพนธ์ร่วม: ศ. ดร. เอกลักษณ์ คาน, 137 หน้า.

อนุภาคเหล็กศูนย์ขนาดนาโนเป็นอนุภาคขนาดเล็กและมีความไวต่อการเกิดปฏิกิริยาสูง จึงเป็นวิธีหนึ่งที่นิยมนำใช้ในการบำบัดสารปนเปื้อนในสิ่งแวดล้อม ถึงแม้การใช้งานอนุภาคเหล็กศูนย์ขนาดนาโนจะเป็นวิธีที่มีประสิทธิภาพ แต่อนุภาคเหล็กศูนย์ขนาดนาโนจำนวนมากที่เข้าสู่สิ่งแวดล้อมเองก็ก่อให้เกิดความกังวลถึงผลกระทบทางสิ่งแวดล้อมที่อาจตามมา งานวิจัยชิ้นนี้จึงมีวัตถุประสงค์เพื่อศึกษาผลและกลไกความเป็นพิษของอนุภาคเหล็กศูนย์ขนาดนาโนต่อแบคทีเรียในธรรมชาติ โดยใช้ *Pseudomonas putida* เป็นแบคทีเรียตัวอย่าง พบว่าอนุภาคเหล็กศูนย์ขนาดนาโนความเข้มข้น 1 กรัมต่อลิตร ทำให้การอยู่รอดของแบคทีเรียลดลงหนึ่งพันเท่า ในขณะที่อนุภาคเหล็กศูนย์ขนาดนาโนที่สูญเสียความไวในการเกิดปฏิกิริยาแล้วความเข้มข้น 1 กรัมต่อลิตร ทำให้การอยู่รอดของแบคทีเรียลดลงสิบเท่า จากการติดตามการเปลี่ยนแปลงในการแสดงออกของโปรตีนของแบคทีเรียพบว่าปริมาณโปรตีนที่เกี่ยวข้องกับเยื่อหุ้มเซลล์ลดลง ทั้งยังมีการแสดงออกของโปรตีนที่เกี่ยวข้องกับการม้วนตัวของโปรตีนบริเวณเยื่อหุ้มเซลล์เพิ่มมากขึ้น บ่งชี้ว่าอนุภาคเหล็กศูนย์ขนาดนาโนทั้งสองรูปแบบส่งผลต่อเยื่อหุ้มเซลล์แบคทีเรีย อย่างไรก็ตามเมื่อเลี้ยงเซลล์ต่อในสภาวะที่มีแหล่งคาร์บอนพบว่าแบคทีเรียกลับมาเจริญได้อีกครั้งแสดงถึงความสามารถในการปรับตัวของแบคทีเรียในสภาวะที่มีอนุภาคเหล็กศูนย์ขนาดนาโน การวิเคราะห์ TEM แสดงให้เห็นอนุภาคเหล็กศูนย์ขนาดนาโนปกคลุมและแทรกตัวบริเวณเยื่อหุ้มเซลล์ การวิเคราะห์องค์ประกอบกรดไขมันในเยื่อหุ้มเซลล์พบว่าแบคทีเรียมีการเปลี่ยนรูปกรดไขมันไม่อิ่มตัวจากรูปแบบ *cis* เป็น *trans* ทำให้เยื่อหุ้มเซลล์จัดเรียงตัวแน่นขึ้นและมีความแข็งขึ้นเพื่อปรับตัวต่อ fluidizing effect ในเยื่อหุ้มเซลล์ที่เกิดจากอนุภาคเหล็กศูนย์ขนาดนาโน นอกจากนี้ยังพบว่าแบคทีเรียที่สัมผัสอนุภาคเหล็กศูนย์ขนาดนาโนความเข้มข้น 0.1 กรัมต่อลิตรซ้ำ ๆ มีลักษณะฟีโนไทป์เปลี่ยนแปลงไป โดยมีขนาดโคโลนีเล็กลง และมีความทนทานมากต่ออนุภาคเหล็กศูนย์ขนาดนาโนมากขึ้น การสัมผัสอนุภาคเหล็กศูนย์ขนาดนาโนความเข้มข้น 0.5 และ 1.0 กรัมต่อลิตรเพียงครั้งเดียวทำให้ลักษณะฟีโนไทป์ดังกล่าวเพิ่มขึ้นประมาณสิบเท่า สภาวะเครียดออกซิเดชั่นจากอนุภาคเหล็กศูนย์ขนาดนาโนเป็นปัจจัยสำคัญที่เหนี่ยวนำให้เกิดฟีโนไทป์ดังกล่าว ถึงแม้ลักษณะฟีโนไทป์ที่เกิดขึ้นดังกล่าวเป็นความเปลี่ยนแปลงแบบชั่วคราว การวิจัยครั้งนี้สามารถคัดแยกเชื้อที่มีการเปลี่ยนแปลงฟีโนไทป์แบบถาวรได้ด้วย เมื่อศึกษาลักษณะด้านต่าง ๆ ของฟีโนไทป์ที่เปลี่ยนแปลงแบบถาวรพบว่าความสามารถในการว่ายน้ำ การสร้างไบโอฟิล์มและการทนโทลูอีนลดลง และมีสภาวะ lag นานขึ้นสี่เท่าเมื่อเลี้ยงเชื้อในสภาวะที่มีโทลูอีนเป็นแหล่งคาร์บอนเพียงอย่างเดียว จากการทดลองทั้งหมดแสดงให้เห็นถึง ผลของอนุภาคเหล็กศูนย์ขนาดนาโนต่อเยื่อหุ้มเซลล์แบคทีเรียและกลไกการตอบสนองของแบคทีเรียต่อความเสียหายที่เกิดขึ้น โดยความสามารถในการปรับตัวของแบคทีเรียเป็นปัจจัยที่ควรคำนึงถึงในการประเมินผลของอนุภาคเหล็กศูนย์ขนาดนาโนต่อสิ่งแวดล้อม นอกจากนี้กลยุทธ์ในการใช้อนุภาคเหล็กศูนย์ขนาดนาโนเพื่อบำบัดสารพิษในพื้นที่ปนเปื้อน อาทิ ความถี่ในการเติมอนุภาคเหล็กศูนย์ขนาดนาโน เป็นอีกปัจจัยหนึ่งที่ควรคำนึงเนื่องจากมีโอกาสเหนี่ยวนำให้เกิดการเปลี่ยนแปลงฟีโนไทป์ในเชื้อแบคทีเรียตามธรรมชาติได้

สาขาวิชา การจัดการสิ่งแวดล้อม ลายมือชื่อนิสิต .....

ปีการศึกษา 2559 ลายมือชื่อ อ.ที่ปรึกษาหลัก .....

ลายมือชื่อ อ.ที่ปรึกษาร่วม .....

5287546320 : MAJOR ENVIRONMENTAL MANAGEMENT
KEYWORDS: NANOSCAL / BACTERIAL RESPONSE / BACTERIAL MEMBRANE MODIFICATION / PHENOTYPIC VARIATION

PANAYA KOTCHAPLAI: EFFECT OF NANOSCALE ZERO VALENT IRON TOWARD BACTERIA AND THEIR RESPONSE. ADVISOR: ASSOC. PROF. ALISA VANGNAI, Ph.D., CO-ADVISOR: PROF. EAKALAK KHAN, Ph.D., 137 pp.

Nanoscale zero valent iron or nZVI is a reactive iron nanoparticle which has been considered as a promising treatment agent for various contaminants due to its small size and high reactivity. While the successful in-situ environmental application of nZVI has been demonstrated, the increasing use of nZVI possibly leads to the potential environmental impact of nZVI. This research aims to understand the effect of nZVI particularly on environmental bacteria. In this study, *Pseudomonas putida* were selected as the model bacteria as they are ubiquitous in the environment. Exposure of *P. putida* to 1.0 g/L of reactive nZVI (R-nZVI) decreased the bacterial viability by three order of magnitude. Bacterial exposure to oxidized nZVI (O-nZVI), a non-toxic form remained in the environment, resulted in one-order of magnitude reduction in cell viability. Proteomic analysis revealed the significant effect of both forms of nZVI on bacterial membrane as suggested by the decreased abundance of membrane-bound proteins and the up-regulation of proteins playing a role in membrane protein folding. Prolonged exposure in the presence of carbon source resulted in the rebound in number of viable cells, suggesting that bacterial cells can adapt themselves to the nZVI-induced damage. According to TEM analysis, nZVI heavily adsorbed onto the bacterial surface and partially localized around the bacterial membrane, fluidizing bacterial membrane. Fatty acid profile analysis showed the significant conversion of *cis*-isomer to *trans*-unsaturated fatty acid upon nZVI exposure. The altered membrane composition resulted in the tightly packed bilayer, and more rigid membrane as confirmed by fluorescent anisotropy measurement. It is likely that this membrane rigidification is a bacterial adaptive response to counteract the membrane fluidizing effect of nZVI. Interestingly, repetitive exposures of bacteria to an environmentally relevant concentration of R-nZVI (0.1 g/L) induced the emergence of the small colony variant (SCV) of *P. putida* exhibiting much smaller colony size and higher persistence to nZVI exposure. Single bacterial exposure to higher concentration of R-nZVI (i.e. 0.5 and 1.0 g/L) also increased the number of this SCV phenotype by approximately ten-fold. It appears that nZVI-induced oxidative stress involves in the emergent SCV phenotype. While most of the SCV phenotype could revert back to normal phenotype in the absence of nZVI, the irreversible SCV phenotype was also detected. Characterization of this irreversible SCV phenotype reveals partial loss of the environmentally relevant traits including swimming motility and biofilm formation. While *P. putida* F1 is a model strain for toluene degradation study, its irreversible SCV phenotype is slightly more susceptible to toluene and showed four-fold longer lag phase of growth under toluene as sole carbon source, compared to the normal phenotype. Overall, this study unveils the significant effect of nZVI on bacterial membrane (i.e. membrane fluidizing effect) as well as bacterial adaptation responses to the occurred damage. It demonstrates that the bacterial adaptation should be considered for accurately predicting the toxicity of nZVI. The study on adaptability of other microorganisms is also required. Additionally, nZVI in-situ injection strategies (e.g. single and repetitive injection) should be taken into concern since it may induce the variation in bacterial phenotype.

Field of Study: Environmental Management
Academic Year: 2016

Student's Signature .....
Advisor's Signature .....
Co-Advisor's Signature .....

ACKNOWLEDGEMENTS

I would like to express my sincere gratitude to my advisor, Associate Professor Dr. Alisa Vangnai, who gave me the opportunity to conduct research under her supervision. Under her guidance, I have learned the way of critical thinking, research planning, professional working, and manuscript writing. I could have never imagined having better mentor for my PhD study. Besides my advisor, I express my thankfulness to my co-advisor, Professor Dr. Eakalak Khan, who motivates and encourages me to improve myself during my study. His guidance always reaches me out wherever I am. My special gratitude is extended to the committee members: Assoc. Prof. Dr. Ekawan Leupromchai, Assoc. Prof. Dr. Tawan Limpiyakorn, Assoc. Prof. Dr. Rungaroon Waditee Sirisattha and Asst. Prof. Dr. Tanapon Phenrat. Their insightful comments are crucial to improving and completing this dissertation.

I would like to acknowledge the professors, researchers, and technicians who have helped me since the beginning of my study. I could not have completed my research without them. I would like to thank Dr. Sittirak Roytrakul and Mrs. Atchara Paemanee from Proteomic Research Laboratory, Biotec, Thailand for their help in proteomics analysis. I am very thankful to Dr. Nawaporn Vinayavekhin, Deptartment of Chemistry, Faculty of Science, CU for her help in untargeted metabolomics.

My deepest thanks go to my family and friends who have always supported me. First and foremost I would like to thank dad, mom, brother, and my beloved grandmas. Their love, compassion, and support allows me to succeed today. I would like to thank all of my friends from AV lab, who have shared precious memories (and of course, those suffered one too) of being graduate student together. You guys made this long journey a lot more fun.

CONTENTS

Page

THAI ABSTRACT iv

ENGLISH ABSTRACT v

ACKNOWLEDGEMENTS vi

CONTENTS vii

Chapter 1 INTRODUCTION 15

1.1) Background 15

1.2) Research Problem Statement 17

1.3) Research objectives 19

1.4) Hypotheses 20

1.1) Dissertation organization 20

Chapter 2 LITERATURE REVIEWS 22

2.1) Nanoscale Zero Valent Iron 22

2.1.1) Characteristics 22

2.1.2) Environmental applications 24

2.2) Effects of nZVI on living organisms/microorganism 29

2.2.1) Effects of nZVI on mammalian cells 30

2.2.2) Effects of nZVI on aquatic organisms 30

2.2.3) Effects of nZVI on microorganisms 31

2.3) Proposed mechanisms of action of nZVI and bacterial responses 37

2.3.1) Oxidative stress 37

2.3.2) Membrane disruption 43

2.3.3) DNA/RNA damage 46

Page

2.4) Roles of nZVI in bioremediation 47

Chapter 3 Materials and methods 49

3.1) Part 1 Elucidation of effects of reactive and oxidized nZVI on bacterial membrane by proteomic analysis 49

3.1.1) nZVI source and iron content determination. 49

3.1.2) Cell preparation and determination of effects of nZVI on cell viability 49

3.1.3) Proteomic analysis of nZVI-treated cells 50

3.1.3.1 Sample preparation for proteomic analysis 50

3.1.3.2 GeLC-MS/MS 51

3.2) Part 2 Bacterial response to short-term and repetitive nZVI exposure: Modification in bacterial membrane 51

3.2.1) nZVI source and characterizations. 51

3.2.2) Bacteria, media, and cultivation conditions. 52

3.2.3) nZVI toxicity assessment 52

3.2.4) Sample preparations for scanning and transmission electron microscopy, and cell surface charge measurement. 53

3.2.5) Alterations in bacterial membrane fatty acid profile 53

3.2.6) Alterations in phospholipid headgroup 54

3.2.7) Bacterial membrane fluidity 55

3.2.8) Statistical analysis 55

3.3) Part 3 Emergence of phenotypic variants of *P. putida* F1 due to nZVI exposure and their environmentally relevant characteristics 55

3.3.1) nZVI source 55

3.3.2) Bacteria, media, and cultivation conditions. 55

Page

3.3.3) Determination of the emergence of the SCV phenotype 56
3.3.3.1 Effect of nZVI concentration on the emergence of the SCV phenotype 56
3.3.3.2 Effects of oxidative stress and different forms of iron on the emergence of the SCV phenotype 56
3.3.4) Characteristics of the SCV phenotype 57
3.3.4.1 Bacterial growth rate 57
3.3.4.2 Toluene tolerance 57
3.3.4.3 Toluene degradation 58
3.3.4.4 Swimming motility 58
3.3.4.5 Biofilm formation 58
3.3.5) Fourier transform infrared spectroscopy (FTIR) analysis 59
3.3.6) Statistical analysis 59
Chapter 4 Elucidation of effects of reactive and oxidized nZVI on bacterial membrane by proteomic analysis 60
4.1) Introduction 60
4.2) Results and discussion 62
4.2.1) Effects of R-nZVI and O-nZVI on bacterial viability 62
4.2.2) Proteomic analysis 63
4.2.2.1 Differentially expressed proteins in P. putida KT2440 cells after exposed to R-nZVI and O-nZVI 67
4.2.2.2 Differentially expressed proteins only in cells exposed to R-nZVI 72

Page

4.2.2.3 Differentially expressed proteins only in cells exposed to O-nZVI 78

4.3) Summary 84

Chapter 5 Bacterial response to short-term and repetitive nZVI exposure: Modification in bacterial membrane 86

5.1) Introduction 86

5.2) Results and discussion 88

5.2.1) nZVI characteristics 88

5.2.2) Rebound in bacterial viability after prolongation of nZVI exposure 91

5.2.3) Repetitive nZVI exposure induced the emergence of bacterial phenotypic variant 95

5.2.4) Visualization of bacterial membrane-nZVI interaction 98

5.2.5) Decreasing membrane fluidity after nZVI exposure 102

5.2.6) Changes in bacterial fatty acids response to nZVI exposure 104

5.2.7) Changes in bacterial surface charges 108

5.2.8) Phospholipid headgroup analysis 110

5.3) Summary 112

Chapter 6 Emergence of phenotypic variants of *P. putida* F1 due to nZVI exposure and their environmentally relevant characteristics 114

6.1) Introduction 114

6.2) Results and discussion 116

6.2.1) Emergence of phenotypic variant induced by nZVI exposure 116

6.2.2) Mechanism triggering emergence of the SCV phenotype 119

6.2.3) Environmental fitness-related traits of the stable SCV phenotype 122

Page

6.2.4) FTIR analysis 128
6.3) Summary 132
Chapter 7 Conclusions, Implications and Suggestions for Future Research 134
7.1) Conclusions 134
7.2) Environmental implications 136
7.3) Suggestions for future researches 137
REFERENCES 2
VITA 32

List of Figures

Figure 1.1 Proposed distribution of nZVI particles during in-situ application 17

Figure 1.2 Research outline 20

Figure 2.1 Core-shell structure of (A) nZVI and (B) mechanisms involved in transformation of arsenic. 23

Figure 2.2 In situ environmental application of nanoparticles..... 25

Figure 2.3 Contaminants removal by iron oxide shell of nZVI. 26

Figure 2.4 Proposed fate and transport of nZVI particles in the environmental and interaction between nZVI and environmental microorganisms..... 29

Figure 2.5 TEM images of (A) *E.coli* cell and (B) *E. coli* treated with nZVI..... 35

Figure 2.6 Proposed mechanisms of nZVI-induced toxicity in bacterial cells. 37

Figure 2.7 Simplified overview of factors affecting oxidative stress and response system in *P. putida* KT2440..... 38

Figure 4.1 Direct injection of reactive nZVI (R-nZVI) to contaminated site. After interact with the contaminants, large amount of the oxidized form of nZVI (O-nZVI) may remain in the environment..... 61

Figure 4.2 Time-dependent effect of nZVI exposure on bacterial viability of (A) *P. putida* KT2440 and (B) *B. subtilis* 168..... 64

Figure 4.3 Protein profile of *P. putida* KT2440 after R- and O-nZVI exposure..... 65

Figure 5.1 Percentage of the iron content of nZVI as a function of time..... 90

Figure 5.2 Time-dependent survival of *P. putida* F1 cells after nZVI exposure..... 91

Figure 5.3 Survival of *P. putida* F1 cells after exposed to Fe(II), Fe(III) and polyacrylic acid (PAA)..... 92

Figure 5.4 Susceptibility to nZVI of cell obtained from rebound phase after nZVI exposure..... 94

Figure 5.5 (A) Altered colony morphology of *P. putida* F1 after repeatedly exposed to 0.1 g/L of nZVI. (B) The relationship between repetitive nZVI exposure and proportion of persistent phenotype. (C) Comparison between survival of normal and nZVI-persistent phenotype of *P. putida* F1 after exposed to various nZVI concentrations for one hour. 97

Figure 5.6 Susceptibility to nZVI of normal cells, persistent phenotype and reverted phenotypic variant. 98

Figure 5.7 TEM micrographs of *P. putida* F1 cells 100

Figure 5.8 SEM micrographs of *P. putida* F1 cells 101

Figure 5.9 Membrane fluidity of *P. putida* F1 cells after exposure to 0.1 g/L of nZVI for one hour. 103

Figure 5.10 (A) Degree of membrane fatty acid saturation, which is the ratio between unsaturated fatty acids and saturated fatty acid. (B) The ratio between trans and cis isomer of unsaturated fatty acid 106

Figure 5.11 Fatty acid modification in bacteria. 107

Figure 5.12 Possible scenarios for the increasing negative charge of *P. putida* F1 cells after nZVI exposure: 110

Figure 5.13 Percentage of phospholipids of interest which are PS, PE and PG in *P. putida* F1 cells. 112

Figure 6.1 The relationship between the SCV phenotype of *P. putida* F1 and cycles of nZVI exposure. 118

Figure 6.2 Roles of oxidative stress and different forms of iron on the emergence of the SCV phenotype. 119

Figure 6.3 Characteristics of the SCV phenotype in comparison to the normal phenotype of *P. putida* F1. 126

List of tables

Table 2.1 Common environmental contaminants that can be transformed by nZVI . 28

Table 2.2 Summary of reported nZVI effect on bacterial cells. 32

Table 6.1 Bacterial growth in various mediums 125

Chapter 1
INTRODUCTION

1.1) Background

Nanoscale zero-valent iron refers to as zero-valent iron (Fe^0) with particle size typically in a range between 1 and 100 nm (Zhang and Elliott, 2006). A typical structure of iron nanoparticles consists of two parts: Fe^0 core and iron oxide/hydroxide shell structure generated by oxidation of the Fe^0 core (Mukherjee et al., 2016; Ramos et al., 2009b; Yan et al., 2010b). The Fe^0 core as a redox active material exhibits the property of reducing agent with high tendency for electron donation while chemical adsorption or precipitation can occurs at the iron oxide shell. Due to its small size, high reactivity and cost effectiveness, nZVI has been considered as promising treatment for various environmental contaminants (Mukherjee et al., 2016). These contaminants include chlorinated hydrocarbons, inorganic anions, heavy metals and radioactive compounds (Mukherjee et al., 2016; Zhang and Elliott, 2006). In addition to the mentioned mechanisms, nZVI can also interact with O_2 generating H_2O_2 as well as other reactive oxygen species (ROS) via Fenton reaction(He et al., 2016). Thus, nZVI has also been used as a catalyst for oxidative degradation of the contaminants (Li et al., 2015a; Moon et al., 2011).

In addition to lab-scale, the pilot tests and field-scale remediation of pollutants by nZVI have been demonstrated in various environmental context, for instance, groundwater (Mueller et al., 2012a), soil (El-Temsah and Joner, 2013; Singh and Bose, 2015), activated sludge (Wu et al., 2013) and industrial wastewater (Hansson et al., 2012). Typically, nZVI particles are directly injected into the contaminated site (Grieger et al., 2010; Henn and Waddill, 2006; Kim et al., 2017; Zhang and Elliott, 2006) which are more convenient and cost-effective than

constructing macroscale-ZVI-based reactive barrier (Kim et al., 2017). The nZVI dose for *in-situ* contaminant remediation depends on contaminated sites which range from 55 kg to 380 kg for pilot test (Stefaniuk et al., 2016). For the field scale application, the total dose of nZVI ranges from 150 kg to 1 ton (Stefaniuk et al., 2016).

The direct contact between contaminants and nZVI particles is important to the remediation efficiency (Shi et al., 2015). However, during *in-situ* injection of nZVI particles, the mobility of nZVI particles is limited to the area around the injection point due to their electrostatic and magnetic attraction (Phenrat et al., 2007), thus limiting their contaminant removal efficiency in the subsurface area. Accordingly, several approaches, for example, surface modification of nZVI or co-injection with surfactants, have been adopted to enhance the mobility of nZVI particles in the contaminated sites (Shi et al., 2015). However, the surface modification of nZVI could reduce their reactivity (Phenrat et al., 2009b).

While nZVI is considered highly reactive material, nZVI rapidly become oxidized resulting in a limited lifetime of nZVI (Kim et al., 2017). The presented oxidant in groundwater for example O_2, nitrate nitrite, sulfate are potent electron acceptor competing with reduction of the contaminants (Shi et al., 2015) and resulting in rapid oxidation of nZVI (Ahn et al., 2016). Recently, it was found that the aging or the oxidization of nZVI could result in the remobilization of the adsorbed heavy metals (Calderon and Fullana, 2015; Su et al., 2014). In order to maintain the efficacy of heavy metal immobilization, nZVI re-dosing has been proposed (Su et al., 2014). The typical injection of nZVI as well as nZVI re-dosing if practiced will likely result in an extensive amount of nZVI released into and retained in the environment.

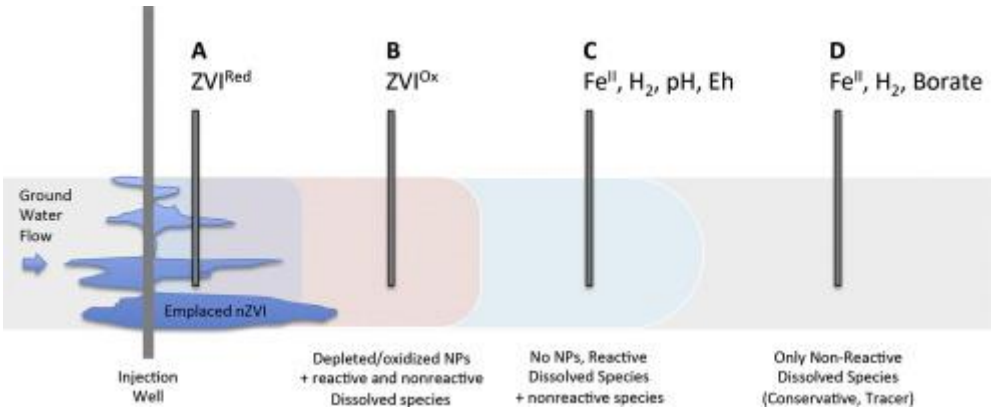

Figure 1.1 Proposed distribution of nZVI particles during *in-situ* application

Source: ((Shi et al., 2015))

1.2) Research Problem Statement

The intensive environmental applications of nZVI both *in situ* and *ex situ* lead to the concern on the environmental impact especially environmental bacteria, which are the key players in various biological processes. On the contrary to the burgeoning literature/interest regarding the characteristics, environmental fate and applications of nZVI, the environmental impact of these nanoparticles is still limited and yet controversial. Many studies reported the bactericidal effect of nZVI toward various strains of bacterial including *Escherichia coli* (Auffan et al., 2008; Chaithawiwat et al., 2016b; Chen et al., 2011b; Kim et al., 2010; Lee et al., 2008a; Li et al., 2010), *Pseudomonas* (Diao and Yao, 2009a; Sacca et al., 2014) and *Bacillus* (Chen et al., 2011b; Diao and Yao, 2009a). Lee et al. (2008) reported that exposure to 0.09 g/L of nZVI under aerobic condition reduces the viability of *E. coli* by 3 to 3.5 order of magnitude within 60 minutes; whereas the exposure to 0.009 g/L of nZVI in anaerobic condition reduce cell viability by 3.5 order of magnitude within 10 minutes (Lee et al., 2008b). The exposure to 0.1 g/L of nZVI under aerobic condition decreased viability of *P. fluorescens* and *B. subtilis* by 99% and 80%, respectively (Diao and Yao, 2009a). On the contrary, the survival *Klebsella oxytoca* decrease by

only 40% after exposed to 10 g/L of nZVI under aerobic condition (Saccà et al., 2013). The combined systems between nZVI and bacteria have been reported to enhance the efficiency of remediation processes (Bose et al., 2016; Murugesan et al., 2011; Shin and Cha, 2008). Bose et al. (2016) reported that *P. putida* (MTCC 1194) could grow in the presence of 10 g/L of nZVI and the aniline degradation by cell-nZVI system is higher than system containing only cells or nZVI (Bose et al., 2016). Microbial nitrate reduction was found greater in the presence of nZVI comparing to system containing only nZVI or microbial process (Shin and Cha, 2008). The variations in experimental results are due to the different experimental conditions including selected bacterial strains (Chaithawiwat et al., 2016a), types and concentrations of nZVI and exposure conditions (Lefevre et al., 2016).

To relate and generalize the toxicity of nZVI to environmentally relevant situation, several studies were conducted using a microbial microcosm (Kirschling et al., 2010; Ma et al., 2015; Saccà et al., 2014; Tilston et al., 2013). While a toxicity study using a mixed culture could represent the complex and ecologically relevant environment, using a pure bacterial culture is more suitable/eligible for deciphering the toxicity mechanism (Maurer-Jones et al., 2013). Several approaches have been used to elucidate the toxicity mechanism or the effect of nZVI on bacteria, for example, electron microscopes (Auffan et al., 2008; Fajardo et al., 2013; Lee et al., 2008a; Sacca et al., 2014), fluorescent probes (Kim et al., 2010), proteomic analysis (Fajardo et al., 2013; Saccà et al., 2013; Sacca et al., 2014), gene expression (Chaithawiwat et al., 2016b; Fajardo et al., 2013; Sacca et al., 2014) or using mutants strains lacking of defense enzymes (Auffan et al., 2008; Chaithawiwat et al., 2016b). Accordingly, effects on bacterial membrane and oxidative damage have been proposed as the two main mechanisms of bacterial inactivation (Lefevre et al., 2016). Using proteomic analysis could reveal the big picture of nZVI effect on bacterial cells i.e. membrane damage and induction of oxidative stress (Sacca et al., 2014).

However, most studies focused only the toxicity mechanism of fresh or reactive nZVI, whereas nZVI mainly remained in the environment in less reactive or oxidized form (Adeleye et al., 2013) and can cause a considerable toxicity to bacteria **(Auffan et al., 2008)**.

While the toxicity mechanism of nZVI on bacteria has been concerned, the information regarding bacterial response to nZVI-induced damages is still limited. Bacteria, for example, *P. putida*, is capable to adapt themselves to several stresses including organic solvents, making them a commonly found bacteria in the environment (Nelson et al., 2002a). The information about bacterial stress response may explain the discrepancy of nZVI toxicity on bacteria. This information may also provide the understanding about shift in bacterial community following nZVI exposure or predicting the nZVI-susceptible bacterial strain in worst case scenario of nZVI-injection since some bacterial stress responses are strain-dependent. Furthermore, the understanding about bacterial response can be adopted in designing and improving the combined cell-nZVI degradation system.

1.3) Research objectives

The goals of this research were to understand the effects of nZVI on environmental microorganism particularly those potential bacteria involved biological processes in the contaminated site**.** To achieve these goals, several objectives are established as follows**.**

1. To elucidate the different effects of two forms of nZVI, reactive-nZVI and oxidized-nZVI, by inferring from bacterial protein expression.
2. To investigate morphological and physiological adaptation in bacteria after nZVI exposure.

3. To investigate the biological consequence of bacterial adaptation to nZVI exposure.

Figure *1.2* Research outline

1.4) Hypotheses

1. R-nZVI exposure differently affects the expression of bacterial proteins comparing to O-nZVI exposure. Proteins related to oxidative stress are highly up regulated in R-nZVI exposure.
2. During short-term exposure, bacterial membrane as an initial target for cell-nZVI interaction, becomes more rigid to counteract the fluidizing effect of nZVI.
3. Bacterial cells partially lose their fitness, in order to compensate with the survival under nZVI-induced stress condition.

1.1) Dissertation organization

This dissertation is divided into 7 chapters. This chapter includes background, research problem statement, objectives, hypotheses, and dissertation organization. Chapter 2 provides a literature review on environmental application of nZVI as well as bacterial stress response mechanisms. Chapter 3 provides detail of materials and methods used in this study. Chapter 4 presents a proteomic analysis of

environmental bacterial exposed to reactive nZVI and nonreactive (oxidized) nZVI. Chapter 5 is based on a publication entitled “Membrane modification of *P. putida* F1 in response to nZVI exposure: Effect of short term and repetitive nZVI exposure” which was published in *Environmental Science and Technology*. Chapter 6 is a part of a manuscript entitled “Emergence of phenotypic variants of *P. putida* F1 due to nZVI exposure and their environmentally relevant characteristics.” This manuscript will be submitted for publication in a peer reviewed journal. Conclusions and recommendations for future work are presented in Chapter 7.

Chapter 2
LITERATURE REVIEWS

2.1) Nanoscale Zero Valent Iron

2.1.1) Characteristics

Nanoscale zero-valent iron (Fe^0) refers to as zero-valent iron with particle size is typically in a range between 1 and 100 nm (Zhang and Elliott, 2006). nZVI is known as a highly redox active material. Due to their size, nZVI have much higher specific surface area than granular or macro- or micro-scale zero valent iron which is known as an effective reducing agent (Zhang et al., 1998). A typical structure of nZVI consist of two parts: Fe^0 core and iron oxide/hydroxide shell structure (Figure 2.1). The metallic core exhibits the property of reducing agent, serving as electron donors or reductants for the reduction of the contaminants such as chlorinated hydrocarbons (Liu et al., 2007; Singh and Bose, 2015; Taghavy et al., 2010). High reactivity of nZVI is driven by the oxidation of Fe^0 core (Liu et al., 2005). In the presence of oxygen, the metallic core of nZVI will be oxidized to hydroxide or oxyhydroxide shell (Li et al., 2006). This oxide/hydroxide shell of nZVI can act as a protective phase to stabilize the particles in aqueous suspension (Nurmi et al., 2004). The (hydrous) oxide shell provides sites for metal ions adsorption (Li and Zhang, 2006; Üzüm et al., 2008) which can be further reduced by the Fe^0 core (Li and Zhang, 2006). On the other hand, the formation of oxide shell and an impurity on oxide shell can decrease the reactivity of metallic core of nZVI (Sarathy et al., 2008). The composition of the oxide shell and the nature of its surface are influenced by particle size and the environment. Under subsurface condition, the oxidation of nZVI will result in both magnetite (Fe_3O_4) and maghemite (γ-Fe_2O_3) formation within the oxide layer (Reinsch et al., 2010).

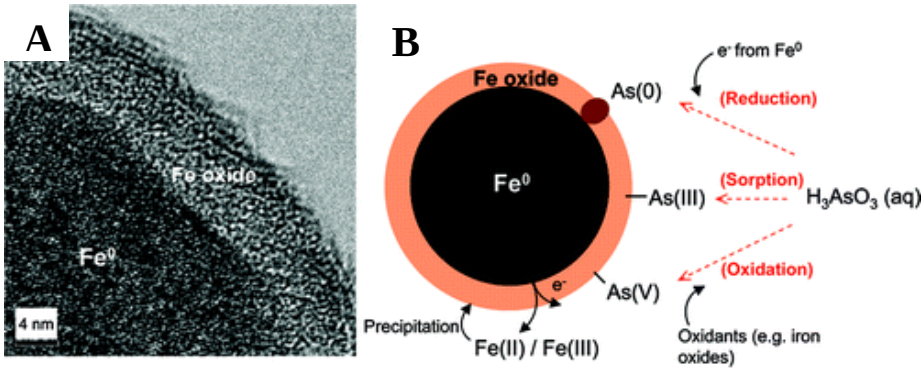

Figure 2.1 Core-shell structure of (A) nZVI and (B) mechanisms involved in transformation of arsenic. Source: (Ramos et al., 2009b))

Specific surface area is an important factor affecting properties of nanoparticles. Recent researches have shown that nZVI has a greater rate of reaction with contaminants than microscale zero valent iron (mZVI) (Singh and Bose, 2016; Wang and Zhang, 1997). Such a large specific area provides more sites where reaction occurs, which is one reason why nanoscale iron particles might exhibit greater rates of reaction with contaminants, thus making them more effective in reducing certain kinds of contaminants.

In Fe^0 core, the oxidation that occurs upon its addition to acidic, oxygen saturated aqueous solutions results in the formation of the surface-bound Fe(II) and either hydrogen peroxide (eq 1). The generated H_2O_2 can be further reduced to H_2O by transferring electrons from Fe^0 (eq 2).

$$Fe^0(s) + O_2(aq) \xrightarrow{H+} Fe(II)(aq) + H_2O_2(aq) \quad (1)$$

$$Fe^0(s) + O_2(aq) \xrightarrow{H+} Fe(II)(aq) + 2H_2O(l) \quad (2)$$

The products of reaction (1) can further react according to equation (3), generating hydroxyl radicals (Fenton's reaction).

$$Fe(II)(aq) + H_2O_2(aq) \longrightarrow Fe(III)(aq) + OH\cdot(aq) + OH^-(aq) \quad (3)$$

Lee et al. (2014) compared the generation of oxidants by nZVI and mZVI under aerobic conditions (Lee et al., 2014). While the oxidant production by mZVI is steadier and results in higher yield, nZVI particles rapidly generate oxidants and reach the saturation level within few hours (Lee et al., 2014). The same study also reported that the addition of EDTA, an iron chelator, could enhance the production of oxidant since a soluble Fe(II)-EDTA complexes could reduce the passivation of nZVI surface (Lee et al., 2014). Additionally, the higher redox potential of Fe(III)–EDTA/Fe(II)–EDTA couple than that of Fe(III)/Fe(II) couple involves in the faster reaction of Fe(II)–EDTA with O_2 and H_2O_2 than that of free Fe(II) (Lee et al., 2014).

2.1.2) Environmental applications

nZVI is extensively used in environmental application such as wastewater remediation because of its higher reactivity and larger specific surface area than microscale zero-valent iron (mZVI) (Chang and Kang, 2009; Macé et al., 2006; Nurmi et al., 2004; Wang and Zhang, 1997) , which is also known as an excellent electron donor. mZVI has been used in creating permeable reactive barriers (PRBs) which are trenches filled with reactive material (mZVI) designed to allow contaminated groundwater to pass through and react with it.

Because of its small size and ability to remain in suspension, nZVI is typically injected directly into contaminated sites and effectively transported by groundwater flow (Figure 2.2). The concentrations of injected nZVI vary from 0.75 to 50.0 g/L (Elliott and Zhang, 2001; Tuomi, 2008). A benefit of using nZVI is being able to inject

it directly into a contaminated aquifer, which avoids the need to dig a trench for installation of the PRB. Using this injection technique is believed to be faster and more effective for groundwater treatment than either pump-and-treat or PRB methods.

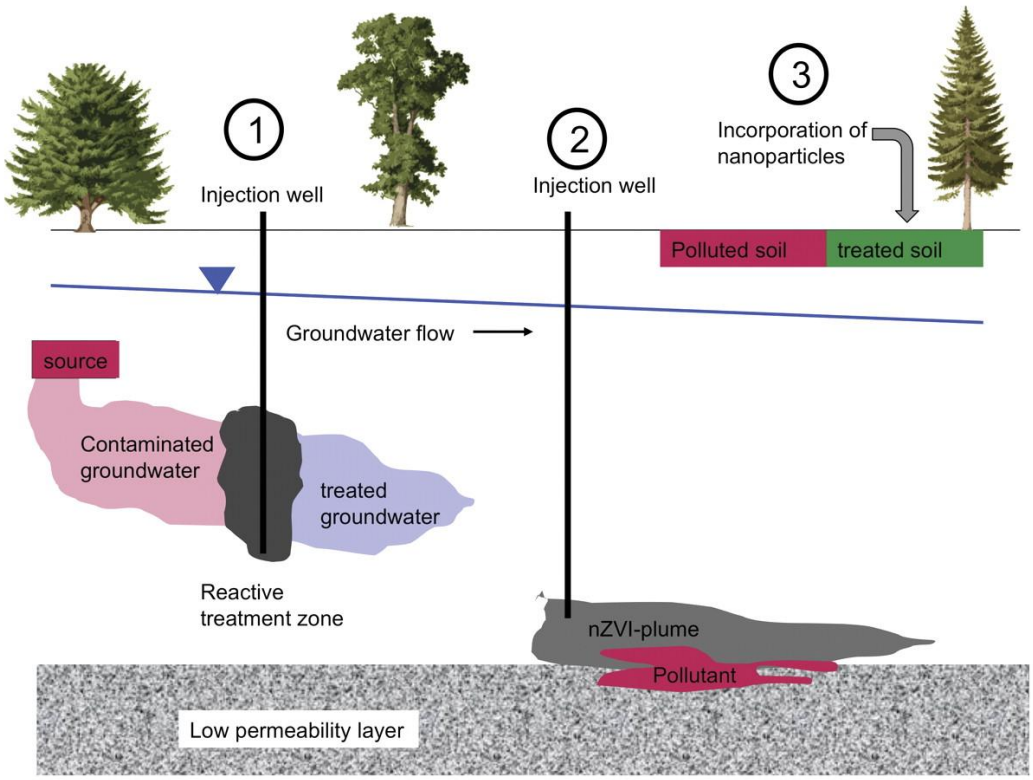

Figure *2.2* In situ environmental application of nanoparticles.

Source: (Mueller and Nowack, 2010)

nZVI has been known as an alternative for transformation of variety of common environmental contaminants such as chlorinated organic compounds, pesticides, organic dyes, heavy metal ions, inorganic anions (Zhang, 2003) and radioactive compound (Yan et al., 2010a) (Table 2.1).

The core-shell structure of nZVI exhibits the distinctive mechanisms in contaminants removal. Zero valent iron core or metallic core can serve as electron donors or reductants for the reduction and precipitation of metal ions (Li and Zhang, 2006). At low pH (pH ≤ 8), iron oxides are positively charged and attract ligands (e.g., phosphate). The increase in solution pH above the isoelectric point results in the negatively charged oxide which can form surface complexes with cations (Li and Zhang, 2006).

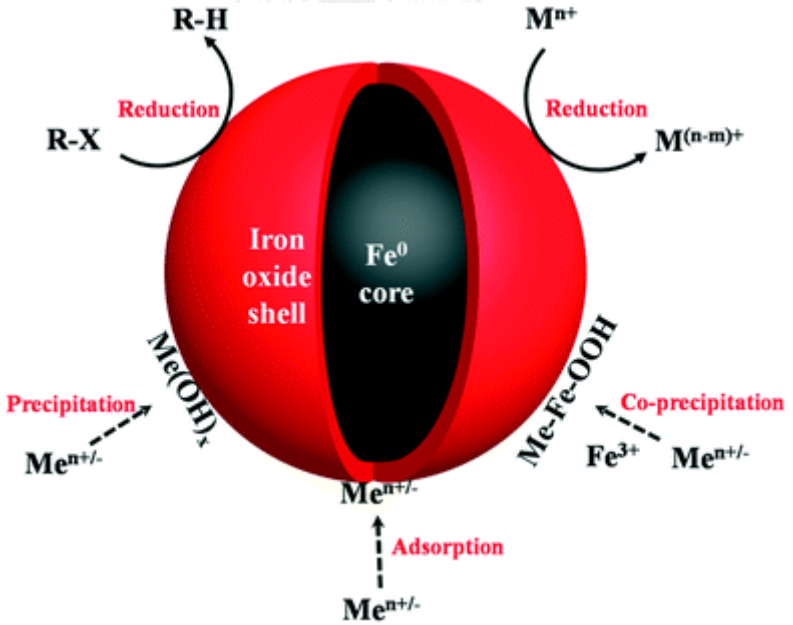

Figure *2.3* Contaminants removal by iron oxide shell of nZVI. R-X: chlorinated organic contaminants, M^{n+}: organic/inorganic contaminants and $Me^{n+/-}$: metal cations. Source: (Mu et al., 2017)

One limitation of nZVI for *in situ* application is that nZVI has a strong tendency to agglomerate in solutions (Nurmi et al., 2004),(Phenrat et al., 2007). This is difficult to avoid under environmental conditions and may result in reduced potential surface area of applied nZVI. Because of the potential agglomeration and attachment to soil surface (Lowry, 2009), the migration of injected nZVI is very limited (Saleh et al., 2008). There are several ways to form stable suspensions of dispersed nZVI in laboratory, for example, modifying surface of nZVI with polymers (He et al., 2006; Phenrat et al., 2008; Sirk et al., 2009; Tiraferri et al., 2008). In 2006, He et al. reported that coating palladized iron nanoparticles with sodium carboxymethyl cellulose (CMC) can increase their mobility in soil and reduce their aggregation(He et al., 2006). The reactivity of trichloroethelene degradation of CMC-coated nanoparticles was also greater than non-coated nanoparticles. In contrast, Phenrat et al. reported that surface modifications can reduce nZVI reactivity (Phenrat et al., 2009b). They suggested that coating materials may block the reactive site at the surface.

Common groundwater anions, for example, NO_3^-, Cl^-, SO_4^{2-}, HPO_4^{2-} and HCO_3^-, can also affect nZVI reactivity for contaminant remediation (Lim and Zhu, 2008; Liu et al., 2007; Reinsch et al., 2010). Reinsch et al. (2010) reported that the degree of passivation of nZVI surface by these constituents after one month are $HCO_3^- < HPO_4^{2-} < SO_4^{2-} < Cl^- < NO_3^-$, and that the oxidation of nZVI can be limited at more than 5 mN NO_3^- (Reinsch et al., 2010). Similarly, Lim et al. (2008) reported the inhibitory effect of groundwater anions on the degradation of 1,2,4-trichlorobenzene by Pd/Fe nanoparticles (nPd/Fe) (Lim and Zhu, 2008). They proposed that the effect of these anions on the reactivity of nPd/Fe can be divided into 3 groups based on their inhibitory mechanisms i.e. (1) catalyst poisoning (sulfide and sulfite), (2) redox-active compounds (nitrate and nitrite) which compete for the reductive sites and (3)

passivating compounds (phosphate and carbonate) which reduce the available adsorptive and reductive sites on nZVI surface (Lim and Zhu, 2008).

Table 2.1 Common environmental contaminants that can be transformed by nZVI (Modified from (Zhang, 2003))

Contaminants	Contaminants
Chlorinated methanes	**Trihalomethanes**
Carbon tetrachloride	Bromoform
Dichloromethane	Dibromochloromethane
Chloromethane	Dichlorobromomethane
Chlorinated benzenes	**Chlorinated ethenes**
Hexachlorobenzene	Tetrachloroethene
Pentachlorobenzene	Trichloroethene
Tetrachlorobenzenes	*cis*-Dichloroethene
Trichlorobenzenes	*trans*-Dichloroethene
Dichlorobenzenes	1,1-Dichloroethene
Pesticides	**Other polychlorinated hydrocarbons**
DDT	PCBs
Lindane	Pentachlorophenol
Organic dyes	**Other organic contaminants**
Orange II	N-nitrosodimethylamine
Acid Orange	TNT
Acid Red	**Inorganic anions**
Heavy metal ions	Arsenic
Mercury	Perchlorate
Nickel	Nitrate
Silver	**Radioactive compound**
Cadmium	Uranium

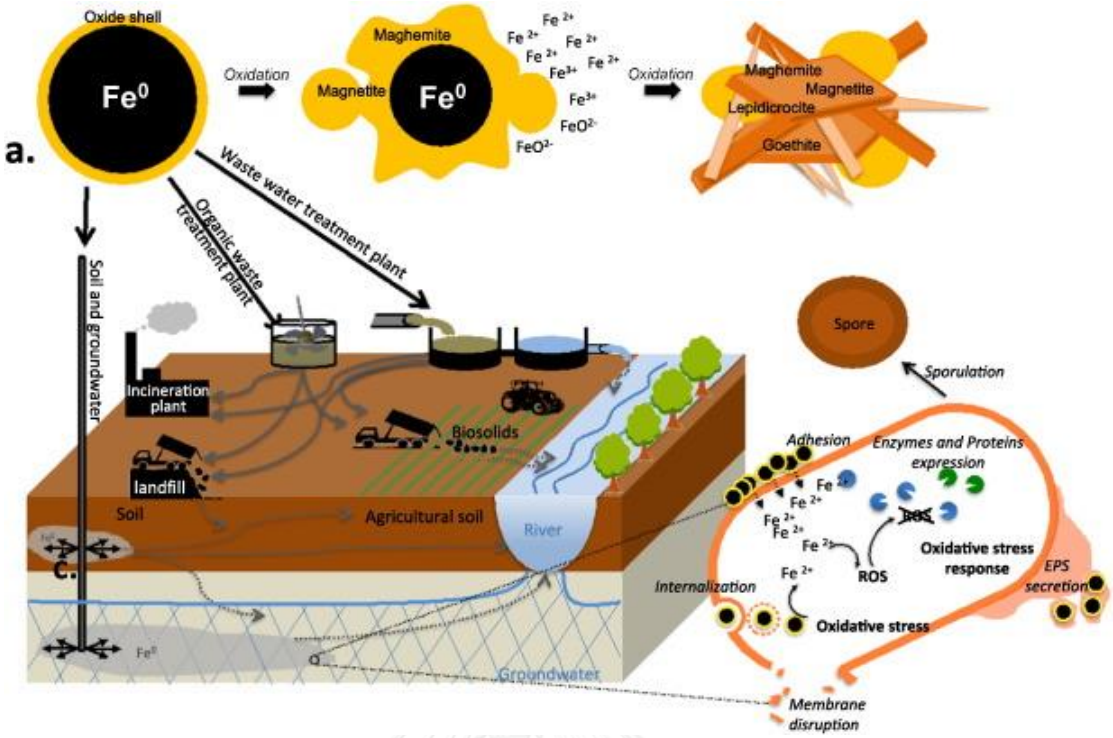

Figure *2.4* Proposed fate and transport of nZVI particles in the environmental and interaction between nZVI and environmental microorganisms. EPS: Extracellular polymeric substances. ROS: Reactive oxygen species. Source: (Lefevre et al., 2016).

2.2) Effects of nZVI on living organisms/microorganism

As an interest in the *in situ* environmental application of nanoscale zero valent iron (nZVI) is increasing, the concern regarding the environmental impact of these reactive iron particles became a topic of interest since high amount of nZVI has been released and retained in the environment (Mueller et al., 2012b). Iron is an essential nutrient for microorganism generally exists in the environment as an soluble Fe(II) and insoluble Fe(III) depending on their environmental conditions (e.g. oxygen concentration or pH) (Straub et al., 2001). Even though large amount of natural-occurred iron is already exist in the environment, the huge release of nZVI particles may cause unintended consequence due to their high reactivity.

2.2.1) Effects of nZVI on mammalian cells

In the study of Keenan and colleagues in 2009, human bronchial epithelial cells were treated with nZVI and ferrous ion (Fe(II)) (Keenan et al., 2009). After a 60 minute-exposure to nZVI or Fe(II), lung cell viability decreased following a dose-response relationship, while cells exposed to weathered nZVI resulted in minimum toxicity. They indicated that Fe^0 does not directly pose a cell damage, while Fe(II) is a prerequisite for cell damage. The relationship between Fe(II) oxidation, cytotoxicity and ROS generation was supported by the observation that the addition of iron chelator which prevents Fe(II) oxidation, limited cell damage, and cell exposed to preoxidized nZVI also resulted in no cell damage (Keenan et al., 2009).

2.2.2) Effects of nZVI on aquatic organisms

In 2009, Li et al. (Li et al., 2009) investigated the potential effect of nZVI on medaka (*Oryzias latipes*). The decreases of superoxide dismutase activities and increases of malondialdehyde, indicating oxidative damaged occurred when fish (medaka) embryos were exposed to nZVI. For adult fishes, they found the disturbance of antioxidant balance in liver and brain in the beginning of exposure, but it could be recovered with the exposure time. Some histopathological and morphological changes in gill and intestine of adult fishes were also observed. They mentioned that desquamated structure of gill filament and secondary gill lamellae, the deformed intestinal villi and intestine wall, swollen cells and iron accumulation, which are observed in gills and intestines exposed to 50 μg/ml nZVI, may affect the corresponding functional performances. This leads to a concern on the potential that direct contact between fish and high concentrations of nZVI slurry (4.5-10 g/L slurry used in pilot remediation) (Gavaskar A., 2005), may induce the aforementioned histopathological and morphological changes.

2.2.3) Effects of nZVI on microorganisms

Effects of nZVI on microorganism, particularly bacteria, have been studied in various bacterial strains as shown in Table 2.2. In 2008, Lee et al. studied the effects of nZVI and other types of iron-based compounds on E. coli (Lee et al., 2008b). They observed a strong bactericidal effect of nZVI under deaerated condition, while under air saturation condition, the inactivation was significantly lower due to corrosion, surface oxidation and formation of iron oxide layer (Lee et al., 2008b). This bactericidal effect was not observed in other types of iron-based compounds (Fe^0 powder, iron oxide and Fe(III) ions). However, Fe(II) also exhibited a significant bactericidal activity under deaerated condition suggested that Fe(II) can contribute to the bactericidal activity of nZVI, while Fe(III) has no cytotoxicity.

Table 2.2 Summary of reported nZVI effect on bacterial cells.

Source: (Lefevre et al., 2016)

Bacterial strain	nZVI characteristics	nZVI concentrations	Effects	References
K. planticola	nZVI (NANOFER 25S)	1000–10,000 mg/l	No effect on viability and activity. Attachment of nZVI to cell surface was observed.	(Fajardo et al., 2013)
K. oxytoca	nZVI (NANOFER 25S)	1000–10,000 mg/l	No bactericidal effects. Attachment of nZVI to cell surface without significant cell damage was observed. Proteomic analysis revealed the overproduction of tryptophanase.	(Saccà et al., 2013)
P. fluorescens	Synthesized nZVI	100–10,000 mg/l	Complete inactivation at all concentrations tested. Iron precipitate coating on cell surface was observed.	(Diao and Yao, 2009a)
P. stutzeri	nZVI (NANOFER 25S)	1000–10,000 mg/l	Slight toxicity, no effect on activity. Proteomic analysis revealed the oxidative stress response. Attachment of nZVI on cell surface and down-regulation of membrane transport proteins suggested effect on bacterial membrane	(Sacca et al., 2014)
Alcaligenes eutrophus	Synthesized bare-nZVI, chitosan-nZVI, sodium-oleate-nZVI	650 mg/l	Decrease of activity in the first 2 days.	(An et al., 2010)
Agrobacterium sp. PH-08 (Gram –)	Synthesized nZVI	100–250 mg/l	Significant toxicity (53.2 and 5.3% survival after 1 h-exposure to 100 mg/l CMC- and bare-nZVI, respectively). Drastic damage of cell membrane was observed.	(Zhou et al., 2014)
Agrobacterium	nZVI (NaBond, China)	100–	11.4 and 32% decrease in cell	(Le et al., 2014)

sp. PH-08		10,000 mg/l	viability after 6 h-exposure to 100 and 1000 mg/l nZVI, respectively. Slightly affect bacterial degradation capabilities. Attachment of nZVI cell surface without disruption or internalization was observed.	
E. coli	nZVI (Toda Kogyo Corp., Japan)	1000 mg/l	Toxic effect is strain-dependent. Bacterial exponential and decline growth phases were more susceptible to nZVI exposure than lag and stationary phases.	(Chaithawiwat et al., 2016a)
E. coli	nZVI (Toda Kogyo Corp., Japan)	1000 mg/l	Bacterial strains lacking antioxidant enzyme or sigma-s factor were more sensitive to nZVI exposure	(Chaithawiwat et al., 2016b)
E. coli	Synthesized nZVI	7–700 mg/l	Severe toxicity (~ 75% inactivation at ≥ 70 mg/l nZVI).	(Auffan et al., 2008)
E. coli	Bare nZVI (Toda Kogyo Corp., Japan) PSS-nZVI PA-nZVI NOM-nZVI	1–2000 mg/l	1.8 and 5.2-log inactivation for 7 and 28% Fe^0 nZVI, respectively. Surface modification of nZVI reduced the toxicity. Attachment of nZVI on cell surface was observed.	(Li et al., 2010)
E. coli	Synthesized nZVI	1.2–110 mg/l	Severe toxicity under de-aerated conditions. Slight toxicity under aerated conditions. Significant cell damage.	(Lee et al., 2008b)
E. coli	Synthesized nZVI	1.2–110 mg/l	Serious damage of cell membrane and respiratory activity was observed under de-aerated conditions. Negligible effect was observed in aerated condition.	(Kim et al., 2010)
B. nealsonii	nZVI (NANOFER 25S)	1000–10,000 mg/l	Slight toxicity was observed at 5000 whereas 10,000 mg/l nZVI drastically damage cells.	(Fajardo et al., 2012)

			Reduced metabolic activity. Cell content leakage was observed.	
B. subtilis	Synthesized nZVI	100–10,000 mg/l	Strong bactericidal effect (100, 95, and 80% inactivation at 100, 1000, and 10,000 mg/l nZVI, respectively). Massive needle-shaped of iron oxide coated on cell surface was observed..	(Diao and Yao, 2009a)
B. cereus	nZVI (NANOFER 25S)	1000–10,000 mg/l	Up-regulation of oxidative stress response proteins. Down-regulation of cell wall and motility proteins. No change in gene expression levels. Early sporulation was observed.	(Fajardo et al., 2013)
Paracoccus sp. YF1	Synthesized nZVI	50–1000 mg/l	50 $mg \cdot l^{-1}$ nZVI promoted bacterial growth and nitrate removal. Higher concentration than 50 mg/l decreased growth and nitrate removal. Attachment of nZVI to cell surface was observed.	(Jiang et al., 2015)

They mentioned that the bactericidal effect may result from the physical disruption of bacterial cell membrane because the transmission electron microscopy (TEM) images (Figure 2.5) of *E. coli* treated with nZVI showed the significant membrane disruption and leakage of the intracellular contents (Lee et al., 2008b). Iron, which is a strong reductant, may induce reductive decomposition of functional group in the proteins and lipopolysaccharides of outer membrane, or nZVI may disturb the respiratory system. They also mentioned that nZVI and Fe(II) may react with intracellular oxygen and pose oxidative damage to cells.

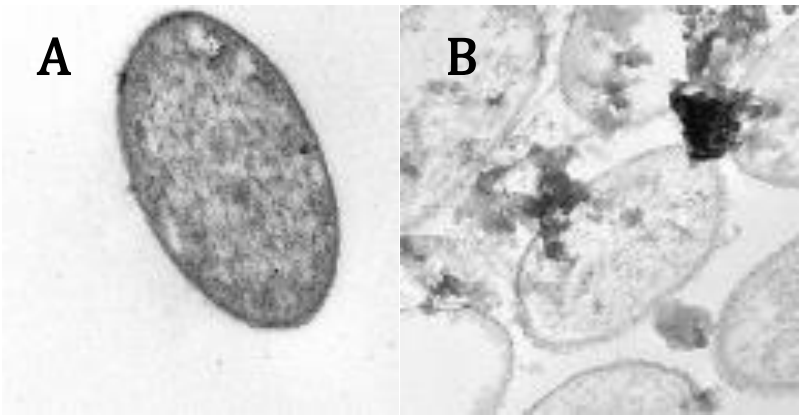

Figure *2.5* TEM images of (A) *E.coli* cell and (B) *E. coli* treated with nZVI
Source: (Lee et al., 2008b).

Diao et al. studied the use of nZVI in inactivating gram-negative and gram-positive bacteria and fungus under aerobic condition (Diao and Yao, 2009a). Both *B. subtilis* (gram-positive) and *P. fluorecens* (gram-negative) were completely inactivated when treated 10 mg/ml nZVI (Diao and Yao, 2009a). When the concentration of nZVI decreased to 0.1 mg/ml, *P. fluorescens* was still completely inactivated, while the inactivation of *B. sutilis* decreased to 80%. They suggested that because *B. subtilis*, a gram-positive bacteria, have a thicker cell wall providing more protection against environmental stress, while P. *fluorescens*, a gram-negative bacteria, have a thinner cell wall resulting in more susceptibility to stress. The exposure of 0.1-10 mg/ml nZVI to *Aspergillus versicolor*, one of the fungal species, showed no inactivation effect which could be because the fungal cell wall is extremely rigid.

Chen and colleagues in 2010 (Chen et al., 2011a) studied the bactericidal effect of nZVI toward gram-negative (*E. coli*) and gram-positive bacteria (*B. subtilis*) in the presence of humic acid. *B. subtilis* was more tolerant to nZVI (1 g/l) than *E. coli* while humic acid significantly reduced the bactericidal effect of nZVI. They also mentioned the recovery of bacterial survival rate after 4 hour exposure to similar level observed for untreated cells.

The effect of nZVI particles on various types of microorganisms have been extensively studied, however, their effect is still controversial and inconclusive. Kirschling et al. studied effect of nZVI on microbial community in aquifer materials from different TCE-contaminated sites and reported that nZVI may be toxic to only certain groups of bacteria (Kirschling et al., 2010). Quantitative polymerase chain reaction (qPCR) analyses , indicated that the introduction of nZVI to aquifer material stimulate both sulfate reducer and methanogen populations due to the increases of the dissimilatory sulfite reductase gene and archaeal 16s rRNA genes and there is no deleterious effect on total bacterial abundance in the microcosms. They also suggested that the initial changes in diversity were caused primarily by the nZVI-induced changes in geochemical conditions such as oxidation and reduction potential, hydrogen evolution and available iron, not by direct interaction between microorganisms and nanoparticle surfaces (Kirschling et al., 2010).

2.3) Proposed mechanisms of action of nZVI and bacterial responses

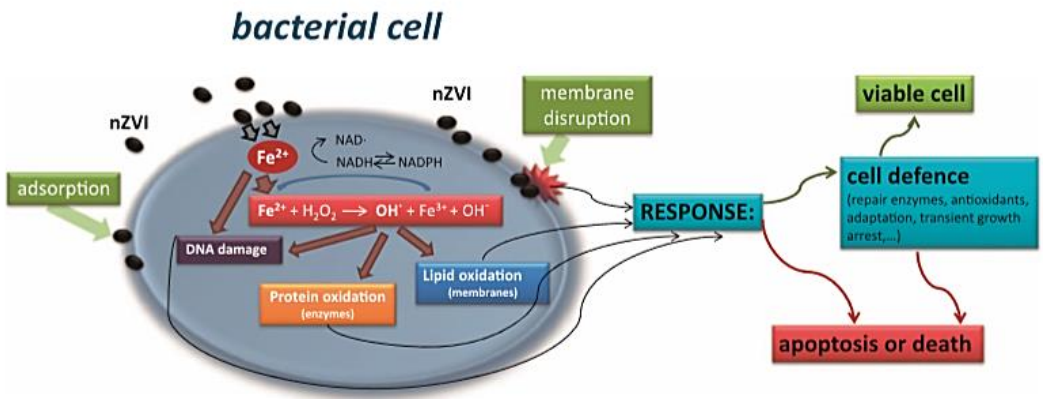

Figure *2.6* Proposed mechanisms of nZVI-induced toxicity in bacterial cells.
Source: (Sevcu et al., 2011).

2.3.1) Oxidative stress

Oxidative damage is caused by the accumulation of ROS including superoxide (O_2^-), hydrogen peroxide (H_2O_2) and hydroxyl radical ($OH^{\bullet}$). These ROS can further damage cellular macromolecules, for example, DNA, RNA, proteins and lipids (Sevcu et al., 2011). Several factors have been reported to induce the oxidative stress/damage in environmental microorganisms including the presence of toxic compounds (e.g. organic pollutants, metal, or antibiotics) or stress conditions (e.g. water limiting condition, osmotic stress) (Figure 2.7) (Kim and Park, 2014). Nanoparticles have also been reported to induce the oxidative stress in environmental microorganisms (Choi et al., 2008; Kim et al., 2007). For instance, Choi et al. reported the correlation between nitrifying bacteria inactivation by silver nanoparticles and silver ions and intracellular ROS concentrations (Choi and Hu, 2008). However, at the same level of the intracellular ROS, silver nanoparticles exhibits more toxicity than silver ions. This suggested the other factors besides ROS involving in silver nanoparticles toxicity.

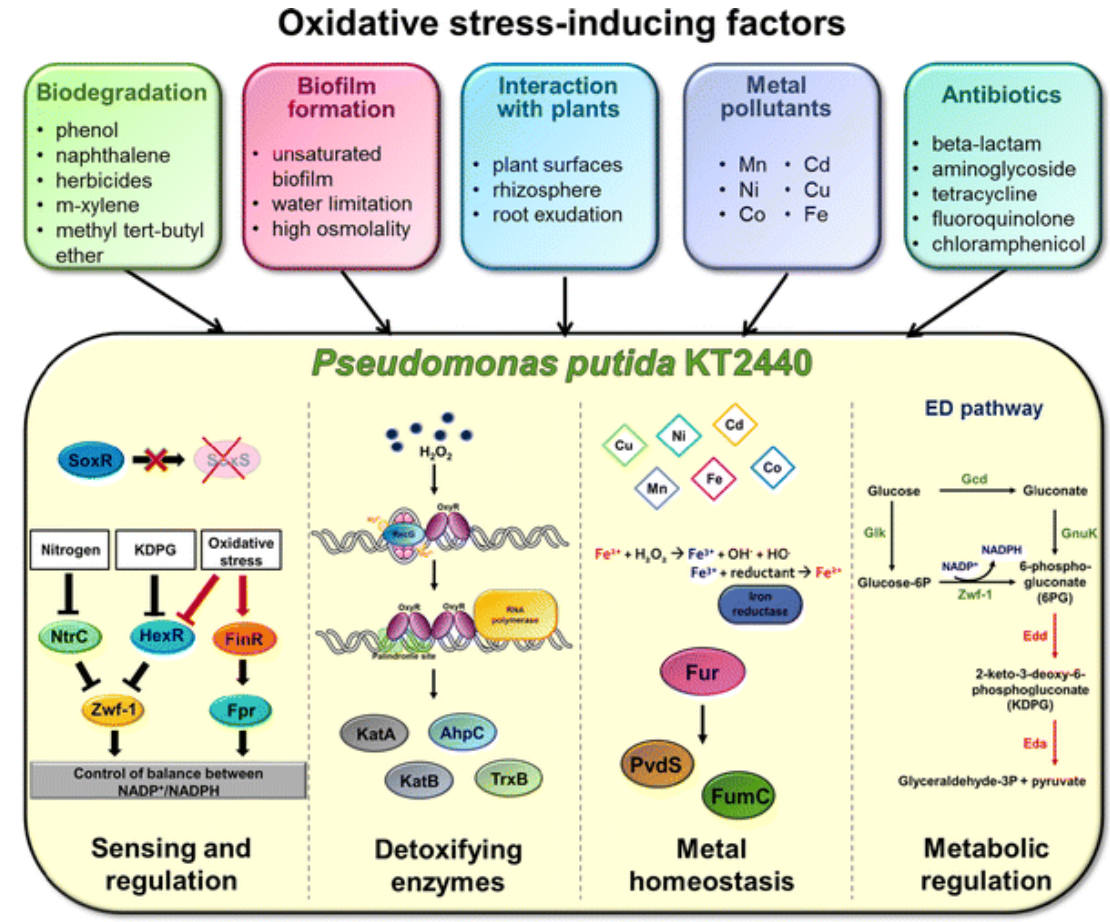

Mechanisms of oxidative stress sensing, regulation, and defense

Figure *2.7* Simplified overview of factors affecting oxidative stress and response system in P. putida KT2440. Source: (Kim and Park, 2014)

So far, the nZVI-induced oxidative damage in various microorganisms is one of the most extensively studied topic (Auffan et al., 2008; Chaithawiwat et al., 2016b; Keenan et al., 2009; Li et al., 2009). A relationship between bactericidal effect of nZVI and oxidative stress has been studied using *E. coli* Qc2472, a double mutant *sodA sodB*, which is completely devoid of the antioxidant enzyme superoxide dismutase, as a model strain . The mutant strain was found to have a greater sensitivity to nMagnetite ($Fe^{II/III}/O_4$) comparing to wildtype (Auffan et al., 2008). Similarly, a study by Chaithawiwat et al. (2016) reported that *E. coli* strains lacking of genes encoding

antioxidant enzyme (catalase and superoxide dismutase) are susceptible to nZVI exposure than the wildtype strains, suggesting the nZVI-induced oxidative stress (Chaithawiwat et al., 2016b). The altered susceptibility to nZVI also depends on bacterial growth phase since the effect of antioxidant enzyme deletion is much more pronounced in cells from lag and exponential phases (Chaithawiwat et al., 2016b). The same study also reported that the deletion of RpoS, a stationary sigma factor controlling the transcription of gene in response to general stresses, significantly enhance bacterial susceptibility to nZVI in growth phase-independent manner (Chaithawiwat et al., 2016b).

In order to counter oxidative stress, cells will express antioxidant enzymes related to detoxifying the ROS and repairing the damaged macromolecules. The major defensive enzymes are superoxide dismutase which dismutate O_2- to H_2O_2, and catalase which disproportionate H_2O_2 into H_2O and O_2, as shown in equation (6) and (7), respectively.

$$O_2\cdot^- + 2H_2 \longrightarrow H_2O_2 + O_2 \quad (6)$$

$$2H_2O_2 \longrightarrow O_2 + 2H_20 \quad (7)$$

In *E. coli*, when cells sense the increased level of O_2^-, some enzymes will be induced such as manganese superoxide dismutase (encoded by *sodA*), the DNA repair enzyme endonuclease IV (*nfo*), and O_2^- resistant izoenzymes of fumarase (*fumC*), aconitase (*acnA*), the cytosolic iron superoxide dismutase (*sodB*), the periplasmic copper-zinc superoxide dismutase (*sodC*) and the Fur repressor (*fur*) (Storz et al., 1990),(Storz and Imlayt, 1999). Several superoxide-induced proteins are known to be regulated by the products of two regulatory genes, soxR and soxS (Storz and Imlayt, 1999). According to Chaithawiwat et al. (2016), the nZVI-induced damage is likely attributed to the intracellular superoxide radical since the increased sensitivity to

nZVI is most pronounced cells with the inactivation of *sodA* and *sodB* (Chaithawiwat et al., 2016b).

Hydroxyl radical, a non-selective strong ROS, can be generated nZVI via Fenton's reaction which is the interaction between Fe(II) and H_2O_2. Accordingly, the bacterial iron homeostasis is strictly controlled. A study on oxidative stress-related genes showed that the activation of oxidative stress induces genes coding for several ion transporters (Ceragioli et al., 2010). Intracellular free iron levels may have been affected by the exposure to oxidative stress. Transcriptomic studies on the response of *Staphylococcus aureus* to hydrogen peroxide and peracetic acid showed that iron uptake systems were initially repressed, suggesting that this bacterium modulates iron uptake in order to prevent secondary oxidative damage (Ceragioli et al., 2010).

Siderophore or iron carrier is the Fe (III) specific chelater, which plays role in scavenging iron and making it available to microbial cells (Neilands, 1995). Aerobic or facultative aerobic microorganisms need iron for a variety of functions including reduction of oxygen for synthesis of ATP, reduction of ribotide precursors of DNA, and for formation of heme. The expression of siderophore is regulated by the ferric uptake regulator (Fur), which is a conserved protein in different Gram-negative bacteria encoded by *fur* and works as a repressor of iron uptake genes (siderophore biosynthesis, receptors) when bound to its co-repressor Fe(II). This Fur protein can directly control some genes involved in iron uptake, or indirectly, via extracytoplasmic sigma factors (ECF**σ**) such as PvdS which controls the transcription of *pvdS* (pyoverdine biosynthesis genes) or AraC regulator (Cornelis et al., 2009). When cells sense some stresses, they typically require higher energy in order to repair or re-synthesize the damaged macromolecules, and also to employ some stress response mechanisms such as efflux pump which require energy to enable the transport of substances across membranes. Enzymes such as glycerol-3-phosphate dehydrogenase (G3PDH), 6 phosphogluconate dehydrogenase (6PGDH), enolase,

citrate synthase, and isocitrate dehydrogenase (IDH) contribute strongly to the control of key pathways of energy metabolism, including glycolysis, pentose phosphate pathway, and the Krebs (citrate) cycle. Not only for energy production, induction of these enzymes during stress may be necessary for generating reducing equivalents (NADH, NADPH) that are needed for cellular antioxidant systems (Kultz, 2005).

Sergura et al., studied the proteomic analysis of response of *P. putida* DOT-T1E to toluene and reported that two groups of highly induced protein based on probably function are proteins involved in the channeling of metabolic intermediates to the Krebs cycle and activation of purine biosynthesis and proteins involved in sugar transport. Some induced proteins involved in general metabolism are glucokinase (encoded by *gck*), fructose-1,6-bisphosphate aldolase (*fda*), phosphoenolpyruvate carboxykinase (*pflu3720*), hydrolipoamide dehydrogenase (E3 component of 2-oxoglutaratedehydrogenase complex, *ipdG*), and succinyl-coenzyme A synthetase (*sucC*). A sugar ABC transport protein was also found induced by toluene. From this result, they suggested that the high energy demand required for solvent tolerance is achieved via activation of cell metabolism.

CyoA (encoded by *cyoABCDE*) is the subunit II of the cytochrome *bo* oxidase. This enzyme functions as the terminal oxidases in the aerobic respiratory chain of *E. coli and* contributes to the generation of a proton motive force (PMF). Cytochromes are the major functional units in the respiratory chain and are essential components in this energy transduction mechanism. The down-regulation of *cyoA* in the investigation of *soxRS* gene deletion can be used as an indicator of the effect on respiratory system and electron transport chain (Kabir and Shimizu, 2006).

In *E. coli*, the succinate dehydrogenase complexes are encoded by the *sdhCDAB* operon (Heinzen et al., 1995). This enzyme complex is involved in aerobic respiration, converting succinate to fumarate. It is composed of cytochrome b556

(SdhC), a hydrophobic protein (SdhD), a flavoprotein (SdhA) and an iron-sulfur protein (SdhB) (Wood et al., 1984). This cytochrome *b* encoded by *sdhC* was reported to primarily responsible for oxidative metabolism and utilization of succinate (Murakami et al., 1985).

Protein damage in cells exposed to stress occurs mainly as oxidative or structural (unfolding) damage. Some damaged proteins are repaired by enzymes that reverse oxidative damage or assist in protein refolding. However, not all damaged proteins are repaired. Many terminally damaged proteins are removed by proteolytic degradation and regenerated. Thus, three processes are mainly responsible for removing protein damage: (*a*) repair of oxidative damage, (*b*) refolding of structurally damaged proteins, and (*c*) proteolysis (Kultz, 2005).

One protein that plays important role in damaged protein repairing is heat shock proteins (HSPs). Molecular chaperones, or the cellular stress response system that utilizes HSPs, under normal condition, do play an essential role in the synthesis, transporting proteins across membrane, folding and degradation of unstable proteins to prevent protein aggregation (Sergios A. Nicolaou, 2010). When cells sense the stress condition, HSPs will play a role in preventing aggregation and assisting in refolding of damaged proteins. Several families can be distinguished and are designated, according to their average molecular mass. Several proteins in heat shock family are Hsp90 (Hsp83 in *S. cerevisiae*), Hsp60 (the chaperonin or GroEL family) (Mager and De Kruijff, 1995). Hsp70 (DnaK in *E. coli*) is known to contains the most highly conserved proteins in the cell.

Studies on Hsp in *E. coli* reported that the heat shock regulon of *E. coli* consists of over 20 genes including *groES*, *groEL*, *dnaK*, and *dnaJ* (Bukau, 1993). In *E. coli*, heat shock proteins GroES and GroEL can be induced by both peroxide- and superoxide-mediated oxidative stresses as well as heat shock, starvation, and SOS. DnaK can be induced by treatment with H_2O_2, nalidixic acid, UV irradiation, and

starvation. The DnaK system of *E*. coli consists of DnaK, DnaJ and GrpE. This chaperone system plays an important role in various cytoplasmic cellular processes. In addition to an ATP-dependent refolding of damaged protein, the DnaK system also assists in translocation through membrane.

There are many sigma factors associated with stress responses, for example, σ^{32}, the product of the *rpoH* gene and σ^{38} or σ^{S} encoded by *rpoS* (Chung et al., 2006). Under normal condition, σ^{32} is a very unstable protein. Its expression is repressed predominantly at the translational level. In response to stresses, for example, temperature upshift, both the stability and synthesis of σ^{32} are transiently elevated, which causes an increase in the concentration of σ^{32}, in turn giving rise to an increase in the rate of Hsp synthesis. The inactivation of RpoS significantly enhance bacterial susceptibility to nZVI (Chaithawiwat et al., 2016b).

2.3.2) Membrane disruption

The significant interaction between nZVI and bacterial cells has been reported in many studies (Lee et al., 2008b; Saccà et al., 2014). While nZVI-induced oxidative stress has been proposed as major toxicity mechanism of nZVI, the interaction between the particles and bacterial surface appears to be essential for the damage. In addition to destructive effect on membrane composition which result in the leakage of intracellular content or affecting bacterial electron transport chain (Lee et al., 2008b), the disturbed membrane permeability may promote the penetration of nZVI or the soluble species thus enhancing the intracellular oxidative stress (Lefevre et al., 2016).

Raffi et al. reported the formation of pits in *E*. coli cell wall and leakage of inner vacuoles caused by the exposure to zero valent copper nanoparticles (Cu^{0}) (Raffi et al., 2010). They suggested that Cu^{2+} ions released from copper nanoparticles

can bind to the surface of bacteria which is negatively charged. The bacterial surface charge is negative because of the excess of the carboxylic groups in the lipoproteins at the surface. The attached Cu^{2+} ions can solidify protein structure or alter enzyme functions (Dan et al., 2005). Hydrogen peroxide generated by Cu^{2+} ions can also cause damage to cytoplasmic membrane (Hoshino et al., 1999). In general, copper ions, with strong reduction ability, can extract electron from bacteria. This can damage cell wall and membrane and subsequently results in cytoplasm leakage and oxidizing the cell nucleus. Cu^{2+} ions can bind with plasma membrane and penetrate into cells through membranes channels. The penetrated Cu^{2+} ions possibly interact with phosphorus- or sulfur-containing compounds in DNA, or combine with intracellular amino acid or protease leading to protein denaturation (Tong et al., 2005).

The formation of pits in bacterial cell wall was also found in *E*. coli after exposed to nAg (Sondi and Salopek-Sondi, 2004). The EDAX qualitative chemical analysis and TEM showed the accumulation of nAg into cell membrane structure. In addition, TEM also showed the leakage of intracellular content. It was suggested that silver nanoparticles interact with building element of cell (Sondi and Salopek-Sondi, 2004).

Gou et al. studied the temporal gene expression in bacteria exposed to nAg and $nTiO_2$ using a whole-cell-array library of *E*. coli K12 with transcriptional green fluorescent protein (GFP)-fusions (Gou et al., 2010) . They found that the toxicity of these two nanoparticles are compound-specific and concentration-dependent. Cell membrane and transportation damage and oxidative stress were reported. However, their toxic mechanisms of nAg and $nTiO_2$ are different due to the difference in the altered expression of specific genes. The up-regulation of genes related to cell membrane barrier function and transportation like *sanA* indicating membrane permeability damages in cells exposed to $nTiO_2$. Whereas, the exposure to nAg leads

to the up-regulations of *bolA* which related to biofilm formation and the alteration of outer membrane properties.

A proteome analysis of *E. coli* cells treated with nAg showed the accumulation of envelop protein precursor, OmpACF (Lok et al., 2006). These protein precursors require energy from adenosinetriphosphate (ATP) and proton motive force to synthesize envelope protein and translocate proteins to membrane. This confers to the dissipation of proton motive force. Silver nanoparticles were also found to destabilize bacterial outer membrane. They suggested that nAg can disrupt outer membrane component such as lipopolysaccharides or porins.

In 2007, Fang studied physiological adaptation of gram negative bacteria, *P. putida* F1, and gram positive bacteria, *B. subtilis* CB310 in response to fullerene exposure. The alteration of membrane lipid composition, phase transition temperature and membrane fluidity were reported as the bacterial responses to fullerene. The bacterial responses depended on the concentration and the cell wall morphology. For *B. subtilis*, gram-positive bacteria, which is more tolerant to fullerene (higher minimum inhibitory concentration), an increase in the level of monounsaturated fatty acid was observed. This suggests the important role of unsaturated fatty acid in gram-positive bacteria adaptation. The exposure to low doses of fullerene resulted in increasing the proportions of iso- and anteiso-branched fatty acids. In *P. putida*, under high concentration exposure, the level of *trans* monounsaturated fatty acids increased. This is known as a general defense mechanisms, which may decrease the permeability of the lipid bilayer. Fourier transform infrared spectroscopy results showed increased phase transition temperatures and membrane fluidity of *P. putida* under fullerene exposure. *B. subtilis* showed increased membrane fluidity but a decrease in phase transition temperatures.

2.3.3) DNA/RNA damage

In 2010, Gou et al. reported that exposure to nAg results in the up-regulation of genes involving DNA repair such *as nfo, recN, uvrA* and *yfbE* (Gou et al., 2010). These up-regulations indicated that nAg exposure can cause DNA damage. This DNA damage was also found in cells exposed to $nTiO_2$. However, genes and magnitude of alterations were different. The exposure to $nTiO_2$ up-regulated *recA* and *lexA*, which are the regulators of SOS system. These two genes subsequently induce genes related to DNA damage such as *polB, ssb, recN, nfo, mutt* and *uvrA*.

In the presence of H_2O_2, the expression of a number of the proteins is regulated by the oxyR transcription factor (Storz and Imlayt, 1999). Several defensive enzymes induced by H_2O_2 are hydroperoxidase I (catalase, *katG*), hydroperoxidase II (*katE*) and glutathione reductase (*gorA*). H_2O_2, can further react with Fe(II), generating HO· which can damage DNA. This results in the expression of several DNA repair enzymes such as exonuclease III (*xthA*), DNA polymerase I (*polA*) (Storz et al., 1990),(Storz and Imlayt, 1999).

As previously mentioned, not only the antioxidant activities have been induced but oxidative stress also induces activities related to the repair of damage caused by oxidants (Storz et al., 1990). When hydroxyl radical attacks on the sugar moiety of DNA, it leads to sugar fragmentation and production of strand breaks with 3'-phosphate or 3'-phosphoglycolate termini (Farr and Kogoma, 1991). Thymine residues in DNA can be hydroxylated to produce 5-hydroxymethyluracil or oxidatively degraded to produce thymine glycol or a urea residue. Exonuclease III, the product of the *xthA* gene, is the major apurinic/apyrimidinic endonuclease (AP endonuclease) activity found in *E. coli,* and has been shown to remove replication blocks from the 3' termini of oxidized DNA *in vitro.* A second AP endonuclease capable of removing 3' replication blocks is endonuclease IV *(nfo).* Several other DNA repair activities are likely to be important for a defense against oxidative stress, as

inferred from the study of hydrogen peroxide sensitivity of mutant strains (Imlay and Linn, 1987). Strains with mutations in *recA,* a regulator of the SOS response (a response induced by several types of DNA damage) are sensitive to hydrogen peroxide (Imlay and Linn, 1987).

2.4) Roles of nZVI in bioremediation

Even though several studies reported the strong bactericidal effects of nZVI (Diao and Yao, 2009b; Lee et al., 2008b), the successful combinations of nZVI together with bioremediation have also been reported (Bose et al., 2016; Jagadevan et al., 2012; Kim et al., 2012; Kocur et al., 2016; Kuang et al., 2013). The abiotic process by nZVI sequesters or concurrent with biotic process are expected to result in synergetic effect on contaminant degradation. The initial degradation by nZVI may decrease the toxicity of the contaminants toward bacteria that may playing a role in remediating some residual or dead-end products. nZVI has also been used as an electron donor or providing H_2 for some microbial reduction (Shin and Cha, 2008) .

Shrout and coworkers reported the decreasing of microbial perchlorate reduction in the presence of ZVI (Shrout et al., 2005). Fe^0 particles, as an electron donor, were added to anaerobic mixed culture capable of reducing perchlorate to chloride. Bacterial perchlorate reduction was inhibited. They suggested that the insoluble product of Fe^0 corrosion may accumulate on bacterial surface and hence inhibit their activity.

In contrast, the advantage of adding nZVI as a reductant for microbial reduction was reported by Shin et al. (Shin and Cha, 2008). Shin et al. reported that co-remediation between nZVI and bacterial can degrade nearly 100% of nitrate within three day, whereas the absence of bacteria under same condition (abiotic system), only 50% of nitrate can be degraded after seven days (Shin and Cha, 2008).

They suggested that Fe(II) from the oxidation of nZVI, may acts as an electron donor for nitrate microbial reduction.

Xiu et al. (Xiu et al., 2010b) studied the effect of nZVI on *Dehalococcoides* spp. *Dehalococcoides* is known for its ability to completely dechlorinate trichloroethylene (TCE) to ethane, nZVI was reported to inhibit bacterial dechlorination but the dechlorination activity, however, can be recovered after lag time. This co-remediation may be an alternative for remediate contaminated site. Nevertheless, they suggested that this is unlikely to be a universal application and more factors need to be studied.

The expression of *tceA* and *vcrA*, encoded for reductive dehalogenases, were down-regulated in bacteria exposed to bare nZVI (Xiu et al., 2010a). On the contrary, *tceA* and *vcrA* were up-regulated in bacteria exposed to nZVI coated with an olefin maleic acid copolymer (Xiu et al., 2010a). The mechanism of *tceA* and *vcrA* gene-expression inhibition by NZVI is still unclear.

The effective degradation of triclosan via palladized iron nanoparticles (nFe-Pd) co-remediate with *Sphingomonas* sp. PH-07 was demonstrated (Murugesan et al., 2011). Triclosan can be completely dechlorinated by nFe-Pd, resulting in the formation of 2-phenoxyphenol, which is the dead-end products. This compound can be subsequently aerobically degraded by *Sphingomonas* sp. PH-07, which was able to grow in the presence of nFe-Pd. The compromising strategy for triclosan degradation by hybrid treatment between nFe-Pd and bacteria has been proposed.

Chapter 3
Materials and methods

3.1) Part 1 Elucidation of effects of reactive and oxidized nZVI on bacterial membrane by proteomic analysis

3.1.1) nZVI source and iron content determination.

The nZVI particles obtained from Toda Kogyo Corp., Japan were used and designated as R-nZVI. These nZVI particles are uncoated nZVI with reported average size of 28 nm (Chaithawiwat et al., 2016a). The same nZVI particles stored under aerobic condition at room temperature for approximately two years were designated as O-nZVI. The Fe(II) content of nZVI was determined using the Ferrozine method (Voelker and Sulzberger, 1996). To determine the total iron and Fe^0, nZVI was digested in concentrated HCl and then quantified for the total iron using the Ferrozine method, while the generated H_2 after acid digestion was used to quantify Fe^0 content (Hwang et al., 2014).

3.1.2) Cell preparation and determination of effects of nZVI on cell viability

P. putida KT2440 was from the American Type Culture Collection. Bacterial cells were cultivated in TSB medium at 150 rpm (orbital shaking) and 30°C. *B. subtilis* 168 cells (obtained from Professor Junichi Kato, Hiroshima University, Japan) were cultivated in TSB medium, 150 rpm, 37°C.

Cells from mid-exponential phase were harvested by centrifugation at 5,000 rpm for 15 min and washed twice with 0.85% NaCl before resuspended in 5 mM carbonate buffer (pH 8.0). The bacterial cell suspension was diluted to an initial cell concentration of 10^8 CFU/mL. For nZVI exposure, 10 mL of cell suspension in 27-mL bottle were exposed 1.0 g/L of R-nZVI or O-nZVI. This nZVI concentration was

selected based on the potential nZVI concentration in contaminated site (Chaithawiwat et al., 2016a, b). Magnetic stirrer (700 rpm) was used to prevent the aggregation of nZVI. Control condition was cells without nZVI exposure. Cell viability at each time point was determined by the plate count method. The experiment was carried out in at least three biological replication.

3.1.3) Proteomic analysis of nZVI-treated cells

3.1.3.1 Sample preparation for proteomic analysis

The proteomic analysis was mainly focused on *P. putida* KT2440. *P. putida* KT2440 cells from mid-exponential phase were collected and prepared as described in section 3.2.2). Cell suspension were then treated with 1.0 g/L of R-nZVI or O-nZVI for 4 hours. To obtain adequate protein content for proteomic analysis, reaction scale was enlarged to 200 ml of cell suspension in 1-L flask. Magnet was used to separate nZVI particles from bacterial cells which subsequently were collected by centrifugation. Cells were washed twice and resuspended in 10 mM Tris-HCl (pH 8.5). Cell suspension was sonicated on ice for four minutes (10% power, M73 ultrasonic homogenizer microtip probe). After sonication, total protein extract was obtained by centrifugation at 15,000 ×*g* for 3 min to remove cell debris.

The obtained supernatant was considered as total protein fraction. For protein fractionation, this fraction was further ultracentrifuged at 99,000 rpm for one hour. The obtained supernatant from this step was considered as bacterial soluble protein fraction. The remained pellets were washed and followed by ultracentrifuged to remove the soluble protein. Then the pellets were solubilized using SDS solution to obtain membrane-bound protein.

Protein concentration was determined using a modified Lowry method(Markwell et al., 1978). Fifteen micrograms of protein were separated on

12.5% SDS-PAGE and stained with Colloidal Coomassie Brilliant Blue G-250(Paemanee et al., 2016).

3.1.3.2 GeLC-MS/MS

In-gel digestion by trypsin and sample preparation for LC-MS/MS were conducted as described in Paemanee et al. (2016) (Paemanee et al., 2016). Quantitative analysis of protein was performed using DeCyder MS differential analysis software (DeCyderMS, GE Healthcare). For protein identification, the PMF data were searched against the NCBInr database for proteobacteria using the MASCOT (version 2.2 Matrix Science, London, UK). Three missed cleavages were allowed. Carbamidomethylation was set as fixed modification and methionine oxidation was set as variable modification. Peptide tolerance are ± 1.2 Da.

3.2) Part 2 Bacterial response to short-term and repetitive nZVI exposure: Modification in bacterial membrane

3.2.1) nZVI source and characterizations.

Nanofer 25S, commercial iron nanoparticles, was obtained from NANOIRON s.r.o., Czech Republic. Nanofer 25S is a polyacrylic acid-modified nZVI produced by the hydrogen reduction of ferrihydrite. The hydrodynamic size and surface charge of Nanofer 25S was determined by Dynamic Light Scattering (Malvern Zetasizer, Malvern Instruments Ltd.). A refractive index of 2.87 was selected for hydrodynamic size determination (Phenrat et al., 2009a). The Fe(II) content of Nanofer 25S was determined using the Ferrozine method (Voelker and Sulzberger, 1996). To determine the total iron and Fe^0, Nanofer 25S was digested in concentrated HCl and then quantified for the total iron using the Ferrozine method, while the generated H_2 after acid digestion was used to quantify Fe^0 content (Hwang et al., 2014). For surface charge measurement, a stock solution of nZVI was dispersed in M9G to obtain a final

concentration of 0.1 g/L and zeta potential of nZVI was measured using a Zetasizer (Malvern Instruments Ltd.) at 25°C.

3.2.2) Bacteria, media, and cultivation conditions.

P. putida F1 was kindly provided by Professor J. Kato from Hiroshima University (Japan). Bacterial cells were cultivated in M9 minimal medium (further referred as M9G) which consists of (per 1 L): $Na_2HPO_4 \cdot 12H_2O$, 15.05 g; KH_2PO_4, 3 g; NaCl, 0.5 g; NH_4Cl, 1 g; $MgSO_4$, 2 mM; $CaCl_2$, 0.1 mM; a solution of trace elements, 1 mL; and 0.4% glucose. One hundred mL of the trace element solution consist of H_3BO_4, 0.116 g; $FeSO_4 \cdot 7H_2O$, 0.278 g; $ZnSO_4 \cdot 7H_2O$ 0.115 g; $MnSO_4 \cdot H_2O$, 0.169 g; $CuSO_4 \cdot H_2O$, 0.038 g; $CoCl_2 \cdot 6H_2O$, 0.024 g; and MoO_3, 0.01g. The cultivation conditions were 200 rpm and 30°C.

3.2.3) nZVI toxicity assessment

Cells from mid-log phase were harvested by centrifugation at 5,000 rpm for 15 min and washed twice with 0.85% NaCl before resuspended in M9G medium. The bacterial cell suspension was adjusted to an initial cell concentration of 10^8 CFU/mL before being exposed to 0.1, 1.0 and 5.0 g/L of nZVI at 150 rpm, 30°C for six hours. Bacterial viability was monitored using the plate count technique. A control experiment was conducted in the same manner but without nZVI addition. The effects of 0.1 g/L of Fe(II), Fe(III) and 3 mg/L polyacrylic acid which is an equivalent to 3% of surfactant in Nanofer 25S, the coating material of Nanofer 25S, were also tested in the same manner as nZVI.

The nZVI concentration of 0.1 g/L was selected to study the effect of repetitive nZVI exposure to bacterial cells. In every exposure cycle, bacterial cells previously treated with nZVI for 24 hours were diluted (1:100) with fresh M9G medium and re-dosed with nZVI. The nZVI re-dosing cycle was conducted for ten

times. The obtained cells were tested for their sensitivity to nZVI by exposing cells from mid-log phase to 0.1, 1.0 and 5.0 g/L of nZVI at 150 rpm and 30°C for one hour.

3.2.4) Sample preparations for scanning and transmission electron microscopy, and cell surface charge measurement.

Scanning electron microscopy (SEM) and transmission electron microscopy (TEM) were used to observe interactions between nZVI and bacterial cell membrane. To prepare a SEM specimen, cells with and without nZVI exposure were washed once with 0.85% saline solution and fixed in 2.5% glutaraldehyde in 0.1 M phosphate buffer (pH 7.2) for 2 hours at 4°C. Specimens were rinsed with phosphate buffer followed by distilled water. After that, they were dehydrated with a series of ethanol (30 to 95%), critical point dried, and coated with gold. Specimens were observed under a scanning electron microscope (JEOL model JSM-5410LV).

Samples for TEM were prepared by the Microscopic Center, Burapha University, Chonburi, Thailand. Briefly, bacterial cells were treated with 0.1 g/L nZVI for one and six hour. Cells were then harvested and washed once with 0.85% saline solution, before fixed in 2.5% glutaraldehyde in **0.1 M phosphate buffer**. Cell resuspension was dropped on carbon-coated Cu grid and allowed to dry before observed under a transmission electron microscope (Philips model TECNAI 20).

For surface charge measurement, the cell concentration in M9G medium was diluted to approximately 10^8 CFU/mL and zeta potential was measured using a Zetasizer (Malvern Instruments Ltd.) at 25°C.

3.2.5) Alterations in bacterial membrane fatty acid profile

Bacterial cells were harvested by centrifugation (5,000 rpm, 15 min) and washed once with 0.85% NaCl. Cell pellets were stored at -80°C before fatty acid extraction. Bacterial fatty acid was extracted using the Bligh and Dyer method(Bligh and Dyer, 1959). Cell pellets were resuspended in 0.4 mL of water. Then, 2 mL of

chloroform and 4 mL of methanol were added followed by 1.2 mL of water. The mixtures were vortexed and left overnight. After that, chloroform and water were added to obtain the final ratio (by volume) of 1:1:0.9. The mixtures were centrifuged at 1,500 rpm for 10 minutes and the upper aqueous phase was discarded. The lower organic phase was collected. Chloroform was evaporated under a gentle stream of nitrogen gas. The obtained lipid was resuspended in hexane and derivatized using a 5% sulfuric/methanol solution at 60°C for two hours.

Fatty acid methyl esters were analyzed by an Agilent 7000C Triple Quadrupole GC/MS system (Agilent Technologies Inc., USA). Separation was performed on a HP-5ms column (30 m × 0.25 mm, 0.25 μm). The initial oven temperature was held at 120°C for 2 min, followed by ramping (10°C/min) to 200°C, holding for 2 min, and ramping (10°C/min) to the final temperature of 280°C, which was maintained for 5 min. The *cis* and *trans* configuration of unsaturated fatty acids was determined using standard *cis*- and *trans*-9-hexadecenoic acids.

3.2.6) Alterations in phospholipid headgroup

Samples were extracted for their metabolites following the protocol by Vinayavekhin(Vinayavekhin and Saghatelian, 2001). Briefly, cells were centrifuged, washed and resuspended in M9G medium. The cell suspension was extracted with chloroform:methanol mixture (2:1) before centrifuged to separate the organic and aqueous phase. The obtained organic phase was then dried under nitrogen steam before dissolved in chloroform. The samples were analyzed by LC-MS as described by Vinayavekhin (Vinayavekhin et al., 2015). The percentage of phospholipid was determined by following equation;

$$\%\text{Phospholipid} = \frac{\text{Peak area of phospholipid of interest}}{\text{Total peak area}}$$

3.2.7) Bacterial membrane fluidity

Membrane fluidity was investigated by measuring fluorescence polarization of a probe compound, 1,6-diphenyl-1,3,5-hexatriene (DPH) incorporated into the cytoplasmic membrane. Bacterial cells were harvested, washed, and resuspended in M9G medium to obtain OD_{600} of 0.2. The 0.6 mM stock solution of DPH in tetrahydrofuran was added to obtain a final concentration of 4 μM DPH. The mixture was shaken at 200 rpm, 30℃ for 10 minutes in the dark. A spectrofluorometer was used to measure fluorescence polarization with excitation at 360 nm and emission at 430 nm, 10- and 10-nm slit width, respectively.The fluorescent anisotropy which inversely correlates with the fluidity of bacterial membrane was calculated according to Mykytczuk et al. (Mykytczuk et al., 2007).

3.2.8) Statistical analysis

Experimental data were statistically analyzed using Two-way ANOVA followed by Tukey's multiple comparisons or Student t-test with Holm-Sidak method (GraphPad InStat version 3.10, 32 bit for Windows, GraphPad Software, San Diego California USA, www.graphpad.com). The standard deviation of the data was calculated and presented as error bars.

3.3) Part 3 Emergence of phenotypic variants of *P. putida* F1 due to nZVI exposure and their environmentally relevant characteristics

3.3.1) nZVI source

nZVI, Nanofer 25S, was obtained as described in section 3.2.1.

3.3.2) Bacteria, media, and cultivation conditions.

P. putida F1 strain and cultivation conditions are as described in section 4.2.2. In addition to M9G, tryptic soy broth (TSB) and M9 medium supplemented with toluene (vapor phase, further designated as M9T) were used.

3.3.3) Determination of the emergence of the SCV phenotype

3.3.3.1 Effect of nZVI concentration on the emergence of the SCV phenotype

An overnight culture of *P. putida* F1 were diluted (1:100) in fresh M9G before treated with 0.1, 0.5 or 1.0 g/L of nZVI at shaking condition 200 rpm, 30°C. After 24 hours of nZVI exposure, cells were diluted in fresh M9G and re-exposed to nZVI at shaking condition 200 rpm, 30°C. The exposure were repeated for three cycles. The frequency of the SCV phenotype in each cycle was determined using the plate count technique. At least three biological replicates were carried out to determine the frequency of the SCV phenotype.

Due to a limitation in detecting the smaller colony occurred at low frequency which could be hindered by the normal cells, antibiotic resistance was selected as an indicator for the SCV phenotype. The method was adopted and modified from Edwards (2012) (Edwards, 2012). While the growth of the normal cells of *P. putida* F1 was inhibited in the presence of 4 mg/L of gentamicin (gm), the stable SCV phenotype could persist up to 4 mg/L of gm (Appendix A). Thus, the SCV phenotype in this study is referred to *P. putida* F1 cells able to grow on TSB agar plate containing 4 mg/L of gentamicin. The following equation (equation 1) was used for the determination of the frequency of the SCV phenotype.

$$\text{Frequency of the SCV phenotype} = \frac{\text{number of cells grown TSB plate} + \text{gm}}{\text{total cells}} \qquad \text{equation 1}$$

3.3.3.2 Effects of oxidative stress and different forms of iron on the emergence of the SCV phenotype

In addition to R-nZVI, the effect of other forms or products of nZVI (i.e. oxidized form (O-nZVI), ionic Fe(II) and Fe(III), on the emergence of the SCV

phenotype was also investigated. Cells were repeatedly exposed to 0.5 g/L of R-nZVI, O-nZVI and soluble iron species in a similar manner as described in 5.2.3.1. To assess the role of nZVI-mediated oxidative stress, cells were exposed to 0.5 mM of H_2O_2 which is the equivalent level of oxidative stress caused by exposure to 0.5 g/L nZVI as determined by H_2DCFDA (Appendix B). The reported frequency of the SCV phenotype are mean of three biological replicates.

3.3.4) Characteristics of the SCV phenotype

3.3.4.1 Bacterial growth rate

An overnight culture in M9G medium was inoculated in 100 ml of M9G, M9T, M9T supplemented with 0.1% glucose, or TSB medium at 30°C, 200 rpm. For M9T medium, cells with toluene induction (toluene-acclimated cells) were also investigated in comparison to non-induced cells. The optical density (OD600) was monitored with timeand exponential growth rate (μ) was calculated according to Zeyer et al. (1985) (Zeyer et al., 1985). For toluene induction, cells were grown in M9T medium, toluene-acclimated cells showing growth in late-exponential phase were used as 1%(v/v) inoculum for fresh M9T medium for monitoring their growth The reported growth rate is a mean based on at least three independent experiments.

3.3.4.2 Toluene tolerance

Cells were grown in TSB medium at 200 rpm until mid-exponential phase (OD600 ≈ 0.6). The harvested cells with an initial concentration of approximately 10^8 CFU/ml were then exposed to various toluene concentrations of 25 – 870 mg/L at 200 rpm for one hour. The survival of the cells after toluene exposure was determined by the plate count technique.

3.3.4.3 Toluene degradation

Toluene degradation was studied using the normal and SCV cells with toluene induction to reduce lag phase during the degradation. For toluene induction, cells were grown in M9T medium, toluene-acclimated cells showing growth in mid-exponential phase were harvested by centrifugation at 5,000 rpm for 15 min before being washed twice with 0.85% NaCl and resuspended in M9 medium. Initial cell concentration was adjusted by diluting cell resuspension to OD600 of 0.05. A toluene degradation test was conducted in 13-ml capped vial containing 2 ml of toluene-acclimatized culture and an initial toluene concentration of 100 mg/L. With time, vials were sacrificed for toluene quantification.

3.3.4.4 Swimming motility

Bacterial swimming motility, a flagella-mediate bacterial movement, was determined in semisolid agar as described by Ha et al. (2014) (Ha et al., 2014). Briefly, bacterial cells from an overnight culture were inoculated to the center of TSB plate containing 0.3% agar using sterile toothpick. Swimming zone size was measured after 48 hours of incubation at 30°C. The reported swimming distance is a mean of at least two independent experiments.

3.3.4.5 Biofilm formation

An overnight culture of *P. putida* F1 was inoculated in fresh M9G medium and biofilm was statically grown in a 24-well polystyrene plate at 30°C. At each time point, cell culture was removed and the wells were washed gently three times to remove loosely bound cells prior to air drying. The attached cells were recovered by resuspending in sterile DI water before serially diluted and plated on TSB agar. Biofilm amount was quantified by crystal violet staining (Thuptimdang et al., 2015). The reported swimming distance is a mean of at least two independent experiments.

3.3.5) Fourier transform infrared spectroscopy (FTIR) analysis

For normal cells and the irreversible SCV phenotype, cells from mig-log phase were resuspended in M9G medium before treated with 0.1 g/L of nZVI. After one hour of nZVI exposure, cells were washed and lyophilized before analyzed by FTIR. For reversible SCV phenotype (persistent phenotype), cells were repeatedly exposed to 0.1 g/L of nZVI for ten cycles. During tenth cycle, cells were cultivated until mid-log phase before divided into two groups. One group was re-dosed with nZVI; the another group was persistent cells without nZVI exposure. Both groups were further cultivated for one hour before collected and washed once with deionized water to remove the excess nZVI particles. Cells were then lyophilized and submitted for FTIR analysis. One mg of lyophilized sample were mixed with KBr (ratio 1:100) and analyzed by FTIR spectroscopy (Spectrum One, PerkinElmer). FTIR spectra were collected from 400 to 4000 cm^{-1}. The obtained FTIR spectra were exported to cvs files and analyzed using the software Spekwin32 (version 1.72.2).

3.3.6) Statistical analysis

The obtained results from 5.2.3.1, 5.2.3.2 and 5.2.4.1 were statistically analyzed using two-way ANOVA with Tukey's test (GraphPad Prism 6.07 for Windows, GraphPad Software, San Diego California USA, www.graphpad.com). The standard deviation of the data was calculated and presented as error bars.

Chapter 4

Elucidation of effects of reactive and oxidized nZVI on bacterial membrane by proteomic analysis

4.1) Introduction

While nZVI is highly effective for contaminant removal, its extensive *in-situ* application also raises a concern about its environmental impact especially impact on environmental bacteria. It induces oxidative stress, membrane damage and subsequently cell death (Lefevre et al., 2016). However, during the *in-situ* application, the oxidation of nZVI which can occur in both aerobic and anaerobic conditions results in various forms of products including magnetite (Fe_3O_4) and maghemite (γ-Fe_2O_3) (Liu et al., 2014). These iron oxide/hydroxide nanoparticles have typically been reported as non-toxic forms of nZVI as determined by insignificant effect on bacterial viability (Auffan et al., 2008); However, considerable toxicity were observed at high concentration of oxidized nZVI (Auffan et al., 2008).

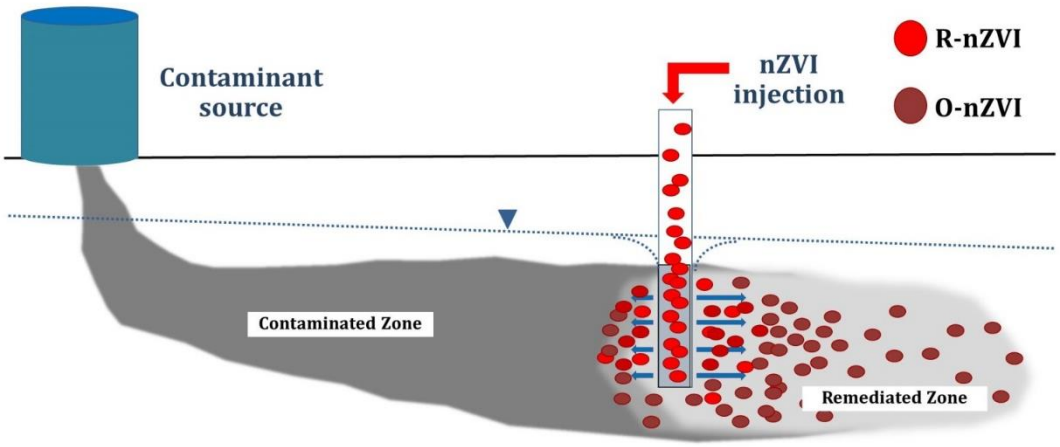

Figure *4.1* Direct injection of reactive nZVI (R-nZVI) to contaminated site. After interact with the contaminants, large amount of the oxidized form of nZVI (O-nZVI) may remain in the environment.

Proteomic analysis is an approach to gain insight in the alteration in bacterial cells upon changing environment. So far, several proteomic analyses of bacterial cells (i.e. *B. cereus* (Fajardo et al., 2013), *P. stutzeri* (Sacca et al., 2014) and *K. oxytoca* (Saccà et al., 2013)) exposed to nZVI have been reported. Bacterial exposure to Nanofer 25S resulted in the down-regulation of membrane-bound proteins including transporter proteins (Sacca et al., 2014) and flagella component (Fajardo et al., 2013), suggesting an important destructive effect of nZVI on bacterial membrane. The up-regulation of oxidative stress response proteins, for instance, catalase (Sacca et al., 2014) and thioredoxin (Fajardo et al., 2013), indicating the nZVI-induced oxidative stress. However, these studies mainly focused on the reactive nZVI (R-nZVI) due to their much higher toxicity, compared to the aged or oxidized form (O-nZVI). While O-nZVI exposure shows no effect on cell viability, adverse effects may be on cell function/activity. Accordingly, a comparative study of bacteria cells treated with two forms of nZVI, R-nZVI and O-nZVI, was conducted. GeLC-MS/MS in which bacterial

protein lysate from each nZVI treatment was separated by SDS-PAGE, followed by gel excision, digestion and analysis by LC-MS/MS was performed to investigate expressed proteins upon bacterial exposure to R-nZVI and O-nZVI. *P. putida* KT2440, an environmental strain with complete genome sequence (Nelson et al., 2002b), was selected as a model bacteria. The susceptibility of Gram positive bacteria, *Bacillus subtilis* 168, to nZVI exposure was also conducted.

4.2) Results and discussion

4.2.1) Effects of R-nZVI and O-nZVI on bacterial viability

The characterization of nZVI before exposure revealed that the Fe^0 content in R-nZVI was 15%, whereas no Fe^0 was detected in O-nZVI. The Fe(II) and Fe(III) contents of R-nZVI were 67% and 38%, respectively. The iron composition of O-nZVI was 71% of Fe(III) and 29% of Fe(II).

R-nZVI particles are redox-active materials and their high toxicity on bacteria has been reported (Lefevre et al., 2016). The toxicity of O-nZVI particles as determined by cell viability is considered low due to their limited reactivity (Auffan et al., 2008). Exposure to 1.0 g/L of R-nZVI decreased viability of *P. putida* KT2440 by almost three orders of magnitude, whereas exposure to 1.0 g/L of O-nZVI resulted in one order of magnitude reduction in cell viability (Figure 4.2A), indicating the considerable toxicity of O-nZVI. Similarly, Auffan et al. (2008) reported the 90% reduction in survival of *E. coli* exposed to 0.7 g/L of magnetite (Fe_3O_4) which is one of an oxidized forms of nZVI (Auffan et al., 2008). This is due to the generated oxidative stress from Fe(II) in Fe_3O_4 (Auffan et al., 2008).

Unfortunately, resuspension of *B. subtilis* 168 in 5 mM carbonate buffer resulted in the steadily decreasing viability over time (Figure 4.2B, control), due to the autolysis of bacterial cells. However, the addition of 1.0 g/L R-nZVI did not affect

cell viability indicating the limited toxicity of R-nZVI on *B. subtilis* cells in this study (Figure 4.2B). According to the limitation of maintaining viability of control *B. subtilis* 168 experiment, the subsequent studies of effect of nZVI on bacterial cells were mainly focused on *P. putida* cells.

4.2.2) Proteomic analysis

The protein patterns of bacterial cells exposed R-nZVI and O-nZVI was shown in Figure 4.3. While the patterns of total protein and soluble protein fraction of cells exposed to either R-nZVI or O-nZVI were not different from those of cells without nZVI exposure, the distinctive smear bands of membrane protein fraction of r-nZVI-treated cells was observed. This may suggests the destructive effect of R-nZVI on bacterial membrane proteins. After SDS-PAGE analysis, protein in each lane was sliced into 15 bands before digested and analyzed by LC-MS/MS.

According to proteomic analysis, the number of proteins from total protein fraction detected in *P. putida* KT2440 cells without nZVI exposure was 3,289. When cells were treated with 1 g/L of R-nZVI, 3,289 proteins were detected, whereas the total detected proteins of cells treated with 1 g/L of O-nZVI were 3367 (Figure 4.4A). Among this, 2,756 proteins were detected in all conditions (i.e. cells treated with R-nZVI or O-nZVI as well as cells without nZVI exposure). In 401 proteins specifically identified as Pseudomonas proteins, 359 of them were found in control experiment, whereas 379 and 371 (Pseudomonas) proteins were detected in cells treated with R-nZVI and O-nZVI, respectively (Figure 4.4B).

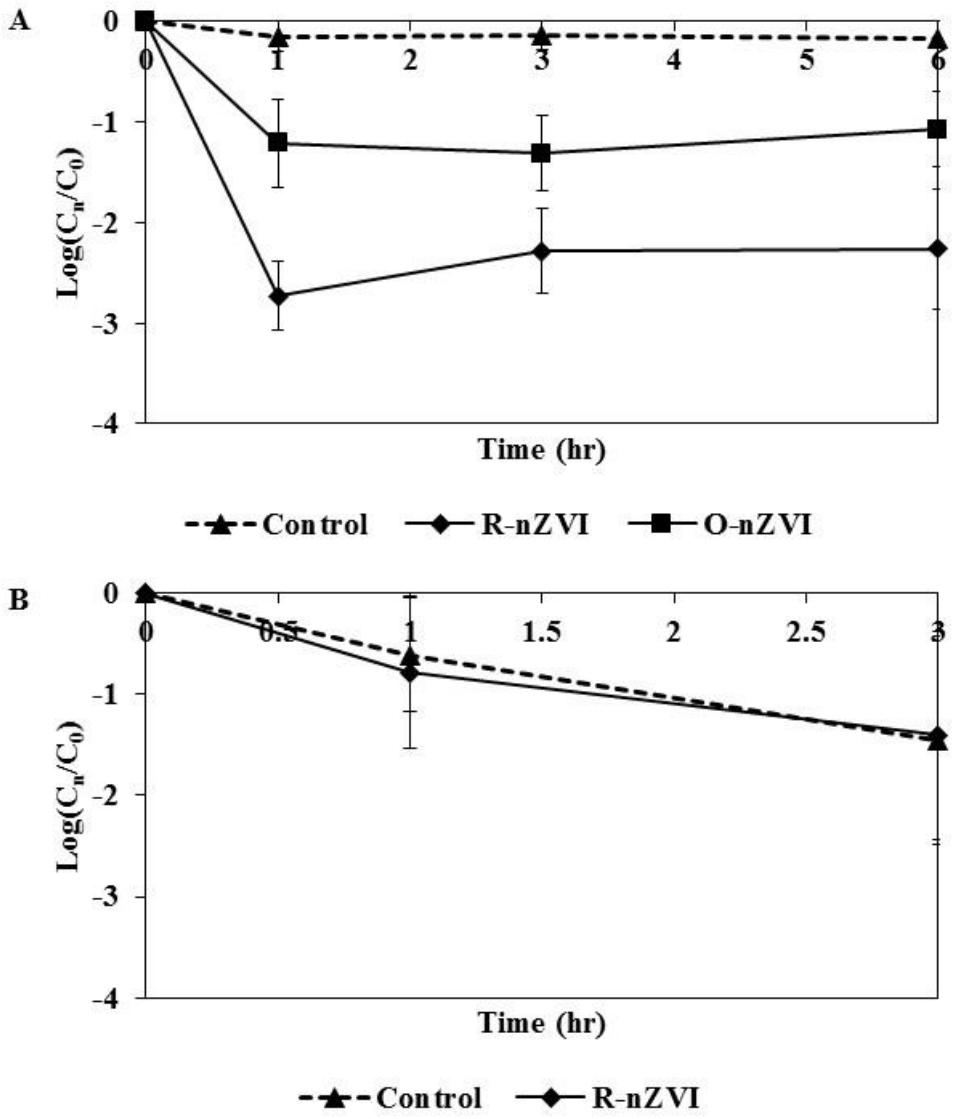

Figure *4.2* Time-dependent effect of nZVI exposure on bacterial viability of (A) P. putida KT2440 and (B) B. subtilis 168. Cells from mid-exponential phase were resuspended in 5 mM carbonate buffer (pH 8.0) before treated with 1.0 g/L of R-nZVI (rectangle symbol) or O-nZVI (diamond symbol). The shown values were calculated from at least three biological replicates.

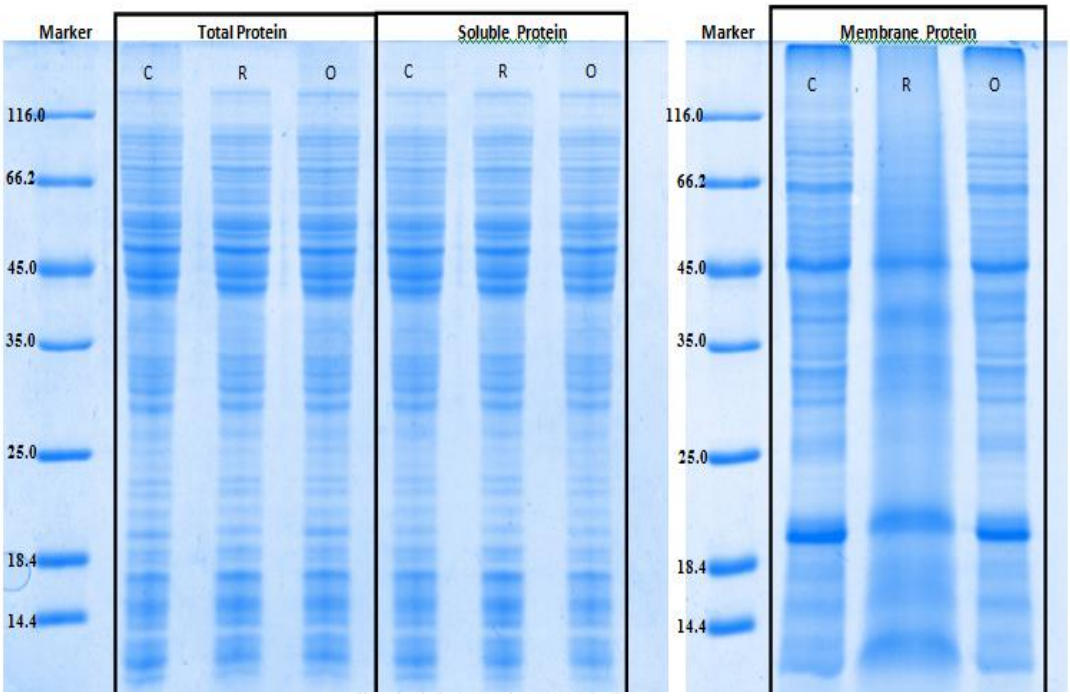

Figure *4.3* Protein profile of *P. putida* KT2440 after R- and O-nZVI exposure. Bacterial cells were exposed to 1 g/L of R- and O-nZVI before extract for total protein solution by sonication. Total protein solutions were subsequent fractionate to obtain soluble and membrane protein solution by ultracentrifuge. Membrane-bound protein was solubilized by SDS buffer. Ten micrograms of each protein solution were analyzed using one-dimensional SDS-PAGE. C, R, O represent control, R-nZVI and O-nZVI, respectively.

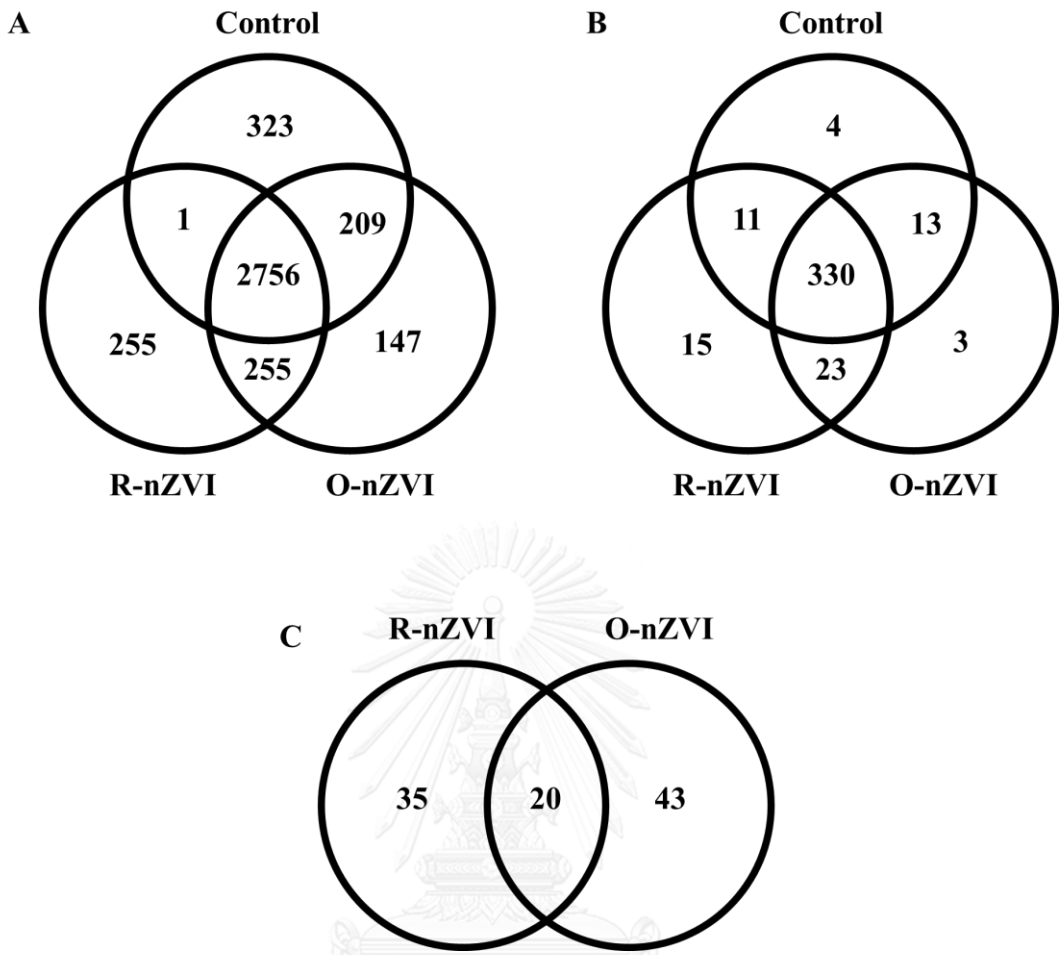

Figure 4.4 Venn diagram illustrating the distribution of identified proteins from P. putida KT2440 cells. (A) Total identified proteins (peptides were searched against the NCBInr database for proteobacteria); (B) Proteins identified as Pseudomonas proteins; and (C) Pseudomonas proteins in cells exposed to R-nZVI or O-nZVI showing altered expression with at least 1.3-fold change, comparing to control which are cells without nZVI exposure.

4.2.2.1 Differentially expressed proteins in P. putida KT2440 cells after exposed to R-nZVI and O-nZVI

Only proteins which belong to Pseudomonas and exhibit a 1.3-fold change were presented and discussed here. The biological functions of the detected proteins were assigned based on Uniprot, KEGG or eggnog database. Among ninety-eight differentially expressed proteins, twenty proteins were found in both cells treated with R-nZVI or O-nZVI (Figure 4.4C). Upon nZVI exposure, the expression of eight proteins which four of them are located at bacterial membrane decreased. These four membrane-bound proteins were inner membrane protein translocase component (YidC), aeroraxis receptor, type IV pilus assembly (PilZ) and NADH dehydrohenase subunit. Eleven proteins were up-regulated in response to both R-nZVI and O-nZVI exposure (Table 4.1).

DsbE is a thioredoxin-domain containing protein involved in bacterial redox homeostasis, as well as lipoprotein biosynthesis. In addition to playing role in maturation of cytochrome c, Dsb protein (sulfide bond forming) is also involved in correct folding of membrane protein (Missiakas and Raina, 1997). Along with other Dsb proteins, DsbE have been reported as important proteins playing roles in bacterial resistance to (redox) metal (e.g. copper) and oxidative stress (Hiniker et al., 2005; Stuart et al., 2013; Teitzel et al., 2006). Peptidylprolyl isomerase (PPIase family protein encoded by *fklB*-2), an enzyme facilitating protein folding in cell membrane (Fischer, 1994), was also up-regulated. Accordingly, proteomic analysis revealed that, regardless of their reactivity, nZVI exposure affected bacterial membrane as indicated by the low abundance of membrane-bound proteins and the up-regulation of proteins involved in bacterial membrane processes. The accumulation of nZVI on bacterial membrane is believed to contribute to nZVI toxicity by interfering the transportation of solutes including nutrients across bacterial membrane (Diao and Yao, 2009c). As a strong electron donor, once interacted with bacterial cells, nZVI

adversely affect their membrane by reducing the phospholipid bilayer as well as bound proteins (Lefevre et al., 2016). Additionally, the disturbance in membrane may further facilitate the internalization of nZVI which could cause the intracellular oxidative stress (Lefevre et al., 2016).

Dihydropyrimidine dehydrogenase was substantially up-regulated by 1.97- and 2.75-fold when cells were treated with R-nZVI and O-nZVI, respectively. This enzyme or NADP-dependent dihydropyrimidine dehydrogenase subunit PreA encoded by *pydA*, is an enzyme in a reductive pathway for pyrimidine degradation (Hidese et al., 2012). Ammonia which is a degradation product of this pathway could serve as nitrogen and carbon source for bacteria (Hidese et al., 2012). The high up-regulation of this protein expression may indicate cell starvation. Carbamate kinase (encoded by *arcC*) is an enzyme in a final step of arginine deiminase, arginine metabolism pathway of which their final products are ammonia, CO_2 and ATP (Dong et al., 2002). The up-regulation of amidase which converts amide, carboxylic acids and

The abundance of succinate dehydrogenase also increased in cells exposed to either R-nZVI or O-nZVI. Succinate dehydrogenase (encoded by *sdhA*) is an enzyme in tricarboxylic acid cycle, catalyzing the synthesis of fumarate from succinate involves in energy production (Benndorf et al., 2006). The generated $FADH_2$ can transfer electron, generating proton gradient thus producing ATP. The higher expression of this protein suggests the elevated demand of energy for energy-dependent nZVI-response mechanisms.

Polynucleotide phosphorylase/polyadenylase (encoded by *pnp*) is an enzyme catalyzing nRNA degradation process. Li et al. (2015) reported the 3- to 10-fold up-regulation of this protein in *P. putida* ND6 exposed to naphthalene, and proposed that the naphthalene-induced high level of polynucleotide phosphorylase/polyadenylase leading to the decreased nucleotide level of naphthalene (Li et al., 2015b).

The interaction between nZVI particles and bacterial membrane is a critical step for nZVI toxicity (Chaithawiwat et al., 2016a; Lefevre et al., 2016). Despite extensive graphical evidence revealing the interaction between nZVI and bacterial cells (Auffan et al., 2008; Fajardo et al., 2013; Lee et al., 2008a; Sacca et al., 2014), studies on nZVI-induced membrane damage are limited. Similar to our observation, the exposure of *P. stutzeri* to 5 g/L of nZVI (Nanofer 25S) significantly affects the abundance of membrane-bound proteins especially transporter proteins (Sacca et al., 2014), while the down-regulation of proteins involved in cell motility and peptidoglycan biosynthesis was observed in nZVI-treated *B. cereus* (Fajardo et al., 2013).

During in-situ injection of nZVI, nZVI particles rapidly aggregate and settle (Phenrat et al., 2007), resulting in high concentration of nZVI particles accumulated around injection point and limited contaminant removal efficiency (Vecchia et al., 2009). This suggested the potential of severe damage on surrounding microorganisms. Several approaches have been reported to enhance the colloidal stability of nZVI, thus increasing their mobility throughout the contaminated sites (Laumann et al., 2014; Phenrat et al., 2009a; Saleh et al., 2008; Vecchia et al., 2009). The greater traveling distance may also increases chance of indigenous bacteria getting contacted with migrated nZVI (Stefaniuk et al., 2016).

In addition to membrane damage, bacterial exposure to either R-nZVI or O-nZVI results in the altered expressions of proteins involved in protein biosynthesis indicating the nZVI-induced protein damage.

Table 4.1 Expressed proteins in *P. putida* KT2440 cells after exposed to R-nZVI and O-nZVI

Protein	**ID Details**	**TR/ TC**[a]	**TO/ TC**[b]	**Subcellular location**[c]	**Function**[d]
gi|26986751	putative inner membrane protein translocase component YidC [*Pseudomonas putida* KT2440]	0.75	0.31	CM	M
gi|26988588	elongation factor P [*Pseudomonas putida* KT2440]	0.59	0.35	C	J
gi|71733714	histone deacetylase [*Pseudomonas syringae* pv. Phaseolicola 1448A]	0.44	0.50	C	B Q
gi|26988981	aerotaxis receptor [*Pseudomonas putida* KT2440]	0.58	0.54	CM	N
gi|26991326	type IV pilus assembly PilZ [*Pseudomonas putida* KT2440]	0.76	0.68	CM	N W
gi|148547037	phenylhydantoinase [*Pseudomonas putida* F1]	0.70	0.72	C	S
gi|26990820	NADH dehydrogenase subunit I [*Pseudomonas putida* KT2440]	0.69	0.72	CM	C
gi|148545524	phosphoenolpyruvate carboxykinase [*Pseudomonas putida* F1]	0.73	0.73	C	G
gi|77457348	phosphopyruvate hydratase [*Pseudomonas fluorescens* Pf0-1]	1.34	0.77	C/CM	G
gi|26991554	50S ribosomal protein L9 [*Pseudomonas putida* KT2440]	1.32	1.30	C	J
gi|313110692	linear gramicidin synthetase subunit D [*Pseudomonas aeruginosa* 39016]	1.64	1.32	U	S
gi|170721726	amidase [*Pseudomonas putida* W619]	1.37	1.34	C	S
gi|26990883	succinate dehydrogenase flavoprotein subunit [*Pseudomonas putida* KT2440]	1.32	1.35	CM	C G
gi|330982087	conjugal transfer coupling protein TraG [*Pseudomonas syringae* pv. Aptata str. DSM 50252]	1.30	1.36	U	S

gi|26987735	carbamate kinase [*Pseudomonas putida* KT2440]	1.41	1.42	C	E
gi|325276169	polynucleotide phosphorylase/polyadenylase [*Pseudomonas* sp. TJI-51]	1.32	1.46	C	F
gi|26988446	FKBP-type peptidylprolyl isomerase [*Pseudomonas putida* KT2440]	1.41	1.61	C	O
gi|289677441	regulatory protein, GntR [*Pseudomonas syringae* pv. Syringae FF5]	1.35	1.71	C	E K
gi|312962225	thiol:disulfide interchange protein DsbE [*Pseudomonas fluorescens* WH6]	1.35	1.82	CM	C O
gi|26990740	dihydropyrimidine dehydrogenase [*Pseudomonas putida* KT2440]	1.97	2.75	C	F C

[a] Fold change of differentially expressed proteins in cells treated with 0.1 g/L of R-nZVI in comparison to cells without nZVI exposure

[b] Fold change of differentially expressed proteins in cells treated with 0.1 g/L of O-nZVI in comparison to cells without nZVI exposure

[c] Subcellular localization: C, Cytoplasmic; CM, Cytoplasmic membrane; OM, Outer membrane; T, Transmembrane; U; Unknown

[d] The abbreviations represent the classification of the Cluster of Orthologous Groups (COG) categories: Un: No related COGs and hypothetical proteins, C: Energy production and conversion, D: cell division and chromosome partitioning, E: Amino acid transport and metabolism, F: Nucleotide transport and metabolism, G: Carbohydrate transport and metabolism, H: Coenzyme metabolism, I: Lipid metabolism, J: translation, ribosomal structure and biogenesis, K: Transcription, L:DNA replication, recombination and repair, M: Cell envelope biogenesis, outer membrane, N: cell motility and secretion, O: post translational modification, protein turnover, chaperones, P: inorganic ion transport and metabolism, Q: secondary metabolites biosynthesis, transport and catabolism, R: general function prediction only, S: function unknown, T: signal transduction mechanisms, U: Intracellular trafficking, secretion and vesicular transport

4.2.2.2 Differentially expressed proteins only in cells exposed to R-nZVI

Thirty five proteins were expressed only in cells exposed to R-nZVI, comparing to cells without nZVI exposure (Figure 4.4C). The expressions of twenty two proteins were down-regulated, of which the altered expressions of five proteins were more than 1.5-fold change (Table 4.2). Bacterial exposure to R-nZVI resulted in the reduced protein biosynthesis since proteins related amino acid biosynthesis and translation process are among the major down-regulated proteins.

While nZVI-induced oxidative stress has been proposed as a main nZVI toxicity mechanism and the presence of antioxidant enzyme is essential for cell viability (Auffan et al., 2008; Chaithawiwat et al., 2016b), the down-regulation of catalase, an antioxidant enzyme, was observed in cell treated with R-nZVI (Table 2). Fajardo et al. (2013) proposed that the insignificant level of catalase upon the exposure of *Bacillus* cereus to nZVI may indicate that the ROS other than H_2O_2 played a role in nZVI toxicity (Fajardo et al., 2013). The abundance of catalase depends on the concentration of H_2O_2 as well as the exposure time (Chaithawiwat et al., 2016b).

The decreased abundance of proteins involved in energy production were also observed (Table 2). Isocitrate dehydrogenase is an enzyme in TCA cycle catalyzing the conversion of isocitrate to **α**-ketoglutarate, generating NADH and CO_2. Dihydrolipoamide acetyltransferase (*aceF*) is a component in pyruvate dehydrogenase complex catalyzing the conversion of pyruvate to acetyl-coA (de Kok et al., 1998); Acetyl-coA which could also be generated from acetate by Acetyl-coA synthetase, will enter TCA cycle. The generated NADH from TCA cycle passes electron to the electron transport chain, generating energy. The down-regulation of NADH dehydrogenase which is a membrane-bound component that shuttles electron from NADH was also observed.

Bacterial exposure to R-nZVI resulted in the up-regulation of 13 proteins (Table 4.2). Interestingly, eight of the up-regulated proteins are membrane-located proteins, contributing to the transportation of solute across membrane. Rare lipoprotein B (encoded by *lptE*), a protein important for lipopolysaccharide assembly, was also up-regulated. In contrast to previously mentioned enzymes in TCA cycle, fumarate hydratase or fumarase, an enzyme catalyzing the conversion of fumarate to malate in TCA cycle, was up-regulated upon R-nZVI exposure.

Several proteins involved TCA cycles, for example, succinate dehydrogenase, aconitase and fumarase (*fumA*), are target for oxidative attack due to the presence of iron-sulfur which is prone to oxidation (Chenier et al., 2008). In contrast to fumarase (*fumA*), the up-regulation of *fumC*, which encodes for iron-independent fumarase, is induced by the exposure to superoxide (Park et al., 2006). In *E. coli*, the expression of *fumC* is regulated by soxRS regulon. The oxidation at [2Fe-S2] cluster of SoxR, for example, by H_2O_2 exposure, induces the expression of soxS (encoding for SoxS protein), which SoxS further control the expression of genes related to oxidative stress response (Kim and Park, 2014). The exposure of *P. putida* KT2440 to superoxide induced the expression of *fumC* but independent of SoxR (Park et al., 2006). However, in this study, the dramatic up-regulation of fumarase encoded by *fumA* (1.74-fold change) in cells treated with R-nZVI was observed. Even though, the down-regulation of proteins involves in TCA cycle suggests the effect of R-nZVI-induced oxidative stress, the reason of the up-regulated fumarase encoded by *fumA* is still unclear.

Dihydrodipicolinate reductase (*dapB*) is an NADH/NADPH-dependent enzyme in lysine biosynthesis via the Diaminopimelate pathway (DAP) (Cox, 1996). Lysine is essential for protein synthesis (Cox, 1996; Hutton et al., 2007). Besides, lysine and *meso*-diaminopimelate (*meso*-DAP), which is an intermediate of the DAP pathway, are necessary for bacterial peptidoglycan synthesis (Cox, 1996; Hutton et al., 2007).

Both two subunits of glycine-tRNA ligase (*glyS* and *glyQ*) or glycyl-tRNA synthetase were also down-regulated in cells treated with R-nZVI. Aminoacyl-tRNA synthetases are enzymes that match tRNA to the corresponding amino acids (Ling et al., 2009). The obtained aminoacyl-tRNA is further delivered to the ribosome for translation process (peptide synthesis) by elongation factor TU (Ling et al., 2009). The down regulation of this protein may suggest the reduced protein synthesis efficiency since this protein plays role in protein translation fidelity.

Table 4.2 Expressed proteins only in *P. putida* KT2440 cells exposed to R-nZVI

Protein	ID Details	TR/TC[a]	Subcellular location[b]	Function[c]
gi|76556191	RNA polymerase beta subunit [*Pseudomonas avellanae*]	0.43	C	K
gi|26986805	**Glycine—tRNA ligase beta subunit** [*Pseudomonas putida* KT2440]	0.59	C	E J
gi|26987139	serine protein kinase PrkA [*Pseudomonas putida* KT2440]	0.59	C	T
gi|26991408	dihydrodipicolinate reductase [*Pseudomonas putida* KT2440]	0.59	C	E
gi|26989191	50S ribosomal protein L20 [*Pseudomonas putida* KT2440]	0.63	C	J
gi|26990716	isocitrate dehydrogenase [*Pseudomonas putida* Kt2440]	0.68	U	C
gi|26986806	Glycine—tRNA ligase alpha subunit [*Pseudomonas putida* KT2440]	0.69	C	E J
gi|26987190	30S ribosomal protein S12 [*Pseudomonas putida* KT2440]	0.69	C	J
gi|26987921	two-component response regulator PhoP [*Pseudomonas putida* KT2440]	0.69	C	T
gi|26990379	catalase/peroxidase HPI [*Pseudomonas putida* KT2440]	0.73	C	P
gi|26991173	acetyl-CoA synthetase [*Pseudomonas putida* KT2440]	0.73	C	I
gi|26988529	GDP-mannose 4,6-dehydratase [*Pseudomonas putida* KT2440]	0.74	C	M
gi|66047582	hypothetical protein [*Pseudomonas syringae* pv. Syringae B728a]	0.74	T	Un
gi|26987220	DNA-directed RNA polymerase subunit alpha [*Pseudomonas putida* KT2440]	0.75	C	K
gi|26991204	TolC family type I secretion outer membrane protein [*Pseudomonas putida* Kt2440]	0.75	OM	M
gi|104782526	NADH dehydrogenase subunit G [*Pseudomonas entomophila* L48]	0.76	CM	C

gi|26987080	dihydrolipoamide acetyltransferase [*Pseudomonas putida* KT2440]	0.76	C	C
gi|148549015	ribonuclease [*Pseudomonas putida* F1]	0.76	C	K
gi|26988805	NAD-glutamate dehydrogenase [*Pseudomonas putida* KT2440]	0.76	CM	S
gi|26991411	heat shock protein GrpE [*Pseudomonas putida* KT2440]	0.77	C	O
gi|146306187	ABC transporter-like protein [*Pseudomonas mendocina* ymp]	0.77	CM	G
gi|26991172	cationic amino acid ABC transporter periplasmic binding protein [*Pseudomonas putida* KT2440]	0.77	CM	E
gi|26991855	spermidine/putrescine ABC transporter ATPase [*Pseudomonas putida* KT2440]	1.30	CM	E
gi|26987211	50S ribosomal protein L18 [*Pseudomonas putida* KT2440]	1.31	C	J
gi|148546410	17 kDa surface antigen [*Pseudomonas putida* F1]	1.32	OM	S
gi|229589165	phosphoserine aminotransferase [*Pseudomonas fluorescens* SBW25]	1.32	C	E
gi|330966208	hypothetical protein PSYAC_16496 [*Pseudomonas syringae* pv. Actinidiae str. M302091]	1.35	U	Un
gi|26991882	secretion protein HlyD family protein [*Pseudomonas putida* KT2440]	1.36	CM	U
gi|28868589	type III helper protein HrpA1 [*Pseudomonas syringae* pv. Tomato str. DC3000] pili	1.37	C/E	S
gi|26988518	hypothetical protein [*Pseudomonas putida* KT2440]	1.40	U	Un
gi|229592159	histidine transport ATP-binding protein [*Pseudomonas fluorescens* SBW25]	1.41	CM	E
gi|26987912	ribonucleotide-diphosphate reductase subunit beta	1.42	C	F

	[*Pseudomonas putida* KT2440]			
gi|26991475	rare lipoprotein B [*Pseudomonas putida* KT2440]	1.47	OM	M
gi|26987633	Fe-S type, tartrate/fumarate subfamily hydro-lyase subunit alpha [*Pseudomonas putida* KT2440]	1.74	C	C
gi|26991353	OmpA/MotB domain-containing protein [*Pseudomonas putida* KT2440]	1.87	OM	M

[a] Fold change of differentially expressed proteins in cells treated with 0.1 g/L of R-nZVI in comparison to cells without nZVI exposure

[b] Subcellular localization: C, Cytoplasmic; CM, Cytoplasmic membrane; OM, Outer membrane; T, Transmembrane; U; Unknown

c The abbreviations represent the classification of the Cluster of Orthologous Groups (COG) categories: Un: No related COGs and hypothetical proteins, C: Energy production and conversion, D: cell division and chromosome partitioning, E: Amino acid transport and metabolism, F: Nucleotide transport and metabolism, G: Carbohydrate transport and metabolism, H: Coenzyme metabolism, I: Lipid metabolism, J: translation, ribosomal structure and biogenesis, K: Transcription, L:DNA replication, recombination and repair, M: Cell envelope biogenesis, outer membrane, N: cell motility and secretion, O: post translational modification, protein turnover, chaperones, P: inorganic ion transport and metabolism, Q: secondary metabolites biosynthesis, transport and catabolism, R: general function prediction only, S: function unknown, T: signal transduction mechanisms, U: Intracellular trafficking, secretion and vesicular transport

4.2.2.3 Differentially expressed proteins only in cells exposed to O-nZVI

Forty three proteins were expressed only in cells exposed to O-nZVI, (compared to cells without nZVI exposure); eleven of them showed a fold-change ≥ 1.5. Three of the expressed proteins were identified as hypothetical protein with unknown function. The abundance of eleven proteins decreased in cells treated with O-nZVI (Table 4.3). Bacterial exposure to O-nZVI caused the up-regulation of thirty-two proteins.

Similar to cells treated with R-nZVI, the expressions of proteins involved in protein biosynthesis were markedly affected by O-nZVI; three proteins were down-regulated and ten proteins were up-regulated. All the down-regulated proteins were ribosomal subunit proteins; the up-regulated proteins included proteins involved in amino acid biosynthesis and transportation, and translation process. This results suggested the notable effect of O-nZVI exposure on bacterial protein biosynthesis process.

The bacterial stress response proteins namely DnaJ and cold shock protein are among down-regulated proteins. However, exposure to O-nZVI increased the expression of heat shock protein 33 (Hsp33). Hsp33 is a cytoplasmic chaperone rapidly acts on the oxidatively damaged proteins, preventing their aggregation (Ruddock and Klappa, 1999). Since this protein functions in ATP-independent manner, it has been proposed that this protein acts as an urgent response by binding to oxidized protein until the suitable redox potential is restored and that other ATP-dependent chaperone proteins can function (Ruddock and Klappa, 1999).

Beside the down-regulation of beta-ketothiolase, an enzyme catalyzing the conversion of acetoacetyl-coA to acetyl-coA, six other proteins related to energy production which are subunit of F0F1 ATP synthase, alcohol dehydrogenase, carbohydrate kinase, dihydrolipoamide acetyltransferase, succinate dehydrogenase and glucose-6-phosphate isomerase were up-regulated. The expression of glucose-6-

phosphate isomerase increased by 2.17 fold compared to cells without nZVI treatment. This enzyme is an important enzyme connecting the different pathways for glucose metabolism by interconverting the glucose-6-phosphate and fructose-6-phosphate (Dos Santos et al., 2004). The addition of Fe(III) has been reported to increase the activity of this enzyme (Yoon et al., 2009).

Two proteins involved in bacterial cell wall biosynthesis were up-regulated. The expression of glucose-1-phosphate thymidilyltransferase increased by 1.58-fold, compared to cells without nZVI treatment. This enzyme catalyzes the first step of deoxy-thymidine di-phosphate (dTDP)–L-rhamnose biosynthesis, which is the precursor of L-rhamnose, a main component of bacterial lipopolysaccharide (Blankenfeldt et al., 2000). The up-regulation of D-ala-D-ala-carboxypeptidase expression with 1.37-fold change was observed. This enzyme is for peptidoglycan biosynthesis and its role in bacterial response to several stresses including metal toxicity has been reported (Príncipe et al., 2009).

Exposure to O-nZVI also caused the notably alteration in the expression of proteins involved in nucleotide, DNA biological processes (Table 4.3). These proteins include DNA-directed RNA polymerase, DNA polymerase II, adenylsuccinate lyase, phosphoribosylglycinamide formyltransferase, RNA polymerase sigma factor (RpoD) and ribonucleotide-diphosphate reductase. DNA-directed PNA polymerase or RpoB catalyzes the RNA synthesis from DNA template of which important for ribosome biosynthesis, whereas ribonucleotide-diphosphate reductase catalyzes the formation of deoxyribonucleotides which is further used in DNA synthesis. DNA polymerase II (Pol-II encoded by *polB*) is an enzyme involved in DNA replication. This enzyme is a part of SOS regulon functioning in response to DNA damage. However, the up-regulation of Pol-II has been reported to enhance the spontaneous untargeted mutagenesis in *E. coli* cells (Al Mamun, 2007).

Adenylosuccinate lyase (ASL) is an enzyme in purine biosynthesis pathway which is important for cell replication. In addition, this enzyme also involved in cellular metabolism since fumarate which is the product from ASL-catalyzed purine biosynthesis is the intermediate of TCA cycles (Tsai et al., 2007). The up-regulation of succinate dehydrogenase, an enzyme catalyzing the conversion of succinate to fumarate, potentially enhances the amount of fumarate (Table 4.3). Fumarate can be further converted oxaloacetate and citrate which can acts a metal chelation thus reducing metal toxicity (Auger et al., 2016; Auger et al., 2013). However, the up-regulation of enzymes, for example, fumarase, malate dehydrogenase or citrate synthase was not observed in this study.

While the exposure caused the notably adverse effect, as determined by the decreased abundance, on proteins involved in energy transduction and protein biosynthesis processes (Table 4.2), bacterial exposure to O-nZVI induced the up-regulation of proteins in response to occurred damages which are chaperone protein, bacterial cell wall modification and enhanced protein biosynthesis (Table 4.3). In addition, the effect of O-nZVI on nucleotide biological processes was also observed.

Table 4.3 Expressed proteins only in *P. putida* KT2440 cells exposed to O-nZVI

Protein	ID Details	TO/TC[a]	Subcellular location[b]	Function[c]
gi|26990459	beta-ketothiolase [*Pseudomonas putida* KT2440]	0.60	C	I
gi|26987185	50S ribosomal protein L1 [*Pseudomonas putida* KT2440]	0.62	C	J
gi|71737742	DnaJ domain-containing protein [*Pseudomonas syringae* pv. Phaseolicola 1448A]	0.69	T	O
gi|237799979	type III effector protein AvrE1 [*Pseudomonas syringae* pv. Oryzae str. 1_6]	0.70	U	S
gi|26991732	phosphoglyceromutase [*Pseudomonas putida* KT2440]	0.72	C	G
gi|26987191	30S ribosomal protein S7 [*Pseudomonas putida* KT2440]	0.73	C	J
gi|325273007	hypothetical protein G1E_08484 [*Pseudomonas* sp. TJI-51]	0.74	CM	Un
gi|26987867	hypothetical protein [*Pseudomonas putida* KT2440] slyB	0.75	OM	M
gi|26990715	Cold shock protein (cspD gene product) [*Pseudomonas putida* KT2440]	0.75	C	K O
gi|26987410	ABC transporter ATP-binding protein [*Pseudomonas putida* KT2440]	0.76	C	S
gi|26987187	50S ribosomal protein L7/L12 [*Pseudomonas putida* KT2440]	0.77	U	J
gi|66044828	cysteine synthase [*Pseudomonas syringae* pv. Syringae B728a]	1.30	C	E
gi|26992092	F0F1 ATP synthase subunit B [*Pseudomonas putida* KT2440]	1.30	CM	C
gi|26987189	DNA-directed RNA polymerase subunit beta' [*Pseudomonas putida* KT2440]	1.30	C	K
gi|26988602	aminotransferase AlaT [*Pseudomonas putida* KT2440]	1.30	C	E
gi|146282579	ribosomal RNA large subunit methyltransferase N [*Pseudomonas stutzeri* A1501]	1.31	C	J

gi|104782409	DNA polymerase II [*Pseudomonas entomophila* L48]	1.31	C	L
gi|26987194	30S ribosomal protein S10 [*Pseudomonas putida* KT2440]	1.32	C	J
gi|15600220	hypothetical protein [*Pseudomonas aeruginosa* PAO1]	1.32	C	Un
gi|26990544	Short chain alcohol dehydrogenase (adhA gene product) [*Pseudomonas putida* KT2440]	1.32	C	C
gi|320324638	ABC transporter protein, ATP binding component [*Pseudomonas syringae* pv. Glycinea str. B076]	1.32	U	M
gi|15598775	carbohydrate kinase [*Pseudomonas aeruginosa* PAO1]	1.33	C	C
gi|26987194	30S ribosomal protein S10 [*Pseudomonas putida* KT2440]	1.34	C	J
gi|15600209	dihydrolipoamide acetyltransferase [*Pseudomonas aeruginosa* PAO1]	1.35	C	C
gi|26990721	adenylosuccinate lyase [*Pseudomonas putida* KT2440]	1.35	U	F
gi|26988190	phosphoribosylglycinamide formyltransferase [*Pseudomonas putida* KT2440]	1.35	U	F
gi|146305738	urea amidolyase-like protein [*Pseudomonas mendocina* ymp]	1.36	U	I, E
gi|70733546	hypothetical protein PFL_0033 [*Pseudomonas protegens* Pf-5]	1.36	C	Un
gi|26991483	D-ala-D-ala-carboxypeptidase [*Pseudomonas putida* KT2440]	1.37	U	M
gi|26988035	general amino acid ABC transporter ATP-binding protein [*Pseudomonas putida* KT2440]	1.39	U	E
gi|257484336	achromobactin transport system permease protein CbrC [*Pseudomonas syringae* pv. Tabaci str. ATCC 11528]	1.41	U	Un
gi|26987129	RNA polymerase sigma factor RpoD	1.42	C	K

	[*Pseudomonas putida* KT2440]			
gi|148545739	50S ribosomal protein L3 [*Pseudomonas putida* F1]	1.43	C	J
gi|26987914	ribonucleotide-diphosphate reductase subunit alpha [*Pseudomonas putida* KT2440]	1.44	C	F
gi|26988494	short chain dehydrogenase (*ycik* gene product) [*Pseudomonas putida* KT2440]	1.57	C	S
gi|26988514	glucose-1-phosphate thymidylyltransferase [*Pseudomonas putida* KT2440]	1.58	U	M
gi|330984350	elongation factor Tu [*Pseudomonas syringae* pv. Lachrymans str. M301315]	1.60	C	J
gi|26986995	heat shock protein 33 [*Pseudomonas putida* KT2440]	1.63	C	O
gi|152984128	hypothetical protein PSPA7_2835 [*Pseudomonas aeruginosa* PA7]	1.63	U	Un
gi|26990882	succinate dehydrogenase iron-sulfur subunit [*Pseudomonas putida* KT2440]	1.81	U	C
gi|26991722	Glutamine synthetase [*Pseudomonas putida* KT2440]	1.93	C	E
gi|26991385	glucose-6-phosphate isomerase [*Pseudomonas putida* KT2440]	2.17	C	G
gi|26988026	PhoH family protein [*Pseudomonas putida* KT2440]	2.76	C	E

[a] Fold change of differentially expressed proteins in cells treated with 0.1 g/L of O-nZVI in comparison to cells without nZVI exposure

[b] Subcellular localization: C, Cytoplasmic; CM, Cytoplasmic membrane; OM, Outer membrane; T, Transmembrane; U; Unknown

[c] The abbreviations represent the classification of the Cluster of Orthologous Groups (COG) categories: Un: No related COGs and hypothetical proteins, C: Energy production and conversion, D: cell division and chromosome partitioning, E: Amino acid transport and metabolism, F: Nucleotide transport and metabolism, G: Carbohydrate transport and metabolism, H: Coenzyme metabolism, I: Lipid metabolism, J: translation, ribosomal structure and biogenesis, K: Transcription, L:DNA replication, recombination and repair, M: Cell envelope biogenesis, outer membrane, N: cell motility and secretion, O: post translational modification, protein turnover, chaperones, P: inorganic ion transport and metabolism, Q: secondary metabolites biosynthesis, transport and catabolism, R:

general function prediction only, S: function unknown, T: signal transduction mechanisms, U: Intracellular trafficking, secretion and vesicular transport

4.3) Summary

When fresh or R-nZVI particles are injected to the contaminated site, they can readily interact with various chemicals including the contaminants and remain in the oxidized form (O-nZVI) in the environment. Bacterial exposure to 1.0 g/L of R-nZVI resulted in the three-order of magnitude reduction in the viability of *P. putida* KT2440, an environmental bacterium. Bacterial exposure to 1.0 g/L of O-nZVI which mainly consists of Fe(III) decreased cell viability by one-order of magnitude. Proteomic analysis of cell treated with nZVI revealed that both forms of nZVI extensively damage bacterial membrane particularly membrane-bound proteins as indicated by the low abundance of membrane proteins, compared to cell without nZVI exposure. Proteins related to bacterial protein biosynthesis were highly affected by nZVI exposure. These proteins include proteins in amino acid biosynthesis pathway, ribosomal subunit and elongation factor which involved in translation process. The up-regulation of proteins playing role in folding of membrane proteins accentuates the potential of nZVI-induced damage on membrane-bound proteins. Oxidative stress has been reported as a major mechanism of nZVI toxicity, this could explain the down-regulation of proteins involved TCA cycles upon bacterial exposure to R-nZVI. However, the evidence for antioxidant enzyme was not observed. During their *in-situ* injection, nZVI particles tend to aggregate around injection point. The notable nZVI toxicity likely limited to bacteria surrounding injection since the contact between nZVI particles and bacterial cells is important for nZVI toxicity. However, the migration of nZVI may poses damage on bacteria residing in distant area from injection point. The recovery of O-nZVI following *in-situ* remediation should be taken

into concern since the contact with O-nZVI can also cause a considerable damage to bacterial cells.

Chapter 5

Bacterial response to short-term and repetitive nZVI exposure: Modification in bacterial membrane

5.1) Introduction

For *in situ* application of nZVI, iron nanoparticles have been introduced to the contaminated sites using various strategies, for instance, single direct injection, re-circulation of nZVI-amended groundwater with nZVI re-dosing or multiple-time injection of nZVI (Grieger et al., 2010; Henn and Waddill, 2006; Singh and Bose, 2015) as well as construction of nZVI-containing reactive permeable wall. In order to maintain the efficacy of heavy metal immobilization, nZVI re-dosing has also been proposed (Su et al., 2014). The nZVI re-dosing if practiced will likely result in an extensive amount of nZVI released into and retained in the environment leading to a concern on potential impact on organisms.

Nanoscale zero valent iron particles were reported to cause adverse effects to microorganisms, aquatic organisms, terrestrial organisms, and mammalian cells (Stefaniuk et al., 2016). Focusing on microorganisms which are the key players in many environmental processes and prone to environmental changes, the level of nZVI toxicity ranges from altering bacterial activities (Jiang et al., 2015; Kumar et al., 2014; Velimirovic et al., 2015) to the reduction in cell viability (Auffan et al., 2008; Diao and Yao, 2009c; Kim et al., 2010; Lee et al., 2008a). Oxidative stress largely contributes to nZVI toxicity in microorganisms. Fe^0 in nZVI particle can directly transfer electron to the oxygen molecule generating hydrogen peroxide (Auffan et al., 2008). The oxidized forms of Fe^0, Fe(II) and Fe(III) species, can further interact with hydrogen peroxide, generating more reactive oxygen species (ROS) which can attack bacterial biomolecules such as DNA, proteins and lipids (Sevcu et al., 2011).

In addition to nZVI-induced oxidative stress, the interaction between bacterial membrane and the iron particles also remarkably attributed to nZVI toxicity on microorganisms and membrane is believed to be a critical step of nZVI toxicity (Chaithawiwat et al., 2016a; Chen et al., 2011b; Lefevre et al., 2016; Li et al., 2010; Popova et al., 2008). Bacterial cytoplasmic membrane, a phospholipid bilayer with embedded protein, serves as a protective layer for cell and provides a site for many cellular processes. During nZVI exposure, iron nanoparticles tend to attach to bacterial membrane, disrupting membrane composition, interfering membrane functionality and promoting the iron-induced intracellular oxidative stress (Lefevre et al., 2016). Sacca et al. reported the down-regulation of the membrane-bound nitrite reductase indicating the susceptibility of membrane-bound protein to nZVI attack (Sacca et al., 2014). The same study revealed the up-regulation of δ-aminolevulinic acid dehydratase after nZVI exposure, suggesting the higher production of heme group which could reduce hydrogen peroxide as well as scavenge the excess intracellular iron (Sacca et al., 2014). Chaithawiwat et al. reported that while a suspension of 1 g/L of nZVI reduced the number of *E. coli* JM109 by 90%, the filtrate of the suspension did not significantly affect bacterial viability (Chaithawiwat et al., 2016a). This observation accentuates the significance of nZVI-membrane interaction in the toxicity mechanism.

Previous studies on nZVI toxicity focused on the batch-based effect of nZVI (Jang et al., 2014; Lefevre et al., 2016). Some nZVI application strategies and the proposed nZVI re-dosing if practiced will likely result in repetitive exposure patterns. Repetitive exposure of organisms to stress may strengthen them through the adaptation while the cumulative effect may weaken them (Reinert et al., 2002; Simonin et al., 2016; Simonin and Richaume, 2015). So far, there has been only one report on the effect of sequential exposure of nZVI on bacteria. Ma et al. studied the effect of sequentially increased concentration of nanoparticles, including nZVI, on

microbial community, but no significant impact was found due to the aggregation of nZVI (Ma et al., 2015).

Due to the limited information regarding the exposure pattern of environmental bacteria to nZVI, herein, the effect of repetitive nZVI exposure was investigated. Susceptibility of bacterial cells to batch and repetitive exposure to nZVI was compared. Despite substantial studies regarding nZVI-mediated membrane damages, bacterial ability to adapt themselves to membrane damage is still unclear. Bacterial membrane is a dynamic layer capable to quantitatively and/or qualitatively adjust their compositions e.g. fatty acids, phospholipid headgroups, or membrane proteins in response to the disturbance in membrane layer (Murinova and Dercova, 2014; Zhang and Rock, 2008). This study evaluates the changes in fatty acid profile as well as phospholipid headgroup of bacterial membrane exposed to nZVI. Membrane fluidity which is a biophysical property associated with the composition of bacterial membrane and important for bacterial survival (Murinova and Dercova, 2014) was also investigated. *P. putida* F1, which is a degrader for several contaminants including toluene and trichloroethylene(Wackett and Gibson, 1988) was selected as a model strain.

5.2) Results and discussion

5.2.1) nZVI characteristics

The toxicity of nanoparticles is known to depend on their physicochemical properties including size (Raghupathi et al., 2011), surface properties, and the reactivity of the particles (Phenrat et al., 2009c), which are influenced by the environmental matrix. While the primary size of pristine nZVI is in a nanometer range, nZVI particles can react and/or interact with environmental constituents such as Ca^{2+}, resulting in rapid aggregation in natural water (i.e. groundwater and seawater) and

formation of micro-sized aggregates during *in situ* applications (Adeleye et al., 2013; Keller et al., 2012). The nanoparticle aggregates were reported to cause lower toxicity than the pristine nanoparticles due to their lower reactive surface area for interaction (Lowry et al., 2012). In this study, in order to diminish the complexity from the organic matter in the biological medium, M9G medium was selected. Based on the dynamic light scattering, Nanofer 25S resuspended in M9G medium gave a z-average hydrodynamic size of 5,064 ± 308 nm and polydispersity index of 0.52 ± 0.05, indicating the broad-size aggregation of iron nanoparticles in M9G medium.

Considering the length of exposure time, the Fe^0 and Fe(II) contents, which are mainly accountable for nZVI reactivity, were investigated. Prior to the exposure, the main iron species of Nanofer 25S was Fe(II) which contributed to 52.4 ± 1.4% of total iron, whereas Fe^0 and Fe(III) contents were 29.3 ± 3.0% and 18.3 ± 1.6%, respectively (Figure 5.1). After one hour of exposure, Fe(III) became the major iron species which contributed to 95.6 ± 0.48%, while Fe(II) decreased to 4.4 ± 0.48 and no Fe^0 was detected. This indicates that the reactive time of Nanofer 25S in this study is considerably short, compared to the reported 2-hour lifetime of nZVI under aerobic condition(Li et al., 2010).

The surface charge of nZVI is one of the factors affecting the interaction between nZVI and bacterial cells. The surface charge of nZVI was determined by measuring their zeta potential. The nZVI particles resuspended in M9G medium (at pH 7) for one and six hours exhibited negative charges of -37.93 ± 0.38 mV and -29.03 ± 0.47 mV, respectively.

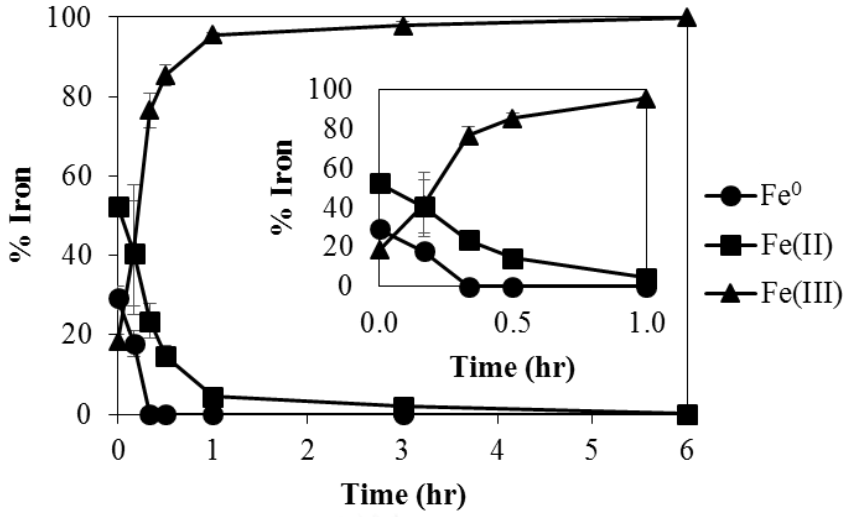

Figure *5.1* Percentage of the iron content of nZVI as a function of time. The inset graph shows the percentage of iron species within one hour.

5.2.2) Rebound in bacterial viability after prolongation of nZVI exposure

Similar to many nZVI toxicity studies, the effect of nZVI on *P. putida* F1 viability is dose-dependent (Lefevre et al., 2016), as shown in Figure 5.2. Within one hour of exposure to 0.1 and 1.0 g/L of nZVI, the viability of *P. putida* F1 decreased by 2.6 and 3.3 order of magnitude, respectively. The one-hour exposure to 5.0 g/L nZVI decreased cell viability by 2.2 order of magnitude and completely eradicated bacterial viability after prolonged exposure, indicating the lethal dose for bacteria in this study. Exposure to 0.1 g/L of Fe(II), Fe(III) or polyacrylic acid, a coating material of Nanofer 25S, did not substantially reduce bacterial viability (Figure 5.3), suggesting that the reduction in cell viability was mainly caused by the iron nanoparticles.

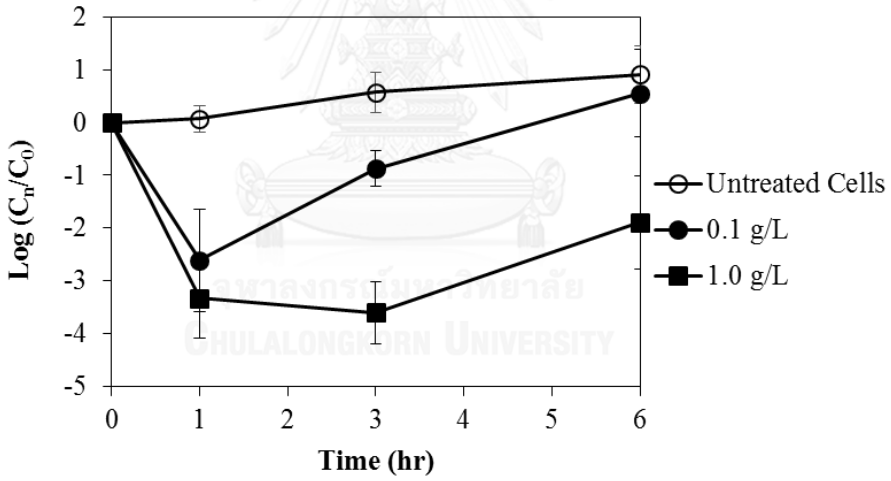

Figure *5.2* Time-dependent survival of P. putida F1 cells after nZVI exposure. Cells from the mid-log phase with an initial concentration of 10^8 CFU/ml were exposed to (●) 0.1 g/L, (■) 1.0 g/L. The control experiment without nZVI addition is indicated by (○).The shown values were calculated from at least three biological replicates.

Exposure conditions is a critical factor for determining and interpreting the environmental impact of nanoparticles(Holden et al., 2016). While 5.0 g/L of Nanofer 25S completely inactivated bacterial viability in this study, Sacca et al. reported that Nanofer 25S, ranging from 1- 10 g/L, inactivated *P. stutzeri* by maximum of two orders of magnitude (Sacca et al., 2014). Despite the strain-dependent susceptibility to nZVI, their substantially lower nZVI toxicity is likely attributed to the deposition of nZVI aggregates since the experiment was conducted in non-shaking condition. Therefore, the contact between nZVI and bacterial cells is limited.

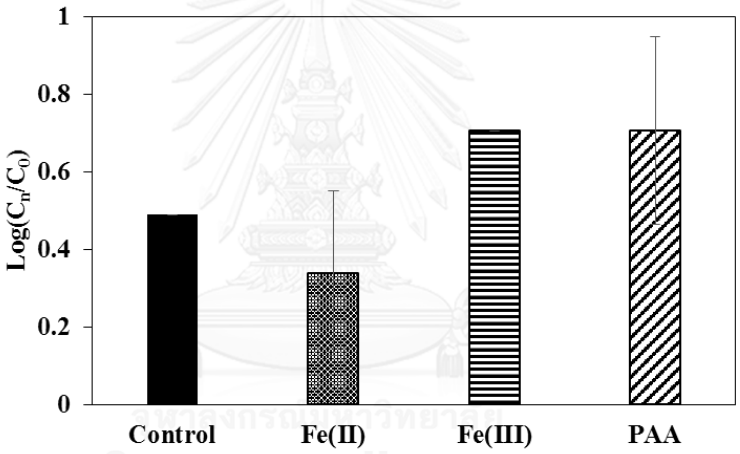

Figure *5.3* Survival of P. putida F1 cells after exposed to 0.1 g/L of Fe(II); 0.1 g/L of Fe(III) and 3 mg/L of polyacrylic acid (PAA). Cells from mid-log phase were exposed under the indicated conditions for one hour before determining their survival by CFU.

A remarkable rebound in a number of viable cells was observed after prolongation of exposure time to six hours (Figure 5.2). Presumptively, at certain nZVI concentrations, after nZVI undergo full oxidation/aging, the remaining cells, which could be uninjured or sublethally injured bacterial population, could resume growth in the less unfavorable condition. To further investigate the susceptibility of the regrown cells to nZVI, cells during the rebound phase were collected, washed and resuspended in fresh M9G medium before exposed to 0.1 g/L of nZVI. The result showed that bacterial cells from the rebound phase remain approximately as susceptible to nZVI as the parental cells (Figure 5.4).

The component of medium is well known to influence the toxicity of nanoparticles by altering the characteristics of nanoparticles (Li et al., 2014) as well as affecting metabolic process of bacterial cells. In this study, the exposure to 1 g/L of Nanofer 25S inactivated *P. putida* F1 cells by almost three orders of magnitude. After nZVI underwent oxidation and lost their reactivity, *P. putida* F1 in this study could use the available nutrient (glucose) to regain their growth and functionality. On the contrary, the toxicity study by Sacca et al. was conducted in NaCl solution with no provided nutrient, thus no rebound in cell viability was observed (Sacca et al., 2014).

Despite the nZVI-induced rapid reduction in bacterial viability leads to a concern on their environmental impact, the regrowth of bacteria under the prolonged exposure suggests limited long-term effect of nZVI. The recovery of bacterial activity after nZVI inhibition has been reported (Tilston et al., 2013; Xiu et al., 2010b). Xiu et al. (2010) reported a lag phase for microbial activity of a dechlorinating-microorganism consortium following the addition of 1 g/L of nZVI (Xiu et al., 2010b). The result, taken together with the observation in this chapter, accentuates the importance of exposure time in ecotoxicity study of nZVI because

the transformation/aging of nanoparticles and bacterial adaptation likely occur (Holden et al., 2016).

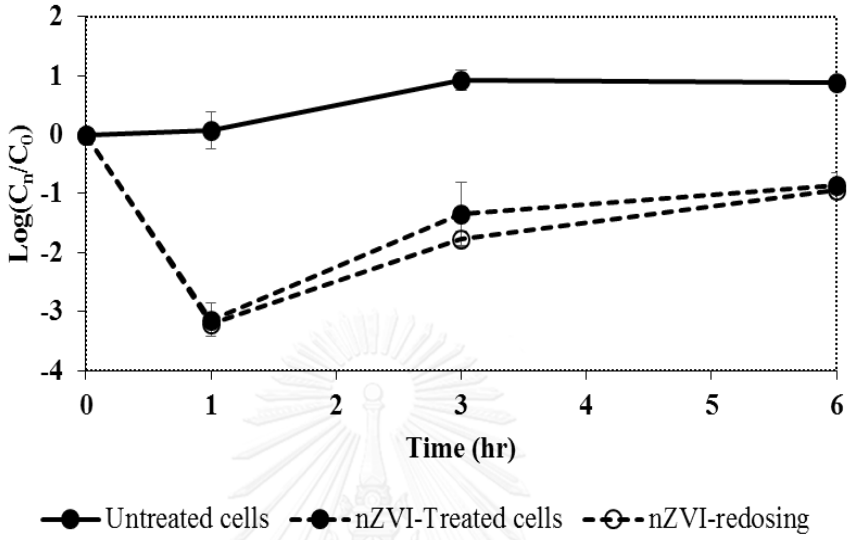

Figure *5.4* Susceptibility to nZVI of cell obtained from rebound phase after nZVI exposure. Normal cells from mid-log phase were exposed to 0.1 g/L of nZVI (●, dash line). After six hours of exposure, bacterial cells were collected and washed twice with 0.85% NaCl solution. The obtained cells were then resuspended in M9G medium before retreated with 0.1 g/L of nZVI (○, dash line). The control experiment without nZVI addition is indicated by bold line (●).The shown values were calculated from at least two biological replicates.

5.2.3) Repetitive nZVI exposure induced the emergence of bacterial phenotypic variant

In practice, the indigenous bacteria potentially encounter the repetitive exposure to nZVI through nZVI-redosing or recirculation of nZVI. To examine the effect of repetitive nZVI exposure, bacterial cells were transferred to fresh M9G and re-dosed with 0.1 g/L nZVI, the environmentally relevant concentration(Yang et al., 2016). Interestingly, after re-dosing with nZVI for three cycles, an altered phenotype of *P. putida* F1 cells, as characterized by a smaller colony morphology was detected (Figure 5.5A). The proportion of small-colony phenotypic variant increased with the number of nZVI re-dosing cycle, and was 75% of total cells after exposed to nZVI for five cycles (Figure 5.5B). To prepare this phenotypic variant for a test to determine its sensitivity to nZVI, bacterial cells were repeatedly exposed to nZVI for ten cycles to ensure that most cells (> 90%) display a small colony characteristic.

While the one-hour exposure of normal *P. putida* F1 cells to 1.0 and 5.0 g/L of nZVI decreased cell viability by more than two orders of magnitude, the exposure of the phenotypic variant (obtained from the tenth nZVI re-dosing) to 1.0 and 5.0 g/L of nZVI decreased cell viability by only 0.42 and 0.24 order of magnitude, respectively (Figure 5.5C). The low concentration of nZVI (0.1 g/L) did not affect the viability of the obtained phenotypic variant. After further cultured in nZVI-free M9G medium for three to five cycles, the obtained phenotypic variants regained the characteristics of normal phenotype i.e. colony morphology and sensitivity to nZVI (Figure 5.6).

This observation suggests that repetitive exposure to nZVI induced the emergence of the transient phenotypic variant capable of surviving or persisting in the presence of lethal dose of compounds or conditions. After the stressor (nZVI) is removed, these persister cells can resume the characteristics (susceptibility to nZVI)

of the parental cells. This small colony phenotypic variant is further noted as the nZVI-persistent phenotype.

There have been only few studies on repetitive exposure of bacteria to nanoparticles. Ma et al. reported that dosing of nZVI, nano titanium dioxide, or nano cerium dioxide in sequencing batch reactors at 0.1, 1, 10, and 20 mg/L sequentially every 2 weeks insignificantly affect nitrification and bacterial community composition in activated sludge (Ma et al., 2015). On the contrary, repetitive exposure to titanium dioxide nanoparticles as well as carbon nanotubes reduces the activity of soil microorganisms (Simonin et al., 2016; Tong et al., 2012). These adverse effect findings should be a concern because releases of nanoparticles to soil through applications of biosolids, nanofertilizers and/or nanopesticides (Simonin et al., 2016) may create a pulse or repetitive exposure condition (Reinert et al., 2002).

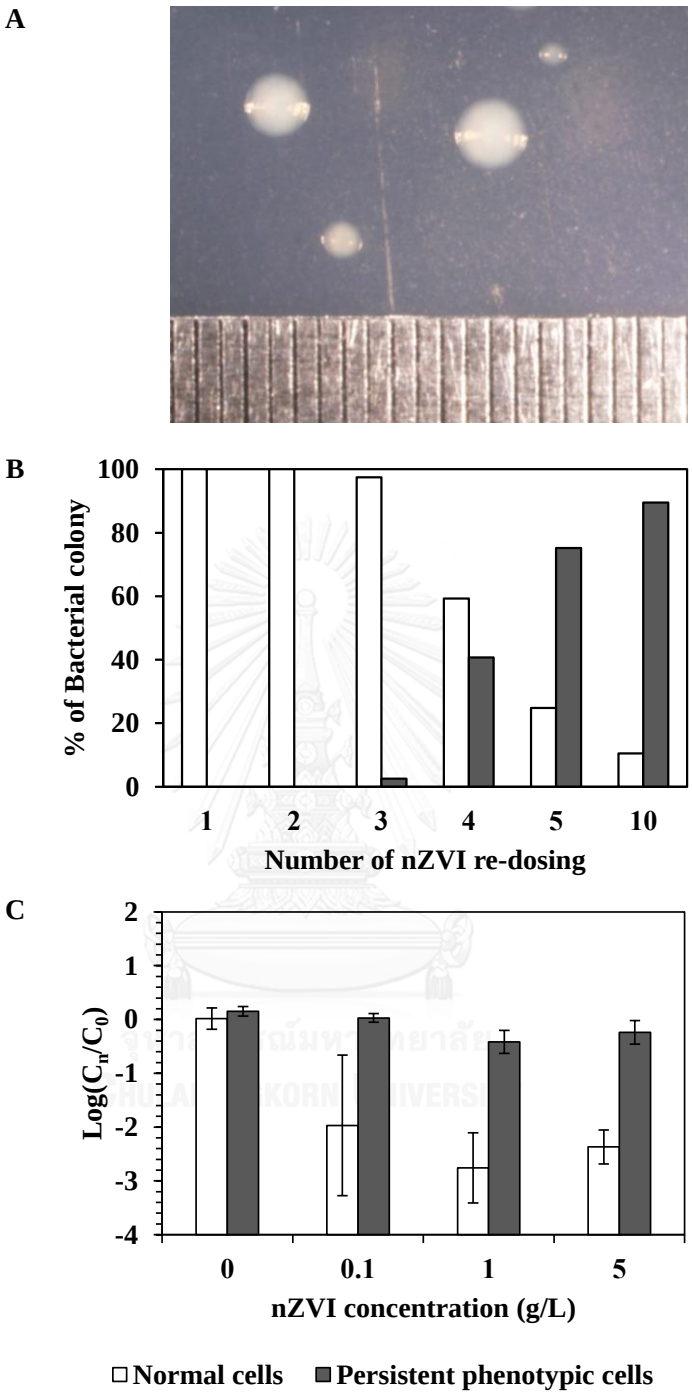

Figure *5.5* (A) Altered colony morphology of P. putida F1 after repeatedly exposed to 0.1 g/L of nZVI. (B) The relationship between repetitive nZVI exposure and proportion of persistent phenotype. (C) Comparison between survival of normal and nZVI-persistent phenotype of P. putida F1 after exposed to various nZVI concentrations for one hour.

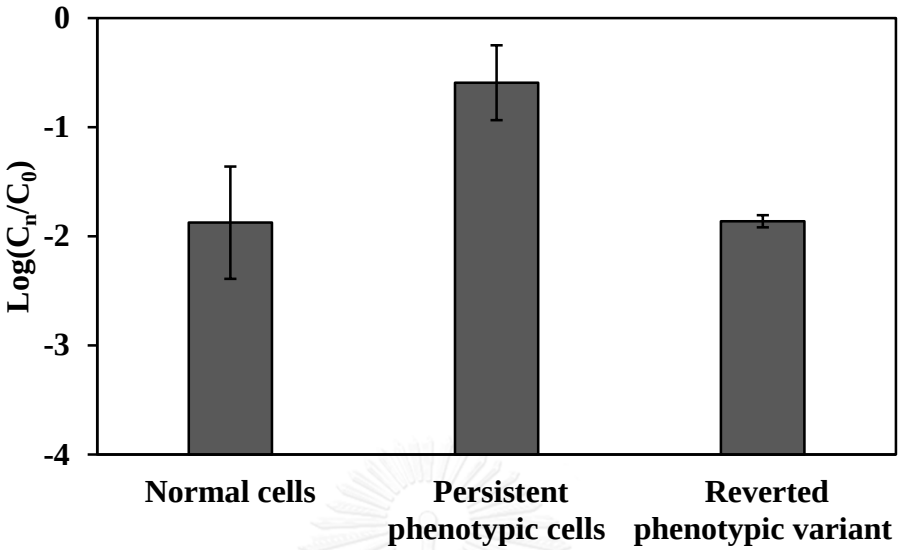

Figure *5.6* Susceptibility to nZVI of normal cells, persistent phenotype and reverted phenotypic variant. Bacterial cells from mid-log phase were exposed to 1.0 g/L of nZVI for one hour. The shown values were calculated from at least two biological replicates.

5.2.4) Visualization of bacterial membrane-nZVI interaction

To explore the interaction between nZVI and bacterial membrane, the electron micrographs of normal and the emergent nZVI-persistent phenotype of *P. putida* F1 cells after exposed to 0.1 g/L of nZVI were examined. Figure 5.7A and B shows the normal rod-shaped cell morphology and intact membrane of *P. putida* F1, respectively. Exposure to 0.1 g/L of nZVI for one hour resulted in extensive accumulation of nZVI onto bacterial cells surface (Figure 5.7C and D), as well as remarkable penetration and localization around the cell membrane (Figure 5.7E). These observations correlated with rough bacterial surface observed by SEM analysis (Figure 5.8B.). The nZVI-induced deformed *P. puitda* F1 cells were shown in Figure 5.7D. Interestingly, this accumulation of nZVI onto bacterial surface was less after

the exposure was prolonged to six hours (Figure 5.7F), or for the nZVI-persistent phenotype (Figure 5.7G and H), thus causing less damage to these cells. SEM results indicated there was no major difference in cell size between normal and the nZVI-persistent phenotype (Figure 5.8), suggesting that the smaller colony size of the persistent phenotype was likely caused by the low growth rate of the phenotype rather than the smaller cell size.

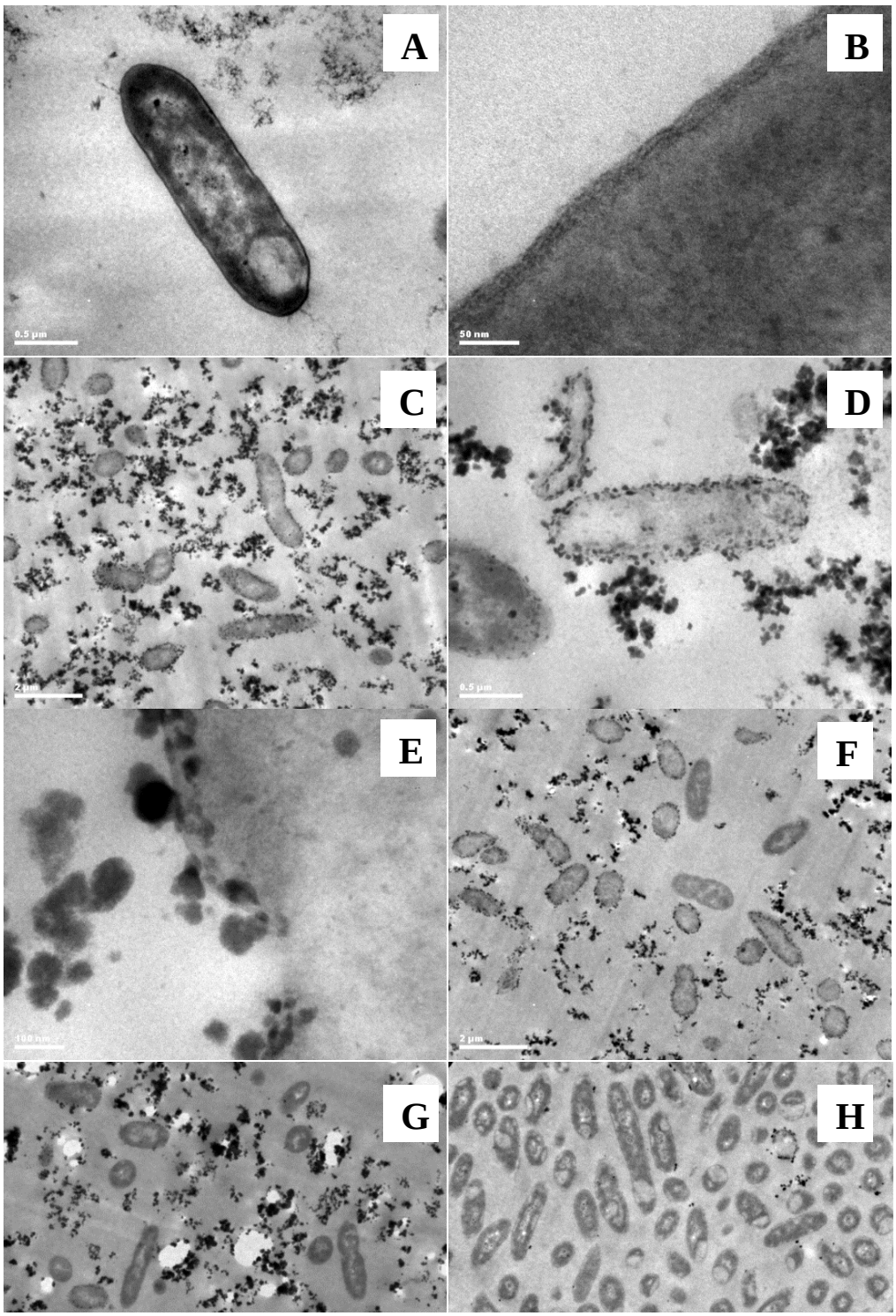

Figure *5.7* TEM micrographs of normal P. putida F1 cells from the mid-log phase (A) and (B) without nZVI exposure; (C), (D) and (E) after exposed to 0.1 g/L of nZVI for one hour and (F) six hour; (G) nZVI-persistent phenotype of P. putida F1 after nZVI exposure for one hour and (H) six hour.

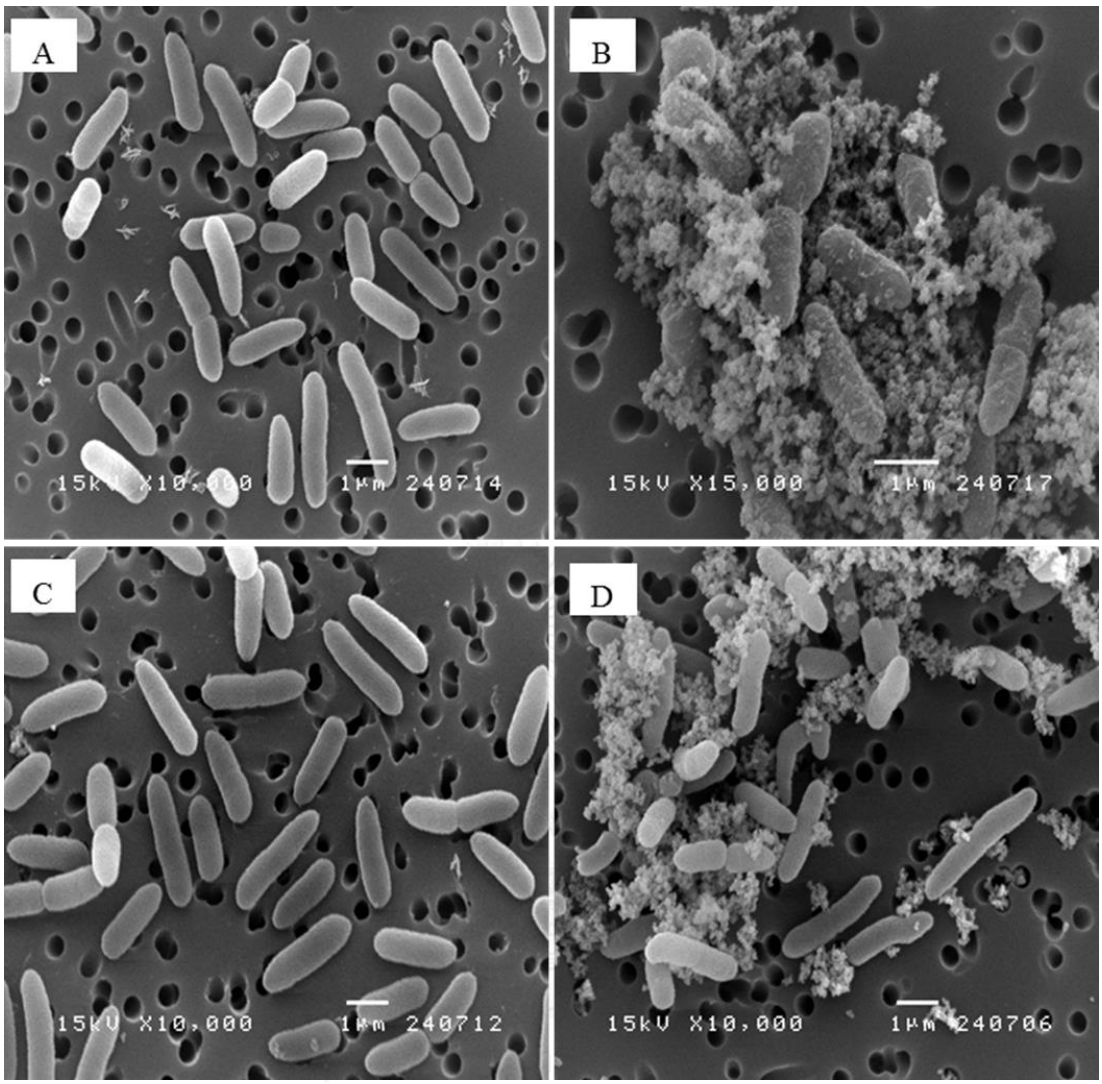

Figure *5.8* SEM micrographs of normal P. putida F1 cells from mid-log phase (a) without nZVI exposure; (b) after exposed to 0.1 g/L of nZVI for 1 hour, and the nZVI-persistent phenotype (c) without nZVI exposure and (d) after exposed to 0.1 g/L of nZVI for 1 hour.

5.2.5) Decreasing membrane fluidity after nZVI exposure

Based on the TEM analysis (Figure 5.7E), the penetration of nZVI in bacterial membrane layer disturbs the property of membrane. Herein, membrane fluidity which is the reversible physical state of the membrane was focused. Fluidity refers to a state in which the organization of membrane composition is disordered while under the opposite condition, rigidity, membrane composition organizes orderly. Membrane fluidity is required for the functionality of membrane-embedded proteins as well as a regulation of bacterial signal transduction, thus is considered vital for bacterial survival (Murinova and Dercova, 2014; Mykytczuk et al., 2007).

The changes in membrane fluidity state were investigated using DPH, which is a fluorescent probe capable of intercalating into the lipid bilayer of the membrane and is sensitive to lipid reorientation. The obtained data was expressed as the fluorescent anisotropy which is inversely proportional to membrane fluidity. Once nZVI particles intercalated into bacterial membrane layer, they disturbed the fluidity of bacterial membrane (Figure 5.9). Before nZVI exposure, the fluorescent anisotropy of normal cells was 0.28 ± 0.02 which significantly increased to 0.56 ± 0.06 after nZVI exposure (Figure 5.9). Before nZVI exposure, the membrane of the nZVI-persistent phenotype is significantly less fluid (i.e. more rigid) than that of the normal cells as indicated by the fluorescent anisotropy of 0.36 ± 0.03. After exposed to nZVI, the fluorescent anisotropy of the persistent phenotype substantially increased to 0.46 ± 0.06.

The reactive oxygen species (Cabiscol et al., 2000) as well as metals such as iron(García et al., 2005) can attack polyunsaturated fatty acids in membrane phospholipid bilayer, thus decreasing membrane fluidity. The exposure of *Escherichia coli* to hematite, an iron oxide nanoparticle, can alter bacterial physical properties including decreasing bacterial elasticity (i.e. bacterial cells become stiffer) (Zhang et al., 2012).

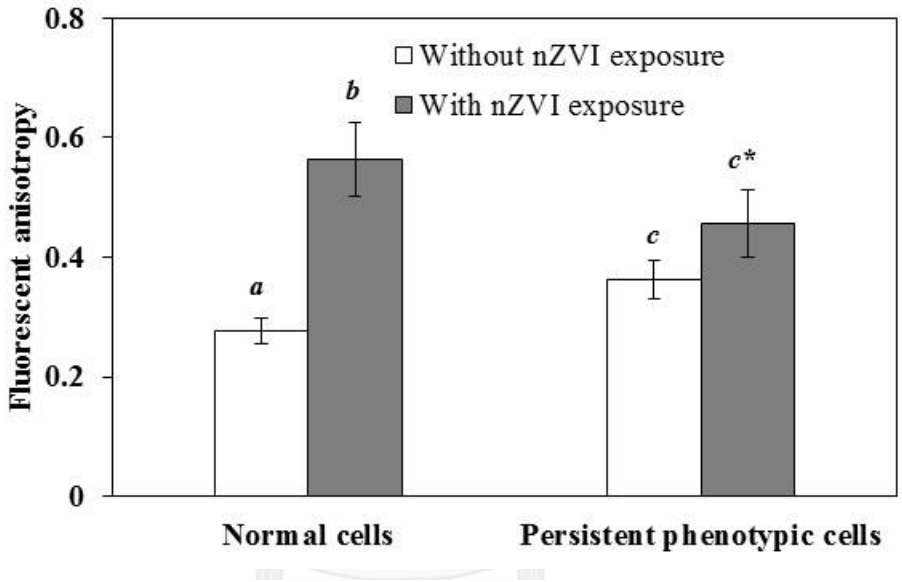

Figure *5.9* Membrane fluidity of P. putida F1 cells after exposure to 0.1 g/L of nZVI for one hour. Results are expressed as fluorescent anisotropy ± SD. The higher fluorescent anisotropy indicates less membrane fluidity (i.e. more membrane rigidity). Different letters indicate significant difference from the normal cells without nZVI exposure (Student t-test, $p < 0.05$). Asterisk indicates insignificance between the fluorescent anisotropy of the persistent phenotype before and after nZVI exposure.

5.2.6) Changes in bacterial fatty acids response to nZVI exposure

As mentioned above, when the organization of membrane (membrane fluidity) is disturbed, bacteria can readjust the components and maintain the proper state of their membrane (Murinova and Dercova, 2014). The membrane modification can be done through various mechanisms such as increase of the proportion of saturated to unsaturated fatty acid (Fang et al., 2007), conversion of *cis* to *trans* isomer of unsaturated fatty acid and synthesis of branched or cyclopropane fatty acids (Murinova and Dercova, 2014; Ramos et al., 2015). The increasing level of saturated fatty acid causes the more orderly and tightly packing of membrane lipid layer, making the bacterial membrane becomes more rigid, while the bended structure of unsaturated fatty acid disorganizes lipid bilayer, causing the fluidity of membrane (Heipieper et al., 2003).

To gain more understanding about the more rigid membrane, the bacterial fatty acid profile after nZVI exposure was investigated. The dominant detected fatty acid components of *P. putida F1* grown in a M9G medium were C16:0, C16:1, and C18:1, similar to a study by Fang et al. (Fang et al., 2007). Upon nZVI exposure, an increase in the degree of saturation, the ratio between saturated fatty acid and unsaturated fatty acid, was observed (Figure 5.10A). In addition, the nZVI exposure significantly increased *trans* to *cis* ratio of monounsaturated fatty acid of normal *P. putida* F1 cells by five times (Figure 5.10B). The trans-unsaturated fatty acid exhibits similar physical properties as saturated fatty acid, resulting in the substantially more tightly packed membrane and increasing membrane rigidity (Bernal et al., 2007; Heipieper et al., 2003; Zhang and Rock, 2008). Under growth-suppressed condition, instead of the energy-dependent de novo biosynthesis of saturated fatty acid, some bacteria can employ the conversion of *cis* to *trans* isomer of unsaturated fatty acid to adjust their membrane state (Heipieper et al., 2003). The inverse correlation

between bacterial growth rate and *trans-cis* ratio has been reported (Hachicho et al., 2014; Naether et al., 2013). Even though the activation mechanism of *cis-trans* isomerization of unsaturated fatty acid is still unclear, it is believed that the loosely packed or disintegrated membrane may allow the cis-trans isomerase enzyme, a periplasmic enzyme, to reach the substrate i.e. *cis*-unsaturated fatty acid (Heipieper et al., 2003).

Apparently, for batch exposure to unacclimated bacteria, the iron nanoparticles were able to intercalate and fluidize bacterial membrane. To withstand severe membrane disturbance, bacterial cells converted the *cis* to *trans* isomer of monounsaturated fatty acid, causing more rigid membrane allowing them to survive and resuscitate in the less toxic condition after nZVI experienced full oxidation.

Before nZVI exposure, the degree of saturation of the persistent phenotypic cells is higher than that of the normal cells (Figure 5.10A). The more rigid membrane of the persistent phenotypic cells may involves in the higher persistence to nZVI exposure as proposed for *A. versilocol*or (Diao and Yao, 2009a). After exposed to nZVI, the degree of saturation significantly increased from 0.6 to 0.9 whereas the *trans* to *cis* ratio remained low (Figure 5.10B). This suggests that the reduced interaction between nZVI and membrane of the persistent phenotypic cells caused much lower damage to bacterial membrane thus the conversion to *cis* to *trans* unsaturated fatty acid which is an urgent response to membrane damage is not induced.

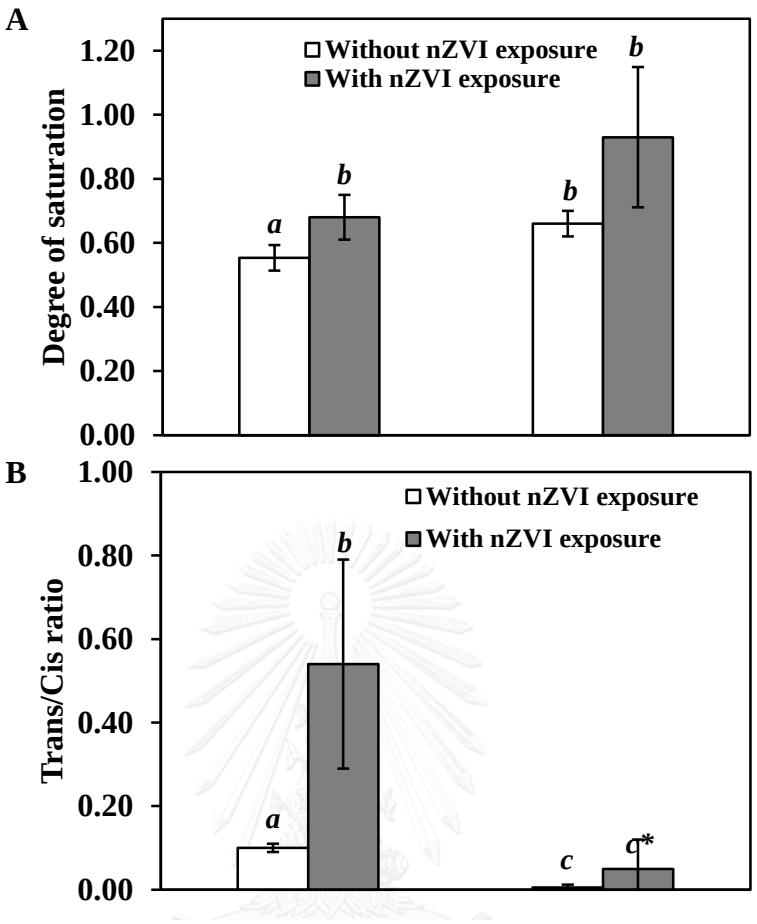

Figure *5.10* (A) Degree of membrane fatty acid saturation, which is the ratio between unsaturated fatty acids and saturated fatty acid. (B) The ratio between trans and cis isomer of unsaturated fatty acid (i.e. C16:1 and C18:1). Bacterial cells were exposed to 0.1 g/L of nZVI for one hour before extracted for total fatty acid. The shown values were calculated from two biological replicates. Different letters indicate significant difference from the normal cells without nZVI exposure (Student t-test, $p < 0.05$). Asterisk indicates insignificance between the fluorescent anisotropy of the persistent phenotype before and after nZVI exposure.

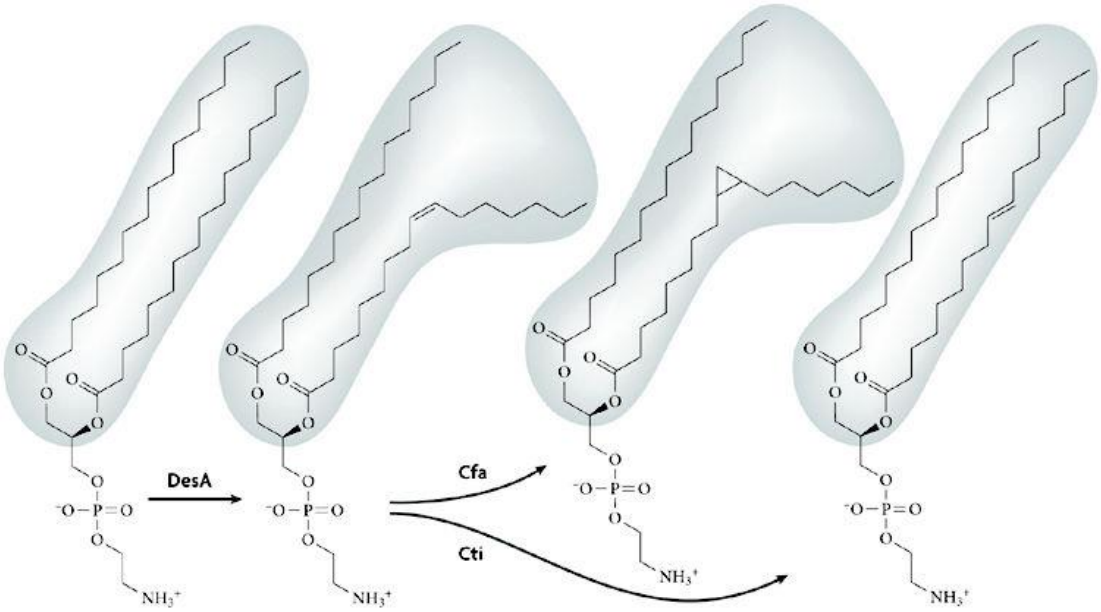

Figure *5.11* Fatty acid modification in bacteria. DesA: The phospholipid acyl-chain desaturase responsible for transformation of saturated fatty acid to unsaturated fatty acid resulting in the increased membrane fluidity. Cfa: Cyclopropane fatty acid synthase responsible for conversion of unsaturated fatty acid to cyclopropane fatty acid. Cti: cis-trans isomerase responsible for the conversion of cis- to trans-double bond in unsaturated fatty acid which resemble the shape of saturated fatty acid, thus decreasing membrane fluidity (i.e. increasing membrane rigidity).
Source: (Zhang and Rock, 2008)

5.2.7) Changes in bacterial surface charges

The interaction between nZVI and bacterial cell is governed by various physicochemical parameters (Xie et al., 2017), including electrostatic interaction (Pagnout et al., 2012). Accordingly, the bacterial surface charge inferring the electrostatic interaction between bacterial cell surface and nZVI particles was investigated. In the absence of nZVI, the surface charge of *P. putida* F1 cells in M9G medium was -10.97 ± 0.47 mV. The exposure of normal and phenotypic variant of *P. putida* F1 cells to nZVI decreased the bacterial surface charge to -17.23 ± 1.20 mV and -15.9 ± 1.25 mV, respectively.

Based on the bacterial surface charge after nZVI exposure, the higher negative charge of normal cells of *P. putida* F1 potentially caused by the sorption of nZVI onto bacterial surface (Figure 5.7D, E). The higher negative surface charge was also observed in nZVI-adapted cells, even though the accumulation of nZVI onto bacterial surface was limited (Figure 5.7G). After repeatedly exposed to nZVI, bacterial cells might adapt by modifying their surface components, for example, lipopolysaccharides, leading to the higher negative charge, thus increasing electrostatic repulsion between nZVI and bacterial surface (Figure 5.12).

While the *cis-trans* isomerization of unsaturated fatty acid acts as an urgent response to membrane disturbance, the mechanism underlying the nZVI-tolerance in the persistent phenotype is not completely conclusive. It is likely that the lower nZVI toxicity on the persistent phenotype was caused by the reduced interaction between bacterial surface and nZVI particles. Several factors have been reported to affect the nZVI-bacteria interaction including the difference in bacterial surface characteristics (Diao and Yao, 2009c; Lefevre et al., 2016; Xie et al., 2017). In 2011, Chen and colleagues reported the toxicity of nZVI on two different bacterial strains, *B. subtilis,* and *E. coli*, and proposed that more negative charge of *B. subtilis* causes less nZVI

toxicity, compared to *E. coli* which is less negatively charged (Chen et al., 2011b). Gram negative bacteria exhibit the negative surface charge due to the presence of the carboxylic acids and phosphate esters (phosphoryl group) in their cell surface components (i.e. phospholipids, lipoproteins, lipopolysaccharides (LPS) and proteins) (Shephard et al., 2008; Wilson et al., 2001), while the negative charge of Gram positive bacteria is mainly attributed to the peptidoglycan and teichoic acid in the outer surface (Wilson et al., 2001). These bacterial surface components play an important role in the interaction between bacterial surface and environmental matrix including soil and sand particles. The cationic metal ion, for example, copper, lead, iron, as well as nanoparticles primarily binds to the phosphate head group of phospholipid and the LPS of bacteria (French et al., 2013; Jiang et al., 2010; Langley and Beveridge, 1999; Yang et al., 2015). The altered surface components exhibit varied affinities for metal binding due to differences in their surface charge (Langley and Beveridge, 1999). Dhas et al. reported the increased negative charge of bacterial cells for both Gram-negative and Gram-positive, after continuously exposed to increasing concentrations of silver and zinc oxide nanoparticles (Dhas et al., 2014). They proposed that the higher production of extracellular proteins and exopolysaccharides in the adapted cells could provide more binding sites for the released metal ion, reducing nanoparticles dispersion and direct contact with bacterial cells (Dhas et al., 2014). Based on this finding, it may be deduced that the repetitive exposure induces the modification of bacterial surface components, thus altering the surface charge and the electrostatic interaction between bacterial cells and nZVI.

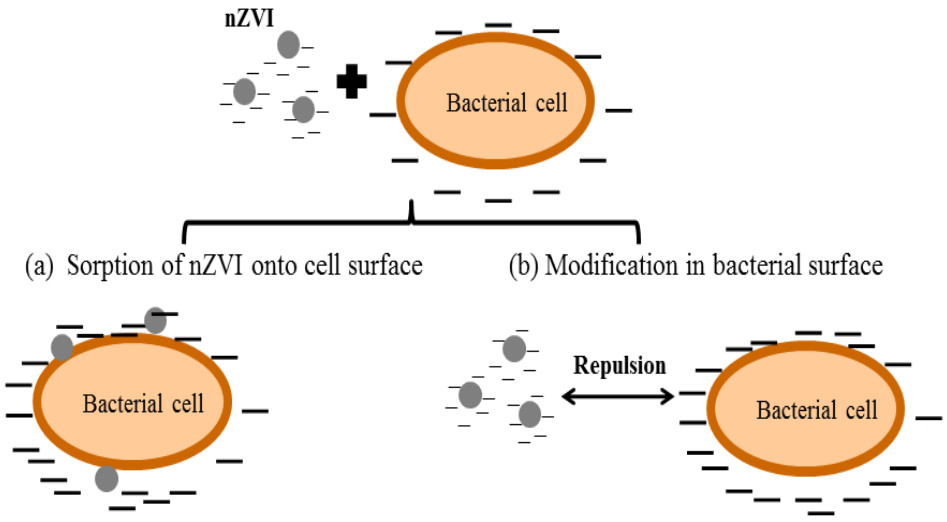

Figure *5.12* Possible scenarios for the increasing negative charge of *P. putida* F1 cells after nZVI exposure: (A) Sorption of nZVI onto the surface of normal cells and (b) Modification in surface biomolecules of nZVI-persistent phenotype of P. putida F1 causing an electrorepulsive force between cells and nZVI.

5.2.8) Phospholipid headgroup analysis

Since phospholipid headgroup is important for the interaction between nanoparticles and bacterial surface (Jiang et al., 2010), in order to obtain more understanding about interaction between nZVI and bacterial membrane, the targeted metabolomics was used to investigate the changes in bacterial phospholipid profile. Targeted metabolomics is the measurement of the metabolites of interest using LC-MS.

For targeted metabolomic data analysis, the obtained fatty acid profile from the previous study was used to generate the list of possible phospholipid. The amount of each phospholipid was extracted from LC-MS profile using the accurate masses of their $[M+H]^+$, $[M+Na]^+$, $[M+NH_4]^+$ or $[M-H]^-$.

The main phospholipids reported in *P. putida* F1 are phosphatidylethanolamine (PE, zwitterion), phosphatidylglycerol (PG, anionic) including the trace amount of phosphatidylserine (PS, anionic) (Fang et al., 2000). Therefore, these three groups of phospholipid were selected as the target metabolites. Before nZVI exposure, PG, PE and PS content of the normal cells of *P. putida* F1 in this study contributed to 65.87%, 24.95% and 9.18% of total phospholipids, respectively (Figure 5.13). After one-hour nZVI exposure, the slightly increasing PE percentage was observed in both normal cells (31.73 ± 0.28%) and persistent phenotypic cells (35.22 ± 6.86% PE), comparing to normal cell without nZVI exposure (24.95 ± 0.52%).

In M9G medium of which pH is approximately 7, PG and PS are negatively charged, whereas PE is neutral phospholipid. The higher anionic phospholipid content may decrease the negative charge on the surface. However, after nZVI exposure, both normal cells and persistent phenotypic cells possess a high content of PE. PE involves in the metal detoxification in *P. fluorescens*, by immobilizing and expulsing intracellular metals, for example, iron and aluminum out of cells (Appanna and Finn, 1995; Auger et al., 2016). The higher PE content of nZVI-treated normal cells of *P .putida* F1 could explain the arrangement of nZVI both inside and on bacterial membrane (Figure 5.7E), similar to the study by Appanna et al. which reported the deposit of iron around bacterial membrane (Appanna and Finn, 1995). Henderson et al (1993) reported that the ratio of PE in total phospholipid was higher in bacterial cells cultivated at 5°C than 20°C (Henderson et al., 1993). Lowering temperature caused the decreasing membrane fluidity i.e. increasing membrane rigidity (Inaba et al., 2003). The elevated PE after nZVI exposure may reflect the increasing membrane rigidity. However, the mechanism underlying the increasing negative charge on bacterial surface is yet understood.

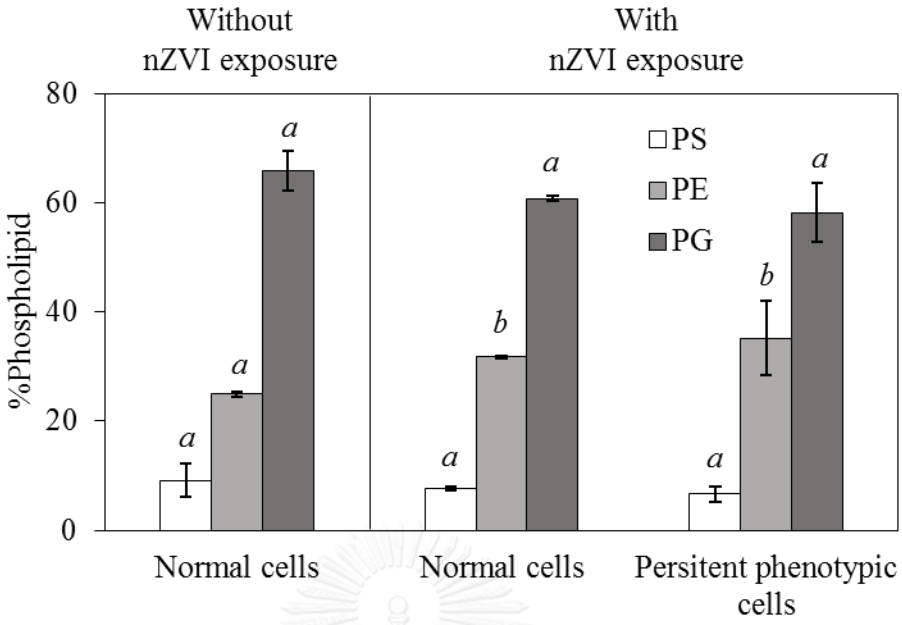

Figure *5.13* Percentage of phospholipids of interest which are PS, PE and PG in *P. putida* F1 cells. The shown values were calculated from two biological replicates. “b” indicates significant difference from the normal cells without nZVI exposure (Student t-test, $p < 0.05$).

5.3) Summary

Exposure of *P. putida* F1 to 0.1 and 1.0 g/L of nanoscale zero valent iron (nZVI) caused the reduction in cell viability substantially for almost three order of magnitude; however, a rebound in cell number was observed after prolonged exposure. Upon exposure, nZVI heavily accumulated on and penetrate into the bacterial membrane. Cell membrane composition analysis revealed the conversion of *cis* to *trans* isomer of unsaturated fatty acid upon short-term nZVI exposure, resulting in a more rigid membrane counteracting the membrane-fluidizing effect of nZVI. Several cycles of repetitive exposure of cell to 0.1 g/L nZVI induced a persistent phenotype of *P. putida* F1 as indicated by smaller colony morphology, more rigid membrane and higher tolerance to nZVI. A low interaction between nZVI

particles and the surface of the nZVI-persistent phenotype reduced the nZVI-induced membrane damage. This study unveils the significance of nZVI-membrane interaction on toxicity of nZVI toward bacteria.

Chapter 6

Emergence of phenotypic variants of *P. putida* F1 due to nZVI exposure and their environmentally relevant characteristics

6.1) Introduction

In the environment, bacteria typically confronts the dynamically fluctuated/challenged situations such as alteration in temperature, pH, water stress or the presence of xenobiotic compounds. Accordingly, bacterial adaptability is an important factor determining their survival. Pseudomonas is one of the versatile bacteria capable of adapting themselves to several stress conditions (Ramos et al., 2009a; Ramos et al., 2015; Silby et al., 2011; Thompson et al., 2010; Udaondo et al., 2012). Their versatility particularly tolerance and ability to utilize various toxic hydrocarbon/pollutants as carbon source and ubiquity make them a major degrader in many polluted sites (Samanta et al., 2002; Singh and Fulekar, 2010; Udaondo et al., 2012; Wilson and Jones, 1993).

Bacterial adaptation can occur through many processes, for example, physiological alteration (e.g. modification in their membrane or protein expression), or genetic modification (e.g. mutation or DNA rearrangement). In some cases, these processes can lead to cross protection against other stresses (Rangel, 2011). Bacteria cells which adapted to acidic condition by modifying their membrane and altering the protein expression has been reported for their cross protection/higher tolerance to cold stress (Streit et al., 2008). While bacterial adaptation to encountered stress is beneficial for their survival, some adaptation processes are metabolic burden or cause a disturbance to bacterial metabolism (Händel et al., 2013; Hottes et al., 2013; Martinez et al., 2009). For instance, the presence of 1-decanol did not affect growth behavior of *P. putida* DOT-T1E; however, cell yield decreased by 50% due to high energy consumption by adaptation mechanism (Neumann et al., 2006). The

expression of AmpC β-lactamase which is a β-lactam-degrading enzyme in *Salmonella Typhimurium* results in high tolerance to an antibiotic β-lactam but the reduced growth rate and invasiveness were observed (Morosini et al., 2000).

Phenotypic variation is one of the survival strategies adopted by bacteria during stress condition. The phenotypic or phase variation is generated by mutation, DNA rearrangement or stochastically epigenetic changes, resulting in different physiological states of cells and granting them chances to survive under stress conditions such as antibiotic stress or oxidative stress (van den Broek et al., 2005; Veening et al., 2008). One of the most studied phenotypic variant is a small colony variant (SCV). Generally, the SCV phenotype is described as a slow-growing subpopulation of bacteria exhibiting different characteristics (e.g. increasing resistance to antibiotics or higher biofilm formation), compared to the normal phenotype (Wang et al., 2014). While the bacterial SCV phenotype is extensively studied in pathogenic bacteria due to the association with difficult-to-treat chronic infection caused by distinctive characteristics, the study on environmental microorganisms has been limited. Recently, a small colony variant has been reported to affect various characteristics of rhizospheric bacteria (Wang et al., 2014). The SCV phenotype of *P. chlororaphis* exhibits higher antibiotic resistance and biofilm formation, whereas bacterial motility and production of phenanzine decreased (Wang et al., 2014).

Nanoscale zero valent iron (nZVI) is an extensively used alternative for *in situ* remediation of contaminated sites. Due to its high reactivity and capability of generating oxidants, environmental impact of nZVI is highly concerned. In the preceding chapter, the emergent of a small-colony phenotypic variant of *P. putida* F1 (further designated as the SCV phenotype) showing higher persistent/tolerance to nZVI upon the repetitive exposure to an environmental-relevant concentration of nZVI were reported. Along with the reversible SCV phenotype, we are able to isolate the stable/irreversible SCV during the repetitive exposure to nZVI.

Due to the limited information on the observed phenotypic variant discovered in our previous study, herein we further explored factors affecting the emergence of the SCV phenotype of *P. putida* F1. In addition to the reactive nZVI, we are also concerned about the oxidized form of nZVI of which their large amount are retained in the environment after remediation process. *P. putida* F1 is a well-studied bacteria for the capability to degrade various aromatic hydrocarbons such as toluene and trichloroethene. Additionally, this strain has been recently used as a model strain for a study on bacterial chemotaxis toward pollutants (Parales et al., 2000). Accordingly, the environmentally relevant characteristics which are toluene sensitivity and degradation, swimming ability and biofilm formation of the SCV phenotype were studied in comparison to the normal phenotype.

6.2) Results and discussion

6.2.1) Emergence of phenotypic variant induced by nZVI exposure

The frequency of the SCV phenotype in *P. putida* F1 cells without nZVI exposure was approximately 10^{-5} throughout the study (data not shown), indicating the background (subpopulation) of the SCV phenotype in *P. putida* population. The higher frequency of the SCV phenotype correlates with the increasing cycles of nZVI exposure (Figure 6.1). While the single exposure to 0.1 g/L of nZVI did not induce the emergence of the SCV phenotype, the frequency of this phenotype substantially increased by 10 times following the second cycle of nZVI exposure (Figure 6.1). The third cycle of nZVI exposure increased the proportion of this phenotype by 50 – 2,000 times, making them visually detectable as a distinctive small colony reported in the previous chapter.

The rising of the SCV phenotype is nZVI-concentration dependent (Figure 6.1). The single exposure to higher concentration of nZVI (i.e. 0.5 and 1.0 g/L) resulted in a

considerable higher frequency of the SCV phenotype. However, the repetitive exposure to 1.0 g/L of nZVI does not further increase frequency of this phenotype.

While the gentamicin concentration (4 μg/ml) applied in this study was selected based on the MIC of the stable/irreversible SCV phenotype (Appendix A), the obtained SCV phenotype from this experiment can revert to the normal phenotype on gentamicin-free TSB agar plate. This observation suggests that the stable SCV phenotype are low-level resistant to gentamicin, while the reversible phenotype is considered a persister cell. It is likely that bacterial response to nZVI exposure (i.e. increasing membrane rigidity) may provide cross-protection against gentamicin. On the other hand, the nZVI exposure may create a selection pressure toward subpopulation of *P. putida* F1 cells which can persist gentamicin exposure and display the SCV phenotype.

The environmental consequences of the reversible SCV phenotype mentioned in the previous chapter appears inconsiderable since it is transient variation/incident; their gentamicin persistence should not be neglected. A slight increase of antibiotic MIC can lead to a considerable concern (Baquero, 2001; Kurenbach et al., 2015; Li et al., 2016). Persister cells are a small fraction of isogenic bacterial population which is able to survive antibiotic treatment. Once antibiotic is removed, the persister cells can rise, thus resulting in chronic infection (Fauvart et al., 2011). This persister phenotype possibly further develops into multi-drug or higher level-resistant phenotype which occurs through genetic modification, for example, mutation or acquiring antibiotic-resistant gene from other strains (Li et al., 2016). Recently, the applications of nZVI for antibiotics or pharmaceutical products removal have gained more attention (Chen et al., 2012; Fang et al., 2011; Fu et al., 2015; Hanay and Türk, 2015; Machado et al., 2013). The application of nZVI wastewater or sludge containing antibiotics and pharmaceutical products may promote the occurrence of antibiotic resistant bacteria.

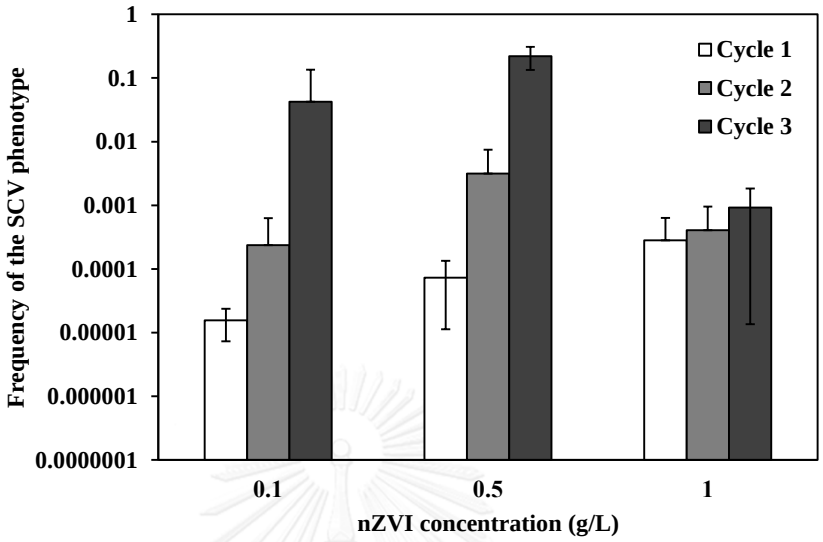

Figure *6.1* The relationship between the SCV phenotype of *P. putida* F1 and cycles of nZVI exposure. The frequency of the emergent phenotypic variant was determined as described in equation 1. The data are based on mean and standard deviation of at least three experimental replications. Some error bars are missing due to the large value of lower SD exceeding the log scale.

6.2.2) Mechanism triggering emergence of the SCV phenotype

Similar to cells exposed 0.5 g/L of R-nZVI (Figure 6.1), the single exposure to 0.5 mM of H_2O_2 increased the frequency of the SCV phenotype by ten times (Figure 6.2). However, the repetitive exposure to H_2O_2 did not further increase the frequency of the SCV phenotype suggesting the maximum SCV induction caused by exposure to 0.5 mM H_2O_2. The repetitive exposure to Fe(II), which can interact with intracellular H_2O_2 and generate OH· via Fenton reaction, also induce the emergence of the SCV phenotype. Neither O-nZVI nor Fe(III) exposure affect the emergence of this phenotype (Figure 6.2). These results indicate that the nZVI exposure likely affects the emergence of the SCV phenotype through the mediation of oxidative stress.

Typically, reactive oxygen species (ROS), for example, H_2O_2 or O_2^-, can be

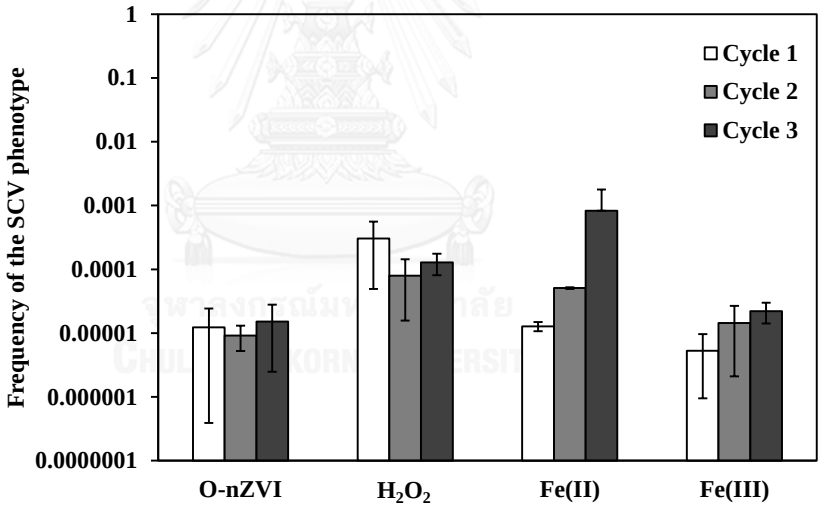

Figure *6.2* Roles of oxidative stress and different forms of iron on the emergence of the SCV phenotype. Cells were exposed to 0.5 g/L of O-nZVI or soluble iron species. To determine role of oxidative stress, cells were exposed to 0.5 mM of H_2O_2 which is equivalent to the oxidative stress induced by 0.5 g/L of R-nZVI. The data are based on mean and standard deviation of at least three experimental replications. Some error bars are missing due to the large value of lower SD exceeding the log scale.

generated intracellularly as a byproduct from bacterial aerobic respiration or the oxidation of biomolecules (Cabiscol et al., 2000). H_2O_2 can further rapidly interact with Fe(II) (Fenton reaction), generating highly reactive, non-selective hydroxyl radicals which can further damage DNA and proteins (Sevcu et al., 2011). The presence of nZVI or Fe(II) significantly promoted the Fenton-mediate oxidative damage, thus increasing chance of phenotypic variation or stress-response induced tolerance against gentamicin. Even though Fe(III) can also interact with $O_2^{-}\cdot$ or H_2O_2 resulting in Fe(II) and oxygen, the lower impact of Fe(III) on bacterial cells is likely due to their low solubility thus reducing their bioavailability (Krewulak and Vogel, 2008). Recent studies found that nZVI does not induce mutagenicity (Barzan et al., 2014; Schiwy et al., 2016). Schiwy et al. (2016) studied the mutagenicity of aged Nanofer 25S and reported that no mutagenicity was observed due low ROS generation (Schiwy et al., 2016).

H_2O_2-induced DNA damage has also been reported to trigger and select for the stable gentamicin-resistant SCV phenotype of *Staphylococcus aureus* (Painter et al., 2015). Oxidative DNA damage (e.g. double stranded DNA breaking) could lead to mutated bacterial cells (Boles and Singh, 2008). On the contrary, the expression of Error-prone Polymerase, a low fidelity DNA damage repairing enzyme, upon the activation of the SOS regulon could enhance the mutation rate of bacteria, and may increase the frequency of the SCV (Torres-Barcelo et al., 2013).

The accumulation of iron during repetitive nZVI exposure may play role in the increasing frequency of the SCV phenotype. This leads to a concern on repetitive exposure of nZVI at contaminated sites, regardless of duration time or frequency, because the generated ROS from newly injected nZVI may initiate the Fenton reaction. However, high concentrations of nZVI (≥ 1.0 g/L) may cause an unbearable damage, for example, severe membrane damage and oxidative stress, resulting cell

death. This may explain the limited induction of the SCV phenotype by repetitive exposure to 1.0 g/L.

While the oxidative stress-induced mutation likely explains the emergence of the stable phenotype, the mechanism underlying the emergence of the reversible SCV phenotype showing persistent to gentamicin is still unclear. Beside mutagenesis, the oxidative stress-induced expression of efflux pump and bacterial adaptation to membrane-active compounds have been reported to induce the cross-protection against aminoglycoside antibiotics (Fraud and Poole, 2011; Jassem et al., 2014; Kurenbach et al., 2015). For instance, Kurenbach (2015) reported that bacterial exposure to a sublethal concentration of herbicides affects the susceptibility to various antibiotics through activation of *soxS*-controlled efflux pump (Kurenbach et al., 2015). The *soxRS* regulon controls several proteins involved in bacterial oxidative stress response including superoxide dismutase, fumarase and aconitase(Demple, 1996). A peroxide-induced MexXY-OprM efflux pump system has been reported to play a role in the emergence of aminoglycoside resistant cells of *P. aeruginosa* (Fraud and Poole, 2011).

6.2.3) Environmental fitness-related traits of the stable SCV phenotype

To assess the ecological fitness of the SCV phenotype, bacterial growth under various conditions including using toluene as a sole carbon source were investigated. In minimal medium, except for M9T inoculated with toluene-acclimated cells, the duration of lag phase of the SCV phenotype was much longer than that of the normal phenotype (Table 6.1). It appeared that the SCV phenotype become more susceptible to toluene and requires longer time to adapt to toluene resulting in longer lag phase (at least 24 hours) for growth under toluene as a sole carbon source compared to 6-hour lag phase of the normal phenotype. Despite the four-fold longer lag phase, the maximum growth rate of the SCV phenotype was not significantly different from the normal cells indicating that once SCV cells is acclimated to toluene, they are as effective as the normal cells for toluene utilization. This was confirmed by the growth of toluene-acclimated normal and SCV cells in M9T which exhibit similar lag phase and maximum growth rate (Table 6.1). The growth rate of the SCV phenotype in TSB (rich medium) is slightly lower than the normal phenotype.

Bacterial growth under toluene as a sole carbon source was also examined in the presence of glucose as a co-substrate. The addition of glucose reduced the duration of lag phase and the maximum growth rate of the normal phenotype in M9T. The added glucose could substantially cut down the lag period of the SCV phenotype in M9T; however, the maximum growth rate remained comparable to the case of M9T without glucose supplementation.

The susceptibility to toluene was compared between the normal and the SCV phenotype. The SCV phenotype tolerated up to 100 mg/L of toluene. However, while the exposure to 870 mg/L (0.1%) toluene reduced the survival of the normal phenotype by 0.3 order of magnitude, the survival of the SCV phenotype decreased by 0.5 order of magnitude, indicating that the SCV phenotype is slightly more

susceptible to toluene than the normal phenotype. Toluene degradation by the normal and the SCV phenotype was tested at an initial toluene concentration at 100 mg/L which did not inhibit the viability of both phenotypes. The normal phenotype could degrade toluene faster than the SCV phenotype as shown in Figure 6.3A.

The limited/low bioavailability of pollutant (e.g. trapped in soil pore) is one of the limitations for *in-situ* bioremediation process (Singh et al., 2006). Chemotactic bacteria, for instance, *Pseudomonas* strains are capable of moving in response to several pollutants, thus enhancing the bioavailability of pollutant (Parales et al., 2015) and providing advantages over non-chemotactic or non-motile bacteria (Law and Aitken, 2003; Marx and Aitken, 2000; Paul et al., 2006; Singh and Olson, 2010). After bacteria sense the chemical via the chemoreceptor protein, they can respond by moving toward chemoattractant or moving away from chemorepellent by using flagellar-mediated swimming motility (Figure 6.3). While *P. putida* F1 has been reported for their chemotactic ability toward several pollutants including benzene, toluene and trichloroethylene (Parales et al., 2000), the SCV phenotype is defective in swimming motility. This could strain chemotactic ability of the bacteria (Figure 6.3B).

Biofilm is a complex form/lifestyle of bacteria consisting of surface-associated bacterial cells holding together by the matrix consisting of extracellular polymeric substance. It is a typical form of bacteria in the environment which plays important roles in many biological processes (Davey and O'toole, 2000; Harrison et al., 2007; Ramey et al., 2004; Singh et al., 2006). The effective biodegradation of pollutant by *P. putida* F1 biofilm has been reported (Herzberg et al., 2006; Woo et al., 2000). Several studies proposed that bacterial flagella is necessary for biofilm formation. During the bacterial colonization on surface, the flagella-mediate swimming bacteria reach the surface forming mono-layer of attached bacteria. On the other hand, the absence of bacterial flagella has been reported to increase biofilm forming ability due to the

reduced microbial mobility thus enhancing the amount of attached cells. In this study, while the observed SCV phenotype is non-motile, the amount of attached cells is still considerable high (≈10^7 CFU/ml) (Figure 6.3C). However, no biofilm production was detected by using crystal violet staining method suggesting the reduced/limited EPS production (Figure 6.3C).

Table 6.1 Bacterial growth in various mediums

Conditions	Normal		SCV	
	Lag time (hr)	Growth rate (hr^{-1})	Lag time (hr)	Growth rate (hr^{-1})
TSB	2	0.248 ± 0.011	2	0.217 ± 0.015
M9G	2	0.213 ± 0.026	2 - 7	0.243 ± 0.080
M9T + 0.1% Glucose	2	0.211 ± 0.009	13 - 24	0.067 ± 0.051
M9T (Non-induced)	6 - 7	0.084 ± 0.024	24 - 57	0.089 ± 0.030
M9T (Induced)	2	0.220 ± 0.051	2	0.230 ± 0.040

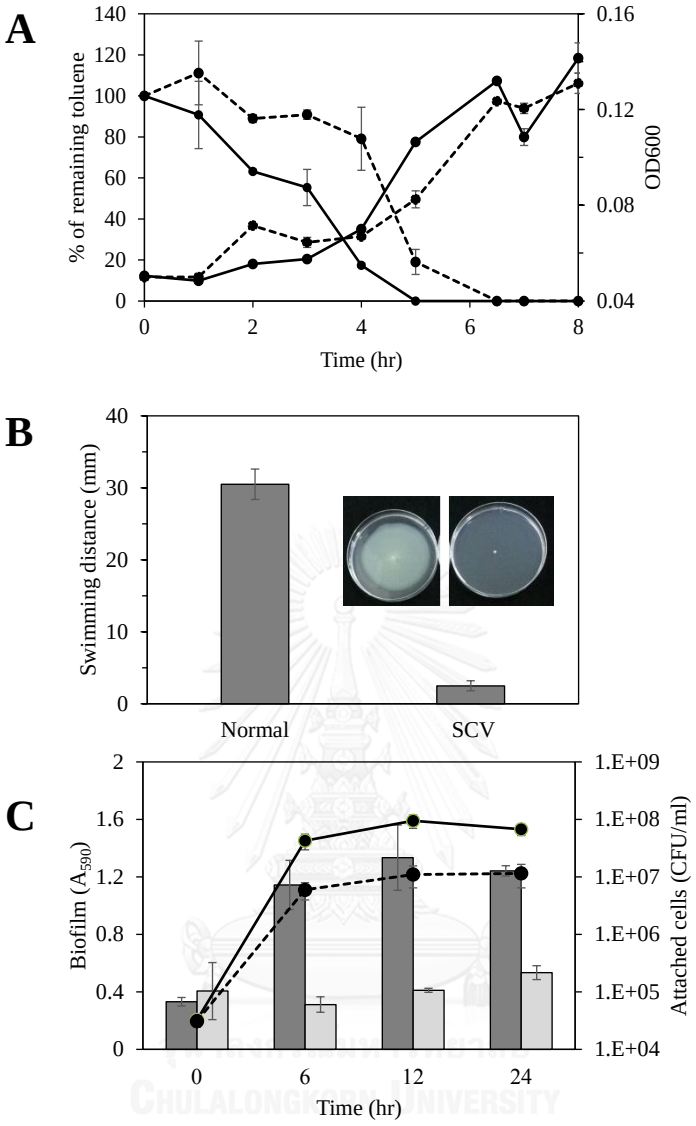

Figure *6.3* Characteristics of the SCV phenotype in comparison to the normal phenotype of *P. putida* F1. (A) Toluene utilization by toluene-induced *P. putida* F1 cells. The normal phenotype is indicated by solid line; the SCV phenotype is indicated by dash line. (B) Bacterial swimming motility and (C) Biofilm formation of the normal phenotype (dark grey bar) and the SCV phenotype (light grey bar). The data are based on mean and standard deviation of at least two experimental replications.

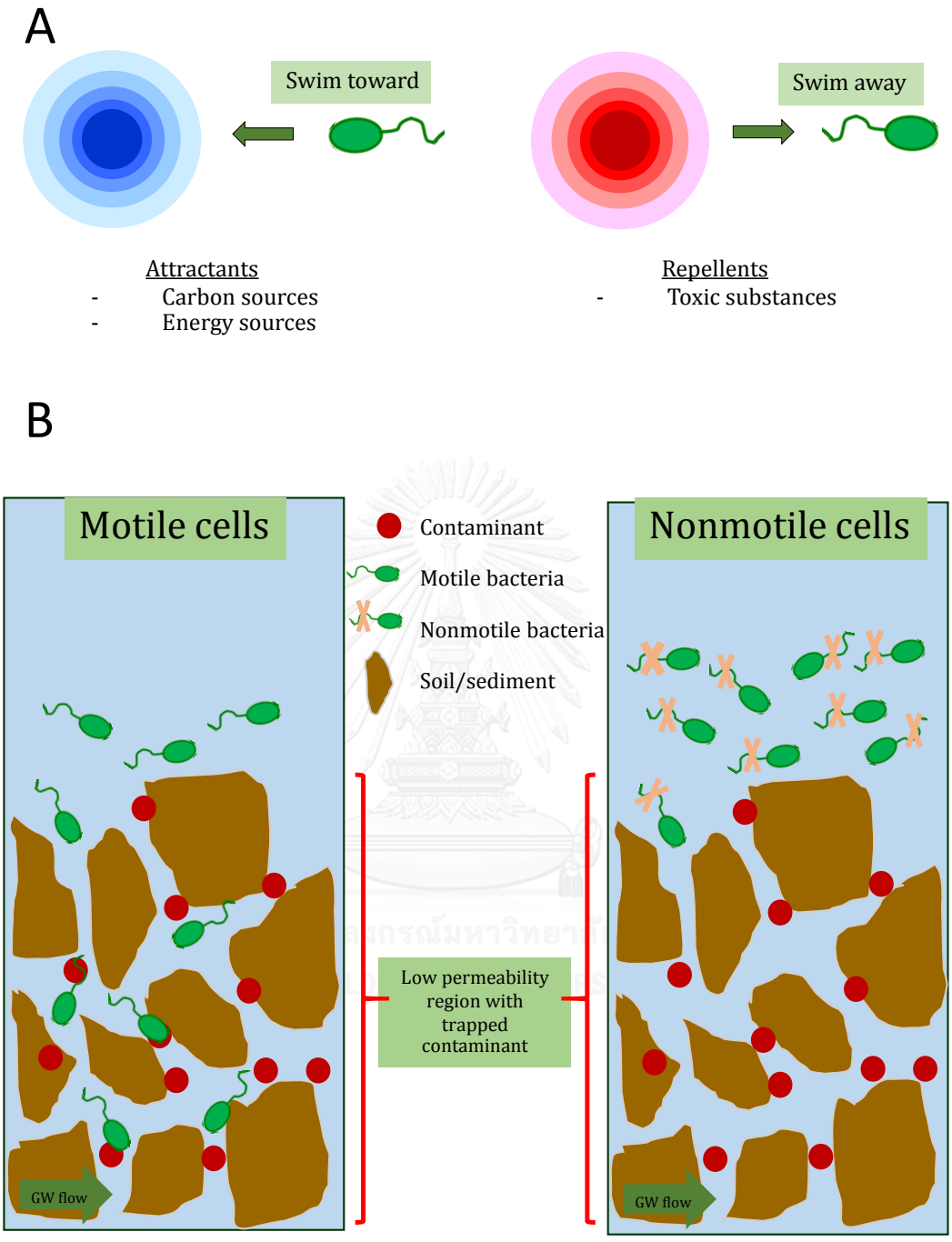

Figure 6.4 (A) Bacterial chemotactic ability allows bacteria to sense and move toward the preferred gradient of beneficial compounds and swim away from an unpreferred condition (e.g. high concentration of toxic compounds). (B) Bacterial chemotaxis may allow bacteria to reach the contaminant in low permeable region, thus increasing bioavailability of the contaminant and the efficiency of bioremediation process.

6.2.4) FTIR analysis

Gram negative bacteria exhibit the negative surface charge due to the presence of the carboxylic acids and phosphate esters (phosphoryl group) in their cell surface components (i.e. phospholipids, lipoproteins, lipopolysaccharides (LPS) and proteins) (Shephard et al., 2008; Wilson et al., 2001). The alteration of these surface components affects the surface properties of bacteria. Fourier Transform Infrared (FTIR) is a rapid and reliable method for detecting the structural changes in bacterial exposed to nanoparticles (Faghihzadeh et al., 2016; Hegde et al., 2016). The spectral region can be assigned to fatty acids (2800 – 3100 cm^{-1}), proteins and peptides (1500-1800 cm^{-1}), carbohydrates (900 -1200 cm^{-1}) and the fingerprint region (600 – 900 cm^{-1})(Faghihzadeh et al., 2016). The broad spectral from 3100 – 3700 cm^{-1} resulted from -OH (~ 3400 cm^{-1}) of water molecules (Naumann, 2006).

Figure 6.5A illustrated the FTIR spectra of nZVI particles. The main peak are at 1035 cm^{-1}, assigning to P-OFe complex (Parikh and Chorover, 2006). From Figure 6.5B, the main absorption bands of normal *P. putida* F1 cells (III), which represented by black line, are 1079 cm^{-1} (polysaccharide ring vibrations); 1236 cm^{-1}; 1392, 1454, 1534 cm^{-1}; 1653 cm^{-1} (amide I band, C=O); and 2928 cm^{-1} (CH_2 asymmetric stretching vibration from fatty acid). When normal cells of *P. putida* F1 were treated with nZVI for one hour, the obtained FTIR spectra (Figure 6.5B, red line) was similar to that of the nZVI particles (Figure 6.5A) showing dominant peaks at 1031 and 1646 cm^{-1}. It is possible that the absorption bands/pattern of nZVI particles sorbed/accumulated onto bacterial surface may mask/hinder the FTIR spectra of bacterial cells, causing the disappearance of of peak at 2800 – 3000 cm^{-1} and 1200 – 1600 cm^{-1} region. Upon nZVI exposure, the decreased peak intensity and shifted amide I at 1653 cm^{-1} from to 1646 cm^{-1}, suggesting the involvement of protein in the interaction between nZVI and bacterial cells.

The FTIR spectra of reversible SCV phenotype (persistent phenotype) obtained from tenth cycle of nZVI re-dosing (Figure 6.5C, black line) showed the similar pattern to that of nZVI (Figure 6.5A). According to previous progress, the accumulation of nZVI particles onto surface of the persistent phenotype is limited. It is possible that the the presence of residual nZVI particles from repetitive exposure or nZVI re-dosing, even though not abserbed onto cells surface, may interfere and hinder the FTIR spectra of bacterial surface. The re-dosing of persistent phenotype to nZVI (Figure 6.5C, red line) caused the shift of peak from 1647 to 1646 cm^{-1}, indicating the interaction between nZVI particles and bacterial proteins. The FTIR spectra of the SCV phenotype (Figure 6.5D, black line) is similar to that of the normal cells of *P. putida* F1 (Figure 6.5B, black line). The exposure of the SCV phenotype to nZVI (Figure 6.5D , red line) also resulted in the similar FTIR spectra to that of the nZVI particles (Figure 6.5A).

Jiang et al. studied the interaction between bacterial surface and metal oxide nanopaticles using FTIR analysis and proposed that the toxicity of metal oxide nanoparticles toward bacteria is due to the destruction of bacterial proteins and phospholipids (Jiang et al., 2010). The exposure of 80 mg/L of metal oxide nanoparticels, which are Al_2O_3, TiO_2, and ZnO nanoparticles, to a standard PE compound showed the presence of peak at 937 cm^{-1} assigned to PO_4^{3-}, which potentially be a product from the breakdown of PE molecules, indicating the destruction of bacterial membrane which subsequently cause cell death (Jiang et al., 2010). While FTIR analysis in this study may suggest the interaction between bacterial protein and nZVI particles, the effect of nZVI on other bacterial components is still unclear.

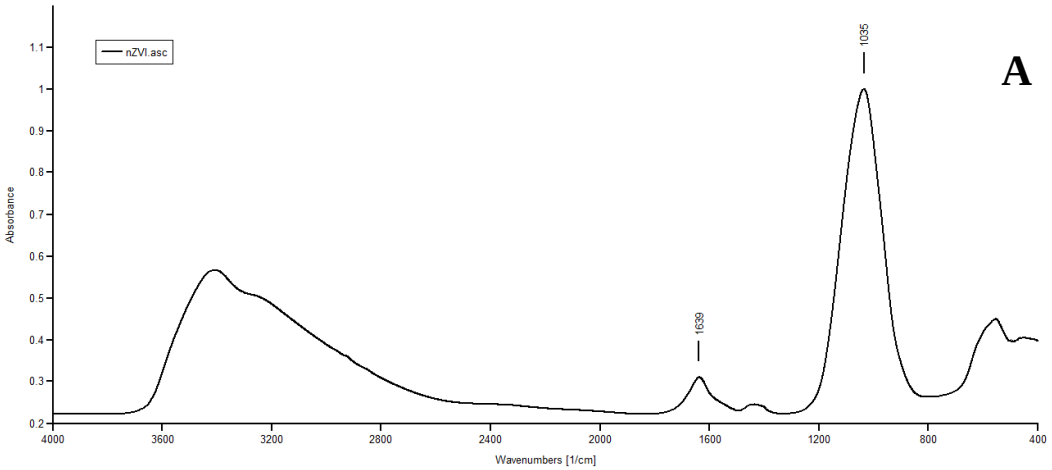
A
nZVI.asc
1035
1639
Absorbance
Wavenumbers [1/cm]

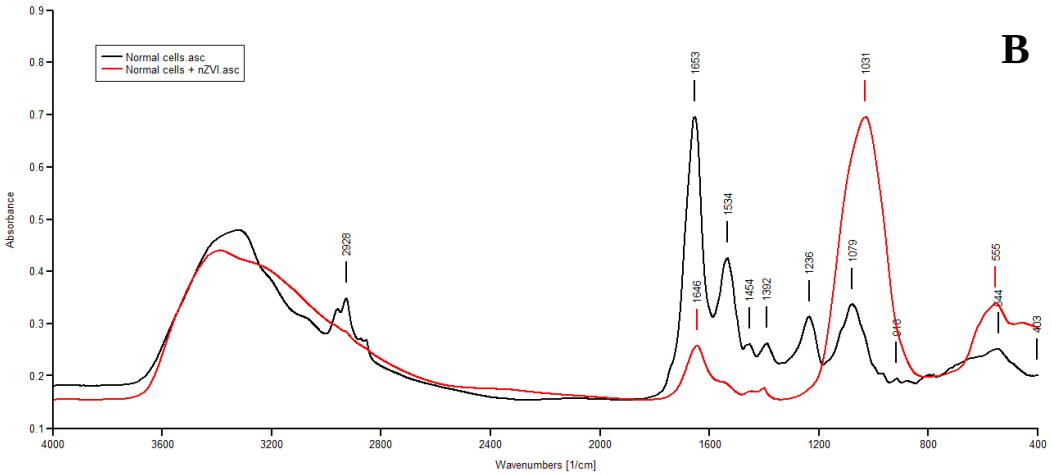
B
Normal cells.asc
Normal cells + nZVI.asc
1653
1031
1534
2928
1646
1454
1392
1236
1079
916
555
544
403
Absorbance
Wavenumbers [1/cm]

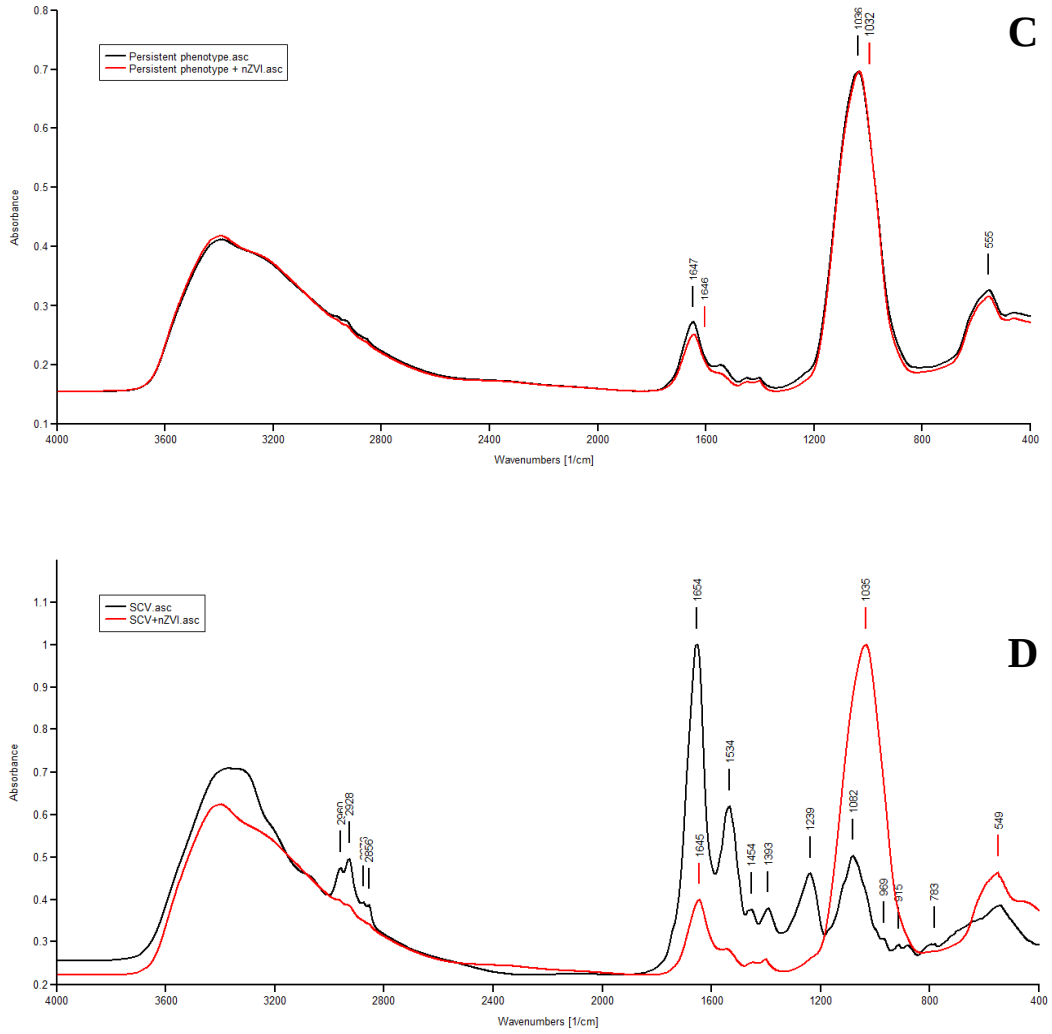

Figure 6.5 Fourier Transform Infrared (FTIR) spectra of (A) nZVI, the exposure of (B) normal cells of P. putida F1, (C) reversible SCV phenotype and (D) irreversible SCV phenotype to nZVI. The black line of (B), (C) and (D) represent the FTIR spectra of cells without nZVI exposure. The red line of (B), (C) and (D) represent the FTIR spectra of cells after exposed to 0.1 g/L of nZVI for one hour.

6.3) Summary

Effect of nZVI concentration, and roles of oxidative stress and iron species on the emergence of the SCV phenotype (or the persistent phenotype as designated in Chapter 4) of *P. putida* F1 upon repetitive exposure to nZVI were investigated. Additionally, the environmental-relevant characteristics of the irreversible phenotype were also reported. Since the SCV was more resistant to gentamicin, this antibiotic was selected as an indicator for determining the SCV phenotype. The higher frequency of the gentamicin-persistent SCV correlated with the increasing cycles of nZVI treatment. Interestingly, only single exposure of *P. putida* F1 to 0.5 and 1.0 g/L of nZVI could substantially increase the frequency of the SCV. It appears that the nZVI-induced oxidative stress mainly contributes to the induction of the SCV phenotype since the non-reactive form of nZVI as well as soluble Fe(III) did not cause the emergence of the phenotype. The re-injection of nZVI should be concerned because the newly injected nZVI may generate ROS which further initiate Fenton reaction with the nZVI remaining in contaminated site. Further characterization of the stable SCV phenotype revealed partial loss of bacterial environmental fitness including reduced growth under toluene as a carbon source and defective swimming motility and biofilm formation. While the environmental consequence of the transient SCV phenotype (Chapter 4) appears inconsiderable since they can revert back to the normal wildtype under nZVI-free condition, their gentamicin persistence should not be neglected as it may contribute to higher or multidrug resistance in the environment. FTIR technique was selected to assess the potential difference in the functional group on the surface of the normal cells and the persistent phenotype which may contribute to higher nZVI tolerance in the persistent phenotype. According to FTIR spectra, no significant difference between the surface functional group of the normal cells and the irreversible SCV phenotype was observed. The presence of residual nZVI during sample preparation or nZVI

exposure likely hinder the FTIR spectra of bacterial cells. Accordingly, the mechanism underlying nZVI tolerance of the persistent phenotype is remain unclear.

Chapter 7

Conclusions, Implications and Suggestions for Future Research

7.1) Conclusions

Despite its high contaminant removal efficiency and cost effectiveness, the potential nZVI toxicity to environmental microorganism could be an important drawback of nZVI application. This research try to fill the knowledge gap regarding environmental impact of nZVI, mainly by focusing on the effects of nZVI on bacterial cells as well as bacterial responses to the occurred damage. In attempt to relate the obtained information to environmentally relevant context, *P. putida* strains were selected as model strains in this study. Two forms of nZVI, the reactive nZVI (R-nZVI) and the oxidized nZVI (O-nZVI), were comparatively studied. As expected, R-nZVI exposure dramatically decreased bacterial viability. The exposure to O-nZVI, a less/non-reactive form of nZVI remained in the environment, still caused a considerable effect on cell viability, possibly due to the presence of small amount of Fe(II) which generate oxidative stress via Fenton reaction. Proteomic analysis revealed the nZVI-induced disturbance in bacterial membrane which is regardless of nZVI reactivity. Once bacterial membrane is disturbed, nZVI particles may internalize bacterial cells, interacting with cellular components or generating intracellular oxidative stress subsequently causing cells death. This observation accentuates the importance of contact between nZVI and bacterial cells for nZVI toxicity.

Despite the drastically reduced cell viability following nZVI exposure, the resilience was observed in prolonged nZVI exposure in the presence of carbon source. In regards to the preceding proteomic analysis, the research emphasized on the importance of nZVI-bacterial membrane interaction on nZVI toxicity as well as the adaptability of bacteria to counteract the disturbance in their membrane. Experimental results suggest that mainly by the conversion of *cis*- to *trans*-isomer of

monounsaturated fatty acid in membrane, to counteract the membrane fluidizing effect of nZVI particles.

The exposure of bacterial cells to nZVI induces the emergence of phenotypic variant of *P. putida* F1 exhibiting a remarkable small colony size and higher tolerance to nZVI thus considered as a nZVI-persistent phenotype or small colony variant. This emergence could be observed during the single exposure to high concentration of nZVI (0.5 and 1.0 g/L of nZVI) as well as the repetitive exposure to lower concentration of nZVI (0.1 g/L or nZVI). The nZVI-induced oxidative stress involves in the emergence of phenotypic variant, since the exposure to O-nZVI did not increase the amount of phenotypic variant. Even though the mechanism underlying the higher tolerance to nZVI is still unclear, the limited interaction between nZVI particles and persistent cells likely reduce nZVI toxicity.

Even though this persistent phenotype can revert to their parental characteristics after several sequential cultivation in the absence of nZVI, the irreversible/stable small colony variant was also detected. This irreversible SCV phenotype is defective in swimming motility and unable to produce exopolysaccharide/exopolymeric substance during biofilm formation. While *P. putida* F1 is well-known for toluene degradability, this phenotype is slightly more susceptible and poses a much longer lag phase in growth under toluene as sole carbon source compared to normal cells of *P. putida* F1. However, once acclimatized to toluene, the irreversible SCV phenotype is as effective as the normal phenotype for using toluene as its sole carbon source.

In conclusion, even though nZVI particles are toxic, bacterial cells can modify themselves, for example, by modifying their membrane composition, to counteract the nZVI-induced damage during nZVI exposure. This response mechanism allows bacterial cells to withstand and survive the occurred damages, resulting the regrowth

of cells (rebound in number of viable cells) after nZVI undergo oxidation and are no longer toxic to bacterial cells. At certain level, the nZVI-induced oxidative stress can induce the emergence of bacterial phenotype variant exhibiting different characteristics from the normal cells of bacteria.

7.2) Environmental implications

The findings from this research will be useful for designing and decision making for environmental application of nZVI. During in-situ injection of nZVI, nZVI particles tend aggregate and settle around the injection point. The high accumulation of nZVI, regardless of their reactivity, likely poses a severe damage to surrounding microorganism due to the high chance of contact between cells and nanoparticles. Several approaches aiming to increase nZVI mobility in the contaminated site may promote the risk of nZVI on non-potentially exposed microorganism residing afar from injection point. Mostly, the nZVI toxicity is concerned at high concentration of nZVI due to their significant effect on cell viability. However, except for nearby the injection point, the environmentally relevant concentration of nZVI is much lower. At certain concentration of nZVI (i.e. 0.1 and 1.0 g/L of nZVI in this research), bacterial cells can response to nZVI-induced damage particularly membrane disturbance thus resulting bacterial survival in the presence of nZVI. Bacterial adaptability is strain-dependent; nZVI exposure may diminish the presence of strains unadaptable to nZVI damage and promote the dominance of strains capable to adapt themselves to nZVI exposure. This may also explain the shift in bacterial community following nZVI exposure. Additionally, some nZVI injection strategies for example, re-dosing or re-circulation, may unintendedly promote the emergence of bacterial cells showing different characteristics and may alter the activity of bacteria in the environment.

7.3) Suggestions for future researches

The *in situ* applications of nZVI were typically conducted in subsurface contaminated area. However, the insightful information regarding nZVI toxicity mechanism under anaerobic condition is relatively limited and the adaptability of anaerobic microorganism is yet reported. The understanding about this subject will be useful for more accurate prediction of the environmental effect of nZVI during *in situ* application.

While the model strain, *P. putida* F1, can modify their membrane composition in response to nZVI-induced membrane damage, it is noteworthy that the *cis-trans* isomerization of unsaturated fatty acid has been reported in only certain bacterial strains (*Pseudomonas* and *Vibrio*) (Heipieper et al., 2003). Additionally, the proper membrane physical state is required for biological processes (Kim et al., 2002). Bacterial cells may lose their fitness, compensating for the survival under stress condition. Therefore, future work is recommended for response capability and mechanism of other common bacterial strains to nZVI as well as consequence of bacterial adaptation to nZVI.

Indigenous microorganisms typically confront the fluctuated/unflavorable environmental condition, especially those microorganisms inhabiting the contaminated site which are challenged by the presence of noxious compounds. Bacterial adaptation to these stressful conditions may affect their susceptibility to nZVI. While the introduction of the reactive nZVI to the contaminated sites may cause an additional adverse effect to indigenous microbes, bacterial adaptation to preexisted stress may induce a cross-protection against nZVI exposure. Accordingly, the studies on the effect of other environmental factors on nZVI toxicity as well as bacterial adaptability are required.

REFERENCES

Adeleye, A.S., Keller, A.A., Miller, R.J., and Lenihan, H.S. (2013). Persistence of commercial nanoscaled zero-valent iron (nZVI) and by-products. J Nanopart Res *15*, 1-18.

Ahn, J.Y., Kim, C., Kim, H.S., Hwang, K.Y., and Hwang, I. (2016). Effects of oxidants on in situ treatment of a DNAPL source by nanoscale zero-valent iron: A field study. Water Res *107*, 57-65.

Al Mamun, A.A. (2007). Elevated expression of DNA polymerase II increases spontaneous mutagenesis in Escherichia coli. Mutation research *625*, 29-39.

An, Y., Li, T., Jin, Z., Dong, M., Xia, H., and Wang, X. (2010). Effect of bimetallic and polymer-coated Fe nanoparticles on biological denitrification. Bioresource technology *101*, 9825-9828.

Appanna, V.D., and Finn, H. (1995). Microbial Adaptation to Iron - a Possible Role of Phosphatidylethanolamine in Iron Mineral Deposition. Biometals *8*, 142-148.

Auffan, M., Achouak, W., Rose, J., Roncato, M.A., Chaneac, C., Waite, D.T., Masion, A., Woicik, J.C., Wiesner, M.R., and Bottero, J.Y. (2008). Relation between the redox state of iron-based nanoparticles and their cytotoxicity toward Escherichia coli. Environmental Science & Technology *42*, 6730-6735.

Auger, C., Appanna, N.D., and Appanna, V.D. (2016). Metabolic Networks to Counter Al Toxicity in Pseudomonas Fluorescens: A Holistic View. In Stress and Environmental Regulation of Gene Expression and Adaptation in Bacteria (John Wiley & Sons, Inc.), pp. 1145-1153.

Auger, C., Han, S., Appanna, V.P., Thomas, S.C., Ulibarri, G., and Appanna, V.D. (2013). Metabolic reengineering invoked by microbial systems to decontaminate aluminum: implications for bioremediation technologies. Biotechnol Adv *31*, 266-273.

Baquero, F. (2001). Low-level antibacterial resistance: a gateway to clinical resistance. Drug resistance updates : reviews and commentaries in antimicrobial and anticancer chemotherapy *4*, 93-105.

Barzan, E., Mehrabian, S., and Irian, S. (2014). Antimicrobial and Genotoxicity Effects of Zero-valent Iron Nanoparticles. Jundishapur J Microbiol *7*, e10054.

Benndorf, D., Thiersch, M., Loffhagen, N., Kunath, C., and Harms, H. (2006). Pseudomonas putida KT2440 responds specifically to chlorophenoxy herbicides and their initial metabolites. Proteomics *6*, 3319-3329.

Bernal, P., Segura, A., and Ramos, J.L. (2007). Compensatory role of the cis-trans-isomerase and cardiolipin synthase in the membrane fluidity of Pseudomonas putida DOT-T1E. Environ Microbiol *9*, 1658-1664.

Blankenfeldt, W., Asuncion, M., Lam, J.S., and Naismith, J.H. (2000). The structural basis of the catalytic mechanism and regulation of glucose-1-phosphate thymidylyltransferase (RmlA). EMBO J *19*, 6652-6663.

Bligh, E.G., and Dyer, W.J. (1959). A rapid method of total lipid extraction and purification. Canadian journal of biochemistry and physiology *37*, 911-917.

Boles, B.R., and Singh, P.K. (2008). Endogenous oxidative stress produces diversity and adaptability in biofilm communities. Proc Natl Acad Sci U S A *105*, 12503-12508.

Bose, R.S., Dey, S., Saha, S., Ghosh, C.K., and Chaudhuri, M.G. (2016). Enhanced removal of dissolved aniline from water under combined system of nano zero-valent iron and Pseudomonas putida. Sustainable Water Resources Management *2*, 143-159.

Bukau, B. (1993). Regulation of the Escherichia coli heat-shock response. Mol Microbiol *9*, 671-680.

Cabiscol, E., Tamarit, J., and Ros, J. (2000). Oxidative stress in bacteria and protein damage by reactive oxygen species. International microbiology : the official journal of the Spanish Society for Microbiology *3*, 3-8.

Calderon, B., and Fullana, A. (2015). Heavy metal release due to aging effect during zero valent iron nanoparticles remediation. Water Res *83*, 1-9.

Ceragioli, M., Mols, M., Moezelaar, R., Ghelardi, E., Senesi, S., and Abee, T. (2010). Comparative transcriptomic and phenotypic analysis of the responses of Bacillus cereus to various disinfectant treatments. Appl Environ Microbiol *76*, 3352-3360.

Chaithawiwat, K., Vangnai, A., McEvoy, J.M., Pruess, B., Krajangpan, S., and Khan, E. (2016a). Impact of nanoscale zero valent iron on bacteria is growth phase dependent. Chemosphere *144*, 352-359.

Chaithawiwat, K., Vangnai, A., McEvoy, J.M., Pruess, B., Krajangpan, S., and Khan, E. (2016b). Role of oxidative stress in inactivation of *Escherichia coli* BW25113 by nanoscale zero-valent iron. Sci Total Environ *565*, 857-862.

Chang, M.C., and Kang, H.Y. (2009). Remediation of pyrene-contaminated soil by synthesized nanoscale zero-valent iron particles. Journal of environmental science and health Part A, Toxic/hazardous substances & environmental engineering *44*, 576-582.

Chen, J., Xiu, Z., Lowry, G.V., and Alvarez, P.J. (2011a). Effect of natural organic matter on toxicity and reactivity of nano-scale zero-valent iron. Water Res *45*, 1995-2001.

Chen, J., Xiu, Z., Lowry, G.V., and Alvarez, P.J.J. (2011b). Effect of natural organic matter on toxicity and reactivity of nano-scale zero-valent iron. Water Research *45*, 1995-2001.

Chen, J.H., Qiu, X.Q., Fang, Z.Q., Yang, M., Pokeung, T., Gu, F.L., Cheng, W., and Lan, B.Y. (2012). Removal mechanism of antibiotic metronidazole from aquatic solutions by using nanoscale zero-valent iron particles. Chemical Engineering Journal *181*, 113-119.

Chenier, D., Beriault, R., Mailloux, R., Baquie, M., Abramia, G., Lemire, J., and Appanna, V. (2008). Involvement of Fumarase C and NADH Oxidase in Metabolic Adaptation of Pseudomonas fluorescens Cells Evoked by Aluminum and Gallium Toxicity. Applied and Environmental Microbiology *74*, 3977-3984.

Choi, O., Deng, K.K., Kim, N.J., Ross, L., Surampalli, R.Y., and Hu, Z.Q. (2008). The inhibitory effects of silver nanoparticles, silver ions, and silver chloride colloids on microbial growth. Water Research *42*, 3066-3074.

Choi, O., and Hu, Z. (2008). Size Dependent and Reactive Oxygen Species Related Nanosilver Toxicity to Nitrifying Bacteria. Environmental Science & Technology *42*, 4583-4588.

Chung, H.J., Bang, W., and Drake, M.A. (2006). Stress Response of Escherichia coli. Comprehensive Reviews in Food Science and Food Safety *5*, 52-64.

Cornelis, P., Matthijs, S., and Van Oeffelen, L. (2009). Iron uptake regulation in <i>Pseudomonas aeruginosa</i&gt. BioMetals *22*, 15-22.

Cox, R.J. (1996). The DAP pathway to lysine as a target for antimicrobial agents. Natural Product Reports *13*, 29-43.

Dan, Z.G., Ni, H.W., Xu, B.F., Xiong, J., and Xiong, P.Y. (2005). Microstructure and antibacterial properties of AISI 420 stainless steel implanted by copper ions. Thin Solid Films *492*, 93-100.

Davey, M.E., and O'toole, G.A. (2000). Microbial Biofilms: from Ecology to Molecular Genetics. Microbiology and Molecular Biology Reviews *64*, 847-867.

de Kok, A., Hengeveld, A.F., Martin, A., and Westphal, A.H. (1998). The pyruvate dehydrogenase multi-enzyme complex from Gram-negative bacteria. Biochimica et Biophysica Acta (BBA) - Protein Structure and Molecular Enzymology *1385*, 353-366.

Demple, B. (1996). Redox signaling and gene control in the Escherichia coli soxRS oxidative stress regulon — a review. Gene *179*, 53-57.

Dhas, S.P., Shiny, P.J., Khan, S., Mukherjee, A., and Chandrasekaran, N. (2014). Toxic behavior of silver and zinc oxide nanoparticles on environmental microorganisms. Journal of Basic Microbiology *54*, 916-927.

Diao, M., and Yao, M. (2009a). Use of zero-valent iron nanoparticles in inactivating microbes. Water Res *43*, 5243-5251.

Diao, M., and Yao, M. (2009b). Use of zero-valent iron nanoparticles in inactivating microbes. Water Res *43*, 5243-5251.

Diao, M.H., and Yao, M.S. (2009c). Use of zero-valent iron nanoparticles in inactivating microbes. Water Research *43*, 5243-5251.

Dong, Y., Chen, Y.-Y.M., Snyder, J.A., and Burne, R.A. (2002). Isolation and Molecular Analysis of the Gene Cluster for the Arginine Deiminase System from

Streptococcus gordonii DL1. Applied and Environmental Microbiology *68*, 5549-5553.

Dos Santos, V., Heim, S., Moore, E., Stratz, M., and Timmis, K. (2004). Insights into the genomic basis of niche specificity of Pseudomonas putida KT2440. Environ Microbiol *6*, 1264 - 1286.

Edwards, A.M. (2012). Phenotype Switching Is a Natural Consequence of Staphylococcus aureus Replication. Journal of Bacteriology *194*, 5404-5412.

El-Temsah, Y.S., and Joner, E.J. (2013). Effects of nano-sized zero-valent iron (nZVI) on DDT degradation in soil and its toxicity to collembola and ostracods. Chemosphere *92*, 131-137.

Elliott, D.W., and Zhang, W.-x. (2001). Field assessment of nanoscale bimetallic particles for groundwater treatment. Environmental Science & Technology *35*, 4922-4926.

Faghihzadeh, F., Anaya, N.M., Schifman, L.A., and Oyanedel-Craver, V. (2016). Fourier transform infrared spectroscopy to assess molecular-level changes in microorganisms exposed to nanoparticles. Nanotechnology for Environmental Engineering *1*, 1.

Fajardo, C., Ortíz, L.T., Rodríguez-Membibre, M.L., Nande, M., Lobo, M.C., and Martin, M. (2012). Assessing the impact of zero-valent iron (ZVI) nanotechnology on soil microbial structure and functionality: A molecular approach. Chemosphere *86*, 802-808.

Fajardo, C., Sacca, M.L., Martinez-Gomariz, M., Costa, G., Nande, M., and Martin, M. (2013). Transcriptional and proteomic stress responses of a soil bacterium Bacillus cereus to nanosized zero-valent iron (nZVI) particles. Chemosphere *93*, 1077-1083.

Fang, J., Barcelona, M.J., and Alvarez, P.J.J. (2000). Phospholipid compositional changes of five pseudomonad archetypes grown with and without toluene. Applied Microbiology and Biotechnology *54*, 382-389.

Fang, J., Lyon, D.Y., Wiesner, M.R., Dong, J., and Alvarez (2007). Effect of a Fullerene Water Suspension on Bacterial Phospholipids and Membrane Phase Behavior. Environmental Science & Technology *41*, 2636-2642.

Fang, Z., Chen, J., Qiu, X., Qiu, X., Cheng, W., and Zhu, L. (2011). Effective removal of antibiotic metronidazole from water by nanoscale zero-valent iron particles. Desalination *268*, 60-67.

Farr, S.B., and Kogoma, T. (1991). Oxidative stress responses in Escherichia coli and Salmonella typhimurium. Microbiol Mol Biol Rev *55*, 561-585.

Fauvart, M., De Groote, V.N., and Michiels, J. (2011). Role of persister cells in chronic infections: clinical relevance and perspectives on anti-persister therapies. Journal of Medical Microbiology *60*, 699-709.

Fischer, G. (1994). Peptidyl-Prolyl cis/trans Isomerases and Their Effectors. Angewandte Chemie International Edition in English *33*, 1415-1436.

Fraud, S., and Poole, K. (2011). Oxidative Stress Induction of the MexXY Multidrug Efflux Genes and Promotion of Aminoglycoside Resistance Development in Pseudomonas aeruginosa. Antimicrobial Agents and Chemotherapy *55*, 1068-1074.

French, S., Puddephatt, D., Habash, M., and Glasauer, S. (2013). The dynamic nature of bacterial surfaces: Implications for metal–membrane interaction. Critical reviews in microbiology *39*, 196-217.

Fu, Y., Peng, L., Zeng, Q., Yang, Y., Song, H., Shao, J., Liu, S., and Gu, J. (2015). High efficient removal of tetracycline from solution by degradation and flocculation with nanoscale zerovalent iron. Chemical Engineering Journal *270*, 631-640.

García, J.J., Martínez-Ballarín, E., Millán-Plano, S., Allué, J.L., Albendea, C., Fuentes, L., and Escanero, J.F. (2005). Effects of trace elements on membrane fluidity. Journal of Trace Elements in Medicine and Biology *19*, 19-22.

Gavaskar A., T.L., Condit W. (2005). Cost and performance report nanoscale zero-valent iron technologie for source remediation. Naval Facilities Engineering Command (NAVFAC) *Contract report: CR-05-007-ENV*.

Gou, N., Onnis-Hayden, A., and Gu, A.Z. (2010). Mechanistic Toxicity Assessment of Nanomaterials by Whole-Cell-Array Stress Genes Expression Analysis. Environmental Science & Technology *44*, 5964-5970.

Grieger, K.D., Fjordbøge, A., Hartmann, N.B., Eriksson, E., Bjerg, P.L., and Baun, A. (2010). Environmental benefits and risks of zero-valent iron nanoparticles (nZVI) for in situ remediation: Risk mitigation or trade-off? Journal of contaminant hydrology *118*, 165-183.

Ha, D.-G., Kuchma, S.L., and O'Toole, G.A. (2014). Plate-Based Assay for Swimming Motility in Pseudomonas aeruginosa. In Pseudomonas Methods and Protocols, A. Filloux, and J.-L. Ramos, eds. (New York, NY: Springer New York), pp. 59-65.

Hachicho, N., Hoffmann, P., Ahlert, K., and Heipieper, H.J. (2014). Effect of silver nanoparticles and silver ions on growth and adaptive response mechanisms of Pseudomonas putida mt-2. FEMS Microbiology Letters *355*, 71-77.

Hanay, Ö., and Türk, H. (2015). Comprehensive evaluation of adsorption and degradation of tetracycline and oxytetracycline by nanoscale zero-valent iron. Desalination and Water Treatment *53*, 1986-1994.

Händel, N., Schuurmans, J.M., Brul, S., and ter Kuile, B.H. (2013). Compensation of the Metabolic Costs of Antibiotic Resistance by Physiological Adaptation in Escherichia coli. Antimicrobial Agents and Chemotherapy *57*, 3752-3762.

Hansson, H., Kaczala, F., Marques, M., and Hogland, W. (2012). Photo-Fenton and Fenton Oxidation of Recalcitrant Industrial Wastewater Using Nanoscale Zero-Valent Iron. International Journal of Photoenergy *2012*, 11.

Harrison, J.J., Ceri, H., and Turner, R.J. (2007). Multimetal resistance and tolerance in microbial biofilms. Nat Rev Micro *5*, 928-938.

He, D., Ma, J., Collins, R.N., and Waite, T.D. (2016). Effect of Structural Transformation of Nanoparticulate Zero-Valent Iron on Generation of Reactive Oxygen Species. Environmental Science & Technology *50*, 3820-3828.

He, F., Zhao, D., Liu, J., and Roberts, C.B. (2006). Stabilization of Fe–Pd Nanoparticles with Sodium Carboxymethyl Cellulose for Enhanced Transport and Dechlorination of Trichloroethylene in Soil and Groundwater. Industrial & Engineering Chemistry Research *46*, 29-34.

Hegde, K., Brar, S.K., Verma, M., and Surampalli, R.Y. (2016). Current understandings of toxicity, risks and regulations of engineered nanoparticles with respect to

environmental microorganisms. Nanotechnology for Environmental Engineering *1*, 5.

Heinzen, R.A., Mo, Y.-Y., Robertson, S.J., and Mallavia, L.P. (1995). Characterization of the succinate dehydrogenase-encoding gene cluster (sdh) from the rickettsia coxiella burnetii. Gene *155*, 27-34.

Heipieper, H.J., Meinhardt, F., and Segura, A. (2003). The cis–trans isomerase of unsaturated fatty acids in Pseudomonas and Vibrio: biochemistry, molecular biology and physiological function of a unique stress adaptive mechanism. FEMS Microbiology Letters *229*, 1-7.

Henderson, R.J., Millar, R.M., Sargent, J.R., and Jostensen, J.P. (1993). Trans-monoenoic and polyunsaturated fatty acids in phospholipids of aVibrio species of bacterium in relation to growth conditions. Lipids *28*, 389-396.

Henn, K.W., and Waddill, D.W. (2006). Utilization of nanoscale zero-valent iron for source remediation—A case study. Remediation Journal *16*, 57-77.

Herzberg, M., Dosoretz, C.G., Kuhn, J., Klein, S., and Green, M. (2006). Visualization of active biomass distribution in a BGAC fluidized bed reactor using GFP tagged Pseudomonas putida F1. Water Research *40*, 2704-2712.

Hidese, R., Mihara, H., Kurihara, T., and Esaki, N. (2012). Pseudomonas putida PydR, a RutR-like transcriptional regulator, represses the dihydropyrimidine dehydrogenase gene in the pyrimidine reductive catabolic pathway. The Journal of Biochemistry *152*, 341-346.

Hiniker, A., Collet, J.-F., and Bardwell, J.C.A. (2005). Copper Stress Causes an in Vivo Requirement for the Escherichia coli Disulfide Isomerase DsbC. Journal of Biological Chemistry *280*, 33785-33791.

Holden, P.A., Gardea-Torresdey, J.L., Klaessig, F., Turco, R.F., Mortimer, M., Hund-Rinke, K., Cohen Hubal, E.A., Avery, D., Barceló, D., Behra, R*., et al.* (2016). Considerations of environmentally relevant test conditions for improved evaluation of ecological hazards of engineered nanomaterials. Environmental Science & Technology *50*, 6124-6145.

Hoshino, N., Kimura, T., Yamaji, A., and Ando, T. (1999). Damage to the cytoplasmic membrane of Escherichia Coli by catechin-copper (II) complexes. Free Radical Biology and Medicine *27*, 1245-1250.

Hottes, A.K., Freddolino, P.L., Khare, A., Donnell, Z.N., Liu, J.C., and Tavazoie, S. (2013). Bacterial Adaptation through Loss of Function. PLOS Genetics *9*, e1003617.

Hutton, C.A., Perugini, M.A., and Gerrard, J.A. (2007). Inhibition of lysine biosynthesis: an evolving antibiotic strategy. Molecular BioSystems *3*, 458-465.

Hwang, Y., Lee, Y.-C., Mines, P.D., Huh, Y.S., and Andersen, H.R. (2014). Nanoscale zero-valent iron (nZVI) synthesis in a Mg-aminoclay solution exhibits increased stability and reactivity for reductive decontamination. Applied Catalysis B: Environmental *147*, 748-755.

Imlay, J.A., and Linn, S. (1987). Mutagenesis and stress responses induced in Escherichia coli by hydrogen peroxide. J Bacteriol *169*, 2967-2976.

Inaba, M., Suzuki, I., Szalontai, B., Kanesaki, Y., Los, D.A., Hayashi, H., and Murata, N. (2003). Gene-engineered Rigidification of Membrane Lipids Enhances the Cold Inducibility of Gene Expression in Synechocystis. Journal of Biological Chemistry *278*, 12191-12198.

Jagadevan, S., Jayamurthy, M., Dobson, P., and Thompson, I.P. (2012). A novel hybrid nano zerovalent iron initiated oxidation – Biological degradation approach for remediation of recalcitrant waste metalworking fluids. Water Research *46*, 2395-2404.

Jang, M.-H., Lim, M., and Hwang, Y.S. (2014). Potential environmental implications of nanoscale zero-valent iron particles for environmental remediation. Environmental health and toxicology *29*, e2014022.

Jassem, A.N., Forbes, C.M., and Speert, D.P. (2014). Investigation of aminoglycoside resistance inducing conditions and a putative AmrAB-OprM efflux system in Burkholderia vietnamiensis. Annals of Clinical Microbiology and Antimicrobials *13*, 2.

Jiang, C., Xu, X., Megharaj, M., Naidu, R., and Chen, Z. (2015). Inhibition or promotion of biodegradation of nitrate by *Paracoccus* sp. in the presence of nanoscale zero-valent iron. Science of The Total Environment *530–531*, 241-246.

Jiang, W., Yang, K., Vachet, R.W., and Xing, B.S. (2010). Interaction between Oxide Nanoparticles and Biomolecules of the Bacterial Cell Envelope As Examined by Infrared Spectroscopy. Langmuir *26*, 18071-18077.

Kabir, M.M., and Shimizu, K. (2006). Investigation into the effect of soxR and soxS genes deletion on the central metabolism of Escherichia coli based on gene expressions and enzyme activities. Biochemical Engineering Journal *30*, 39-47.

Keenan, C.R., Goth-Goldstein, R., Lucas, D., and Sedlak, D.L. (2009). Oxidative stress induced by zero-valent iron nanoparticles and Fe(II) in human bronchial epithelial cells. Environmental Science & Technology *43*, 4555-4560.

Keller, A.A., Garner, K., Miller, R.J., and Lenihan, H.S. (2012). Toxicity of nano-zero valent iron to freshwater and marine organisms. PLoS one *7*, e43983.

Kim, H.-J., Leitch, M., Naknakorn, B., Tilton, R.D., and Lowry, G.V. (2017). Effect of emplaced nZVI mass and groundwater velocity on PCE dechlorination and hydrogen evolution in water-saturated sand. Journal of hazardous materials *322, Part A*, 136-144.

Kim, I.S., Beaudette, L.A., Cassidy, M.B., Lee, H., and Trevors, J.T. (2002). Alterations in fatty acid composition and fluidity of cell membranes affect the accumulation of PCB congener 2,2′,5,5′-tetrachlorobiphenyl by Ralstonia eutropha H850. Journal of Chemical Technology and Biotechnology *77*, 793-799.

Kim, J., and Park, W. (2014). Oxidative stress response in Pseudomonas putida. Applied Microbiology and Biotechnology *98*, 6933-6946.

Kim, J.S., Kuk, E., Yu, K.N., Kim, J.-H., Park, S.J., Lee, H.J., Kim, S.H., Park, Y.K., Park, Y.H., Hwang, C.-Y., *et al.* (2007). Antimicrobial effects of silver nanoparticles. Nanomedicine: Nanotechnology, Biology and Medicine *3*, 95-101.

Kim, J.Y., Park, H.-J., Lee, C., Nelson, K.L., Sedlak, D.L., and Yoon, J. (2010). Inactivation of Escherichia coli by Nanoparticulate Zerovalent Iron and Ferrous Ion. Appl Environ Microb *76*, 7668-7670.

Kim, Y.M., Murugesan, K., Chang, Y.Y., Kim, E.J., and Chang, Y.S. (2012). Degradation of polybrominated diphenyl ethers by a sequential treatment with nanoscale zero valent iron and aerobic biodegradation. Journal of Chemical Technology and Biotechnology *87*, 216-224.

Kirschling, T.L., Gregory, K.B., Minkley, J.E.G., Lowry, G.V., and Tilton, R.D. (2010). Impact of Nanoscale Zero Valent Iron on Geochemistry and Microbial Populations in Trichloroethylene Contaminated Aquifer Materials. Environmental Science & Technology *44*, 3474-3480.

Kocur, C.M.D., Lomheim, L., Molenda, O., Weber, K.P., Austrins, L.M., Sleep, B.E., Boparai, H.K., Edwards, E.A., and O'Carroll, D.M. (2016). Long-Term Field Study of Microbial Community and Dechlorinating Activity Following Carboxymethyl Cellulose-Stabilized Nanoscale Zero-Valent Iron Injection. Environmental Science & Technology *50*, 7658-7670.

Krewulak, K.D., and Vogel, H.J. (2008). Structural biology of bacterial iron uptake. Biochimica et Biophysica Acta (BBA) - Biomembranes *1778*, 1781-1804.

Kuang, Y., Zhou, Y., Chen, Z., Megharaj, M., and Naidu, R. (2013). Impact of Fe and Ni/Fe nanoparticles on biodegradation of phenol by the strain Bacillus fusiformis (BFN) at various pH values. Bioresource technology *136*, 588-594.

Kultz, D. (2005). Molecular and evolutionary basis of the cellular stress response. Annu Rev Physiol *67*, 225-257.

Kumar, N., Omoregie, E.O., Rose, J., Masion, A., Lloyd, J.R., Diels, L., and Bastiaens, L. (2014). Inhibition of sulfate reducing bacteria in aquifer sediment by iron nanoparticles. Water Research *51*, 64-72.

Kurenbach, B., Marjoshi, D., Amábile-Cuevas, C.F., Ferguson, G.C., Godsoe, W., Gibson, P., and Heinemann, J.A. (2015). Sublethal Exposure to Commercial Formulations of the Herbicides Dicamba, 2,4-Dichlorophenoxyacetic Acid, and Glyphosate Cause Changes in Antibiotic Susceptibility in Escherichia coli and Salmonella enterica serovar Typhimurium. mBio *6*.

Langley, S., and Beveridge, T.J. (1999). Effect of O-side-chain-lipopolysaccharide chemistry on metal binding. Appl Environ Microbiol *65*, 489-498.

Laumann, S., Micić, V., and Hofmann, T. (2014). Mobility enhancement of nanoscale zero-valent iron in carbonate porous media through co-injection of polyelectrolytes. Water Research *50*, 70-79.

Law, A.M.J., and Aitken, M.D. (2003). Bacterial Chemotaxis to Naphthalene Desorbing from a Nonaqueous Liquid. Applied and Environmental Microbiology *69*, 5968-5973.

Le, T.T., Murugesan, K., Kim, E.-J., and Chang, Y.-S. (2014). Effects of inorganic nanoparticles on viability and catabolic activities of Agrobacterium sp. PH-08 during biodegradation of dibenzofuran. Biodegradation *25*, 655-668.

Lee, C., Kim, J.Y., Lee, W.I., Nelson, K.L., Yoon, J., and Sedlak, D.L. (2008a). Bactericidal Effect of Zero-Valent Iron Nanoparticles on Escherichia coli. Environ Sci Technol *42*, 4927-4933.

Lee, C., Kim, J.Y., Lee, W.I., Nelson, K.L., Yoon, J., and Sedlak, D.L. (2008b). Bactericidal effect of zero-valent Iron nanoparticles on *Escherichia coli*. Environ Sci Technol *42*, 4927-4933.

Lee, H., Lee, H.-j., Kim, H.-E., Kweon, J., Lee, B.-D., and Lee, C. (2014). Oxidant production from corrosion of nano- and microparticulate zero-valent iron in the presence of oxygen: A comparative study. Journal of hazardous materials *265*, 201-207.

Lefevre, E., Bossa, N., Wiesner, M.R., and Gunsch, C.K. (2016). A review of the environmental implications of in situ remediation by nanoscale zero valent iron (nZVI): Behavior, transport and impacts on microbial communities. Sci Total Environ *565*, 889-901.

Li, D., Zeng, S., He, M., and Gu, A.Z. (2016). Water Disinfection Byproducts Induce Antibiotic Resistance-Role of Environmental Pollutants in Resistance Phenomena. Environmental Science & Technology *50*, 3193-3201.

Li, H., Zhou, Q., Wu, Y., Fu, J., Wang, T., and Jiang, G. (2009). Effects of waterborne nano-iron on medaka (Oryzias latipes): Antioxidant enzymatic activity, lipid

peroxidation and histopathology. Ecotoxicology and Environmental Safety *72*, 684-692.

Li, R., Jin, X., Megharaj, M., Naidu, R., and Chen, Z. (2015a). Heterogeneous Fenton oxidation of 2,4-dichlorophenol using iron-based nanoparticles and persulfate system. Chemical Engineering Journal *264*, 587-594.

Li, S.-S., Hu, X., Zhao, H., Li, Y.-X., Zhang, L., Gong, L.-J., Guo, J., and Zhao, H.-B. (2015b). Quantitative analysis of cellular proteome alterations of Pseudomonas putida to naphthalene-induced stress. Biotechnology Letters *37*, 1645-1654.

Li, X.-q., Elliott, D.W., and Zhang, W.-x. (2006). Zero-valent iron nanoparticles for abatement of environmental pollutants: materials and engineering aspects. Critical Reviews in Solid State and Materials Sciences *31*, 111 - 122.

Li, X.-q., and Zhang, W.-x. (2006). Iron nanoparticles: the core–shell structure and unique properties for Ni(II) sequestration. Langmuir *22*, 4638-4642.

Li, Y., Niu, J., Zhang, W., Zhang, L., and Shang, E. (2014). Influence of Aqueous Media on the ROS-Mediated Toxicity of ZnO Nanoparticles toward Green Fluorescent Protein-Expressing Escherichia coli under UV-365 Irradiation. Langmuir *30*, 2852-2862.

Li, Z., Greden, K., Alvarez, P.J.J., Gregory, K.B., and Lowry, G.V. (2010). Adsorbed Polymer and NOM Limits Adhesion and Toxicity of Nano Scale Zerovalent Iron to E. coli. Environmental Science & Technology *44*, 3462-3467.

Lim, T.-T., and Zhu, B.-W. (2008). Effects of anions on the kinetics and reactivity of nanoscale Pd/Fe in trichlorobenzene dechlorination. Chemosphere *73*, 1471-1477.

Ling, J., Reynolds, N., and Ibba, M. (2009). Aminoacyl-tRNA Synthesis and Translational Quality Control. Annual Review of Microbiology *63*, 61-78.

Liu, A., Liu, J., Pan, B., and Zhang, W.-x. (2014). Formation of lepidocrocite ([gamma]-FeOOH) from oxidation of nanoscale zero-valent iron (nZVI) in oxygenated water. RSC Advances *4*, 57377-57382.

Liu, Y., Majetich, S.A., Tilton, R.D., Sholl, D.S., and Lowry, G.V. (2005). TCE dechlorination rates, pathways, and efficiency of nanoscale iron particles

with different properties. Environmental Science & Technology *39*, 1338-1345.

Liu, Y., Phenrat, T., and Lowry, G.V. (2007). Effect of TCE Concentration and Dissolved Groundwater Solutes on NZVI-Promoted TCE Dechlorination and H2 Evolution. Environmental Science & Technology *41*, 7881-7887.

Lok, C.-N., Ho, C.-M., Chen, R., He, Q.-Y., Yu, W.-Y., Sun, H., Tam, P.K.-H., Chiu, J.-F., and Che, C.-M. (2006). Proteomic Analysis of the Mode of Antibacterial Action of Silver Nanoparticles. Journal of Proteome Research *5*, 916-924.

Lowry, G.V., Casman, E.A. (2009). Nanomaterial transport, transformation, and fate in the environment: a risk-based perspective on research needs. Nanomaterials: Risks and Benefits, 125–137.

Lowry, G.V., Gregory, K.B., Apte, S.C., and Lead, J.R. (2012). Transformations of Nanomaterials in the Environment. Environ Sci Technol *46*, 6893-6899.

Ma, Y., Metch, J.W., Vejerano, E.P., Miller, I.J., Leon, E.C., Marr, L.C., Vikesland, P.J., and Pruden, A. (2015). Microbial community response of nitrifying sequencing batch reactors to silver, zero-valent iron, titanium dioxide and cerium dioxide nanomaterials. Water Research *68*, 87-97.

Macé, C., Desrocher, S., Gheorghiu, F., Kane, A., Pupeza, M., Cernik, M., Kvapil, P., Venkatakrishnan, R., and Zhang, W.-x. (2006). Nanotechnology and groundwater remediation: A step forward in technology understanding. Remediation Journal *16*, 23-33.

Machado, S., Stawiński, W., Slonina, P., Pinto, A.R., Grosso, J.P., Nouws, H.P.A., Albergaria, J.T., and Delerue-Matos, C. (2013). Application of green zero-valent iron nanoparticles to the remediation of soils contaminated with ibuprofen. Science of The Total Environment *461–462*, 323-329.

Mager, W., and De Kruijff, A. (1995). Stress-induced transcriptional activation. Microbiol Rev *59*, 506-531.

Markwell, M.A.K., Haas, S.M., Bieber, L.L., and Tolbert, N.E. (1978). A modification of the Lowry procedure to simplify protein determination in membrane and lipoprotein samples. Analytical Biochemistry *87*, 206-210.

Martinez, J.L., Sánchez, M.B., Martínez-Solano, L., Hernandez, A., Garmendia, L., Fajardo, A., and Alvarez-Ortega, C. (2009). Functional role of bacterial multidrug efflux pumps in microbial natural ecosystems. FEMS microbiology reviews *33*, 430-449.

Marx, R.B., and Aitken, M.D. (2000). Bacterial Chemotaxis Enhances Naphthalene Degradation in a Heterogeneous Aqueous System. Environmental Science & Technology *34*, 3379-3383.

Maurer-Jones, M.A., Gunsolus, I.L., Murphy, C.J., and Haynes, C.L. (2013). Toxicity of engineered nanoparticles in the environment. Analytical Chemistry *85*, 3036-3049.

Missiakas, D., and Raina, S. (1997). Protein folding in the bacterial periplasm. Journal of Bacteriology *179*, 2465-2471.

Moon, B.-H., Park, Y.-B., and Park, K.-H. (2011). Fenton oxidation of Orange II by pre-reduction using nanoscale zero-valent iron. Desalination *268*, 249-252.

Morosini, M.I., Ayala, J.A., Baquero, F., Martínez, J.L., and Blázquez, J. (2000). Biological Cost of AmpC Production forSalmonella enterica Serotype Typhimurium. Antimicrobial Agents and Chemotherapy *44*, 3137-3143.

Mu, Y., Jia, F., Ai, Z., and Zhang, L. (2017). Iron oxide shell mediated environmental remediation properties of nano zero-valent iron. Environmental Science: Nano *4*, 27-45.

Mueller, N., Braun, J., Bruns, J., Černík, M., Rissing, P., Rickerby, D., and Nowack, B. (2012a). Application of nanoscale zero valent iron (NZVI) for groundwater remediation in Europe. Environmental Science and Pollution Research *19*, 550-558.

Mueller, N.C., Braun, J., Bruns, J., Cernik, M., Rissing, P., Rickerby, D., and Nowack, B. (2012b). Application of nanoscale zero valent iron (NZVI) for groundwater remediation in Europe. Environ Sci Pollut Res Int *19*, 550-558.

Mueller, N.C., and Nowack, B. (2010). Nanoparticles for Remediation: Solving Big Problems with Little Particles. Elements *6*, 395-400.

Mukherjee, R., Kumar, R., Sinha, A., Lama, Y., and Saha, A.K. (2016). A review on synthesis, characterization, and applications of nano zero valent iron (nZVI)

for environmental remediation. Critical Reviews in Environmental Science and Technology *46*, 443-466.

Murakami, H., Kita, K., Oya, H., and Anraku, Y. (1985). The Escherichia coli cytochrome b556 gene, cybA, is assignable as sdhC in the succinate dehydrogenase gene cluster. FEMS Microbiology Letters *30*, 307-311.

Murinova, S., and Dercova, K. (2014). Response mechanisms of bacterial degraders to environmental contaminants on the level of cell walls and cytoplasmic membrane. International journal of microbiology *2014*, 873081.

Murugesan, K., Bokare, V., Jeon, J.-R., Kim, E.-J., Kim, J.-H., and Chang, Y.-S. (2011). Effect of Fe-Pd bimetallic nanoparticles on Sphingomonas sp. PH-07 and a nano-bio hybrid process for triclosan degradation. Bioresource technology *102*, 6019-6025.

Mykytczuk, N.C.S., Trevors, J.T., Leduc, L.G., and Ferroni, G.D. (2007). Fluorescence polarization in studies of bacterial cytoplasmic membrane fluidity under environmental stress. Progress in biophysics and molecular biology *95*, 60-82.

Naether, D.J., Slawtschew, S., Stasik, S., Engel, M., Olzog, M., Wick, L.Y., Timmis, K.N., and Heipieper, H.J. (2013). Adaptation of the Hydrocarbonoclastic Bacterium Alcanivorax borkumensis SK2 to Alkanes and Toxic Organic Compounds: a Physiological and Transcriptomic Approach. Appl Environ Microb *79*, 4282-4293.

Naumann, D. (2006). Infrared Spectroscopy in Microbiology. In Encyclopedia of Analytical Chemistry (John Wiley & Sons, Ltd).

Neilands, J.B. (1995). Siderophores: structure and function of microbial iron transport compounds. Journal of Biological Chemistry *270*, 26723-26726.

Nelson, K.E., Weinel, C., Paulsen, I.T., Dodson, R.J., Hilbert, H., Martins dos Santos, V.A.P., Fouts, D.E., Gill, S.R., Pop, M., Holmes, M.*, et al.* (2002a). Complete genome sequence and comparative analysis of the metabolically versatile Pseudomonas putida KT2440. Environ Microbiol *4*.

Nelson, K.E., Weinel, C., Paulsen, I.T., Dodson, R.J., Hilbert, H., Santos, V.A.P.M.d., Fouts, D.E., Gill, S.R., Pop, M., Holmes, M.*, et al.* (2002b). Complete genome

sequence and comparative analysis of the metabolically versatile Pseudomonas putida KT2440. Environmental Microbiology *4*, 799-808.

Neumann, G., Cornelissen, S., van Breukelen, F., Hunger, S., Lippold, H., Loffhagen, N., Wick, L.Y., and Heipieper, H.J. (2006). Energetics and Surface Properties of Pseudomonas putida DOT-T1E in a Two-Phase Fermentation System with 1-Decanol as Second Phase. Applied and Environmental Microbiology *72*, 4232-4238.

Nurmi, J.T., Tratnyek, P.G., Sarathy, V., Baer, D.R., Amonette, J.E., Pecher, K., Wang, C., Linehan, J.C., Matson, D.W., Penn, R.L.*, et al.* (2004). Characterization and properties of metallic iron nanoparticles: spectroscopy, electrochemistry, and kinetics. Environmental Science & Technology *39*, 1221-1230.

Paemanee, A., Wikan, N., Roytrakul, S., and Smith, D.R. (2016). Application of GelC-MS/MS to Proteomic Profiling of Chikungunya Virus Infection: Preparation of Peptides for Analysis. In Chikungunya Virus: Methods and Protocols, J.J.H. Chu, and S.K. Ang, eds. (New York, NY: Springer New York), pp. 179-193.

Pagnout, C., Jomini, S., Dadhwal, M., Caillet, C., Thomas, F., and Bauda, P. (2012). Role of electrostatic interactions in the toxicity of titanium dioxide nanoparticles toward Escherichia coli. Colloids and Surfaces B: Biointerfaces *92*, 315-321.

Painter, K.L., Strange, E., Parkhill, J., Bamford, K.B., Armstrong-James, D., and Edwards, A.M. (2015). Staphylococcus aureus Adapts to Oxidative Stress by Producing H2O2-Resistant Small-Colony Variants via the SOS Response. Infection and Immunity *83*, 1830-1844.

Parales, R.E., Ditty, J.L., and Harwood, C.S. (2000). Toluene-Degrading Bacteria Are Chemotactic towards the Environmental Pollutants Benzene, Toluene, and Trichloroethylene. Applied and Environmental Microbiology *66*, 4098-4104.

Parales, R.E., Luu, R.A., Hughes, J.G., and Ditty, J.L. (2015). Bacterial chemotaxis to xenobiotic chemicals and naturally-occurring analogs. Current Opinion in Biotechnology *33*, 318-326.

Parikh, S.J., and Chorover, J. (2006). ATR-FTIR Spectroscopy Reveals Bond Formation During Bacterial Adhesion to Iron Oxide. Langmuir *22*, 8492-8500.

Park, W., Peña-Llopis, S., Lee, Y., and Demple, B. (2006). Regulation of superoxide stress in Pseudomonas putida KT2440 is different from the SoxR paradigm in Escherichia coli. Biochemical and Biophysical Research Communications *341*, 51-56.

Paul, D., Singh, R., and Jain, R.K. (2006). Chemotaxis of Ralstonia sp. SJ98 towards p-nitrophenol in soil. Environmental Microbiology *8*, 1797-1804.

Phenrat, T., Kim, H.-J., Fagerlund, F., Illangasekare, T., Tilton, R.D., and Lowry, G.V. (2009a). Particle Size Distribution, Concentration, and Magnetic Attraction Affect Transport of Polymer-Modified Fe0 Nanoparticles in Sand Columns. Environmental Science & Technology *43*, 5079-5085.

Phenrat, T., Liu, Y., Tilton, R.D., and Lowry, G.V. (2009b). Adsorbed Polyelectrolyte Coatings Decrease Fe0 Nanoparticle Reactivity with TCE in Water: Conceptual Model and Mechanisms. Environmental Science & Technology *43*, 1507-1514.

Phenrat, T., Long, T.C., Lowry, G.V., and Veronesi, B. (2009c). Partial Oxidation ("Aging") and Surface Modification Decrease the Toxicity of Nanosized Zerovalent Iron. Environ Sci Technol *43*, 195-200.

Phenrat, T., Saleh, N., Sirk, K., Kim, H.-J., Tilton, R., and Lowry, G. (2008). Stabilization of aqueous nanoscale zerovalent iron dispersions by anionic polyelectrolytes: adsorbed anionic polyelectrolyte layer properties and their effect on aggregation and sedimentation. J Nanopart Res *10*, 795-814.

Phenrat, T., Saleh, N., Sirk, K., Tilton, R.D., and Lowry, G.V. (2007). Aggregation and Sedimentation of Aqueous Nanoscale Zerovalent Iron Dispersions. Environmental Science & Technology *41*, 284-290.

Popova, O.B., Sanina, N.M., Likhatskaya, G.N., and Bezverbnaya, I.P. (2008). Effects of copper and cadmium ions on the physicochemical properties of lipids of the marine bacterium Pseudomonas putida IB28 at different growth temperatures. Russian Journal of Marine Biology *34*, 179-185.

Príncipe, A., Jofré, E., Alvarez, F., and Mori, G. (2009). Role of a serine-type d-alanyl-d-alanine carboxypeptidase on the survival of Ochrobactrum sp. 11a

under ionic and hyperosmotic stress. FEMS Microbiology Letters *295*, 261-273.

Raffi, M., Mehrwan, S., Bhatti, T., Akhter, J., Hameed, A., Yawar, W., and ul Hasan, M. (2010). Investigations into the antibacterial behavior of copper nanoparticles against <i>Escherichia coli</i&gt. Annals of Microbiology *60*, 75-80.

Raghupathi, K.R., Koodali, R.T., and Manna, A.C. (2011). Size-dependent bacterial growth inhibition and mechanism of antibacterial activity of zinc oxide nanoparticles. Langmuir *27*, 4020-4028.

Ramey, B.E., Koutsoudis, M., Bodman, S.B.v., and Fuqua, C. (2004). Biofilm formation in plant–microbe associations. Current Opinion in Microbiology *7*, 602-609.

Ramos, J.L., Krell, T., Daniels, C., Segura, A., and Duque, E. (2009a). Responses of Pseudomonas to small toxic molecules by a mosaic of domains. Current Opinion in Microbiology *12*, 215-220.

Ramos, J.L., Sol Cuenca, M., Molina-Santiago, C., Segura, A., Duque, E., Gomez-Garcia, M.R., Udaondo, Z., and Roca, A. (2015). Mechanisms of solvent resistance mediated by interplay of cellular factors in *Pseudomonas putida*. FEMS microbiology reviews *39*, 555-566.

Ramos, M.A.V., Yan, W., Li, X.-q., Koel, B.E., and Zhang, W.-x. (2009b). Simultaneous Oxidation and Reduction of Arsenic by Zero-Valent Iron Nanoparticles: Understanding the Significance of the Core–Shell Structure. The Journal of Physical Chemistry C *113*, 14591-14594.

Rangel, D.E.N. (2011). Stress induced cross-protection against environmental challenges on prokaryotic and eukaryotic microbes. World Journal of Microbiology and Biotechnology *27*, 1281-1296.

Reinert, K.H., Giddings, J.M., and Judd, L. (2002). Effects analysis of time-varying or repeated exposures in aquatic ecological risk assessment of agrochemicals. Environmental Toxicology and Chemistry *21*, 1977-1992.

Reinsch, B.C., Forsberg, B., Penn, R.L., Kim, C.S., and Lowry, G.V. (2010). Chemical transformations during aging of zerovalent iron nanoparticles in the presence of common groundwater dissolved constituents. Environmental Science & Technology *44*, 3455-3461.

Ruddock, L.W., and Klappa, P. (1999). Oxidative stress: Protein folding with a novel redox switch. Current Biology *9*, R400-R402.

Saccà, M., Fajardo, C., Nande, M., and Martín, M. (2013). Effects of Nano Zero-Valent Iron on Klebsiella oxytoca and Stress Response. Microbial Ecology, 1-7.

Saccà, M.L., Fajardo, C., Costa, G., Lobo, C., Nande, M., and Martin, M. (2014). Integrating classical and molecular approaches to evaluate the impact of nanosized zero-valent iron (nZVI) on soil organisms. Chemosphere *104*, 184-189.

Sacca, M.L., Fajardo, C., Martinez-Gomariz, M., Costa, G., Nande, M., and Martin, M. (2014). Molecular stress responses to nano-sized zero-valent iron (nZVI) particles in the soil bacterium *Pseudomonas stutzeri*. PLoS one *9*, e89677.

Saleh, N., Kim, H.-J., Phenrat, T., Matyjaszewski, K., Tilton, R.D., and Lowry, G.V. (2008). Ionic Strength and Composition Affect the Mobility of Surface-Modified Fe0 Nanoparticles in Water-Saturated Sand Columns. Environmental Science & Technology *42*, 3349-3355.

Samanta, S.K., Singh, O.V., and Jain, R.K. (2002). Polycyclic aromatic hydrocarbons: environmental pollution and bioremediation. Trends in Biotechnology *20*, 243-248.

Sarathy, V., Tratnyek, P.G., Nurmi, J.T., Baer, D.R., Amonette, J.E., Chun, C.L., Penn, R.L., and Reardon, E.J. (2008). Aging of iron nanoparticles in aqueous solution: effects on structure and reactivity. The Journal of Physical Chemistry C *112*, 2286-2293.

Schiwy, A., Maes, H.M., Koske, D., Flecken, M., Schmidt, K.R., Schell, H., Tiehm, A., Kamptner, A., Thümmler, S., Stanjek, H*., et al.* (2016). The ecotoxic potential of a new zero-valent iron nanomaterial, designed for the elimination of halogenated pollutants, and its effect on reductive dechlorinating microbial communities. Environmental pollution *216*, 419-427.

Sergios A. Nicolaou, S.M.G., Eleftherios T. Papoutsakis (2010). A comparative view of metabolite and substrate stress and tolerance in microbial processing: From biofuels and chemicals, to biocatalysis and bioremediation. Metabolic Enfineering *12*, 307-331.

Sevcu, A., El-Temsah, Y.S., Joner, E.J., and Cernik, M. (2011). Oxidative stress induced in microorganisms by zero-valent iron nanoparticles. Microbes and environments *26*, 271-281.

Shephard, J., McQuillan, A.J., and Bremer, P.J. (2008). Mechanisms of Cation Exchange by Pseudomonas aeruginosa PAO1 and PAO1 wbpL, a Strain with a Truncated Lipopolysaccharide. Appl Environ Microb *74*, 6980-6986.

Shi, Z., Fan, D., Johnson, R.L., Tratnyek, P.G., Nurmi, J.T., Wu, Y., and Williams, K.H. (2015). Methods for characterizing the fate and effects of nano zerovalent iron during groundwater remediation. Journal of contaminant hydrology *181*, 17-35.

Shin, K.-H., and Cha, D.K. (2008). Microbial reduction of nitrate in the presence of nanoscale zero-valent iron. Chemosphere *72*, 257-262.

Shrout, J.D., Williams, A.G.B., Scherer, M.M., and Parkin, G.F. (2005). Inhibition of bacterial perchlorate reduction by zero-valent iron. Biodegradation *16*, 23-32.

Silby, M.W., Winstanley, C., Godfrey, S.A.C., Levy, S.B., and Jackson, R.W. (2011). Pseudomonas genomes: diverse and adaptable. FEMS microbiology reviews *35*, 652-680.

Simonin, M., Martins, J.M.F., Uzu, G., Vince, E., and Richaume, A. (2016). Combined study of titanium dioxide nanoparticle transport and toxicity on microbial nitrifying communities under single and repeated exposures in soil columns. Environmental Science & Technology *50*, 10693-10699.

Simonin, M., and Richaume, A. (2015). Impact of engineered nanoparticles on the activity, abundance, and diversity of soil microbial communities: A review. Environmental Science and Pollution Research *22*, 13710-13723.

Singh, D., and Fulekar, M.H. (2010). Biodegradation of Petroleum Hydrocarbons by Pseudomonas putida Strain MHF 7109. CLEAN – Soil, Air, Water *38*, 781-786.

Singh, R., and Olson, M.S. (2010). Kinetics of trichloroethylene and toluene toxicity to Pseudomonas putida F1. Environmental toxicology and chemistry *29*, 56-63.

Singh, R., Paul, D., and Jain, R.K. (2006). Biofilms: implications in bioremediation. Trends in Microbiology *14*, 389-397.

Singh, S.P., and Bose, P. (2015). Degradation of soil-adsorbed DDT and its residues by NZVI addition. RSC Advances *5*, 94418-94425.

Singh, S.P., and Bose, P. (2016). Degradation kinetics of Endosulfan isomers by micron- and nano-sized zero valent iron particles (MZVI and NZVI). Journal of Chemical Technology and Biotechnology *91*, 2313-2321.

Sirk, K.M., Saleh, N.B., Phenrat, T., Kim, H.-J., Dufour, B., Ok, J., Golas, P.L., Matyjaszewski, K., Lowry, G.V., and Tilton, R.D. (2009). Effect of Adsorbed Polyelectrolytes on Nanoscale Zero Valent Iron Particle Attachment to Soil Surface Models. Environmental Science & Technology *43*, 3803-3808.

Sondi, I., and Salopek-Sondi, B. (2004). Silver nanoparticles as antimicrobial agent: a case study on E. coli as a model for Gram-negative bacteria. Journal of Colloid and Interface Science *275*, 177-182.

Stefaniuk, M., Oleszczuk, P., and Ok, Y.S. (2016). Review on nano zerovalent iron (nZVI): From synthesis to environmental applications. Chemical Engineering Journal *287*, 618-632.

Storz, G., and Imlayt, J.A. (1999). Oxidative stress. Current Opinion in Microbiology *2*, 188-194.

Storz, G., Tartaglia, L.A., Farr, S.B., and Ames, B.N. (1990). Bacterial defenses against oxidative stress. Trends in Genetics *6*, 363-368.

Straub, K.L., Benz, M., and Schink, B. (2001). Iron metabolism in anoxic environments at near neutral pH. FEMS Microbiology Ecology *34*, 181-186.

Streit, F., Delettre, J., Corrieu, G., and Béal, C. (2008). Acid adaptation of Lactobacillus delbrueckii subsp. bulgaricus induces physiological responses at membrane and cytosolic levels that improves cryotolerance. Journal of Applied Microbiology *105*, 1071-1080.

Stuart, R.K., Brahamsha, B., Busby, K., and Palenik, B. (2013). Genomic island genes in a coastal marine Synechococcus strain confer enhanced tolerance to copper and oxidative stress. ISME J *7*, 1139-1149.

Su, Y., Adeleye, A.S., Zhou, X., Dai, C., Zhang, W., Keller, A.A., and Zhang, Y. (2014). Effects of nitrate on the treatment of lead contaminated groundwater by nanoscale zerovalent iron. Journal of hazardous materials *280*, 504-513.

Taghavy, A., Costanza, J., Pennell, K.D., and Abriola, L.M. (2010). Effectiveness of nanoscale zero-valent iron for treatment of a PCE-DNAPL source zone. Journal of contaminant hydrology *118*, 128-142.

Teitzel, G.M., Geddie, A., De Long, S.K., Kirisits, M.J., Whiteley, M., and Parsek, M.R. (2006). Survival and growth in the presence of elevated copper: transcriptional profiling of copper-stressed Pseudomonas aeruginosa. J Bacteriol *188*, 7242-7256.

Thompson, D.K., Chourey, K., Wickham, G.S., Thieman, S.B., VerBerkmoes, N.C., Zhang, B., McCarthy, A.T., Rudisill, M.A., Shah, M., and Hettich, R.L. (2010). Proteomics reveals a core molecular response of Pseudomonas putida F1 to acute chromate challenge. BMC genomics *11*, 311.

Thuptimdang, P., Limpiyakorn, T., McEvoy, J., Pruss, B.M., and Khan, E. (2015). Effect of silver nanoparticles on Pseudomonas putida biofilms at different stages of maturity. Journal of hazardous materials *290*, 127-133.

Tilston, E.L., Collins, C.D., Mitchell, G.R., Princivalle, J., and Shaw, L.J. (2013). Nanoscale zerovalent iron alters soil bacterial community structure and inhibits chloroaromatic biodegradation potential in Aroclor 1242-contaminated soil. Environ Pollut *173*, 38-46.

Tiraferri, A., Chen, K.L., Sethi, R., and Elimelech, M. (2008). Reduced aggregation and sedimentation of zero-valent iron nanoparticles in the presence of guar gum. J Colloid Interface Sci *324*, 71-79.

Tong, G., Yulong, M., Peng, G., and Zirong, X. (2005). Antibacterial effects of the Cu(II)-exchanged montmorillonite on Escherichia coli K88 and Salmonella choleraesuis. Vet Microbiol *105*, 113-122.

Tong, Z., Bischoff, M., Nies, L.F., Myer, P., Applegate, B., and Turco, R.F. (2012). Response of soil microorganisms to As-produced and functionalized single-wall carbon nanotubes (SWNTs). Environ Sci Technol *46*, 13471-13479.

Torres-Barcelo, C., Cabot, G., Oliver, A., Buckling, A., and Maclean, R.C. (2013). A trade-off between oxidative stress resistance and DNA repair plays a role in the evolution of elevated mutation rates in bacteria. Proceedings Biological sciences *280*, 20130007.

Tsai, M., Koo, J., Yip, P., Colman, R.F., Segall, M.L., and Howell, P.L. (2007). Substrate and product complexes of Escherichia coli adenylosuccinate lyase provide new insights into the enzymatic mechanism. Journal of molecular biology *370*, 541-554.

Tuomi, P., Hains, S., Takala, J., Hyödynmaa, M., Manni-Rantanen, L (2008). Use of nZVI for ground water remediation. Golder Associates.

Udaondo, Z., Duque, E., Fernandez, M., Molina, L., de la Torre, J., Bernal, P., Niqui, J.L., Pini, C., Roca, A., Matilla, M.A*., et al.* (2012). Analysis of solvent tolerance in Pseudomonas putida DOT-T1E based on its genome sequence and a collection of mutants. FEBS Lett *586*, 2932-2938.

Üzüm, Ç., Shahwan, T., Eroğlu, A.E., Lieberwirth, I., Scott, T.B., and Hallam, K.R. (2008). Application of zero-valent iron nanoparticles for the removal of aqueous Co2+ ions under various experimental conditions. Chemical Engineering Journal *144*, 213-220.

van den Broek, D., Bloemberg, G.V., and Lugtenberg, B. (2005). The role of phenotypic variation in rhizosphere Pseudomonas bacteria. Environ Microbiol *7*, 1686-1697.

Vecchia, E.D., Luna, M., and Sethi, R. (2009). Transport in Porous Media of Highly Concentrated Iron Micro- and Nanoparticles in the Presence of Xanthan Gum. Environmental Science & Technology *43*, 8942-8947.

Veening, J.-W., Smits, W.K., and Kuipers, O.P. (2008). Bistability, Epigenetics, and Bet-Hedging in Bacteria. Annual Review of Microbiology *62*, 193-210.

Velimirovic, M., Simons, Q., and Bastiaens, L. (2015). Use of CAH-degrading bacteria as test-organisms for evaluating the impact of fine zerovalent iron particles on the anaerobic subsurface environment. Chemosphere *134*, 338-345.

Vinayavekhin, N., Mahipant, G., Vangnai, A.S., and Sangvanich, P. (2015). Untargeted metabolomics analysis revealed changes in the composition of glycerolipids and phospholipids in Bacillus subtilis under 1-butanol stress. Applied Microbiology and Biotechnology *99*, 5971-5983.

Vinayavekhin, N., and Saghatelian, A. (2001). Untargeted Metabolomics. In Current Protocols in Molecular Biology (John Wiley & Sons, Inc.).

Voelker, B.M., and Sulzberger, B. (1996). Effects of Fulvic Acid on Fe(II) Oxidation by Hydrogen Peroxide. Environ Sci Technol *30*, 1106-1114.

Wackett, L.P., and Gibson, D.T. (1988). Degradation of trichloroethylene by toluene dioxygenase in whole-cell studies with Pseudomonas putida F1. Appl Environ Microb *54*, 1703-1708.

Wang, C.-B., and Zhang, W.-x. (1997). Synthesizing nanoscale iron particles for rapid and complete dechlorination of TCE and PCBs. Environmental Science & Technology *31*, 2154-2156.

Wang, D., Dorosky, R.J., Han, C.S., Lo, C.-c., Dichosa, A.E.K., Chain, P.S., Yu, J.M., Pierson, L.S., and Pierson, E.A. (2014). Adaptation genomics of a small colony variant in the biofilm of Pseudomonas chlororaphis 30-84. Applied and Environmental Microbiology.

Wilson, S.C., and Jones, K.C. (1993). Bioremediation of soil contaminated with polynuclear aromatic hydrocarbons (PAHs): A review. Environmental pollution *81*, 229-249.

Wilson, W.W., Wade, M.M., Holman, S.C., and Champlin, F.R. (2001). Status of methods for assessing bacterial cell surface charge properties based on zeta potential measurements. Journal of Microbiological Methods *43*, 153-164.

Woo, H., Sanseverino, J., Cox, C.D., Robinson, K.G., and Sayler, G.S. (2000). The measurement of toluene dioxygenase activity in biofilm culture of Pseudomonas putida F1. J Microbiol Methods *40*, 181-191.

Wood, D., Darlison, M.G., Wilde, R.J., and Guest, J.R. (1984). Nucleotide sequence encoding the flavoprotein and hydrophobic subunits of the succinate dehydrogenase of Escherichia coli. Biochem J *222*, 519-534.

Wu, D., Shen, Y., Ding, A., Mahmood, Q., Liu, S., and Tu, Q. (2013). Effects of nanoscale zero-valent iron particles on biological nitrogen and phosphorus removal and microorganisms in activated sludge. Journal of hazardous materials *262*, 649-655.

Xie, Y., Dong, H., Zeng, G., Tang, L., Jiang, Z., Zhang, C., Deng, J., Zhang, L., and Zhang, Y. (2017). The interactions between nanoscale zero-valent iron and microbes

in the subsurface environment: A review. Journal of hazardous materials *321*, 390-407.

Xiu, Z.M., Gregory, K.B., Lowry, G.V., and Alvarez, P.J. (2010a). Effect of bare and coated nanoscale zerovalent iron on tceA and vcrA gene expression in Dehalococcoides spp. Environ Sci Technol *44*, 7647-7651.

Xiu, Z.M., Jin, Z.H., Li, T.L., Mahendra, S., Lowry, G.V., and Alvarez, P.J. (2010b). Effects of nano-scale zero-valent iron particles on a mixed culture dechlorinating trichloroethylene. Bioresource technology *101*, 1141-1146.

Yan, S., Hua, B., Bao, Z., Yang, J., Liu, C., and Deng, B. (2010a). Uranium(VI) removal by nanoscale zerovalent iron in anoxic batch systems. Environ Sci Technol *44*, 7783-7789.

Yan, W., Herzing, A.A., Kiely, C.J., and Zhang, W.X. (2010b). Nanoscale zero-valent iron (nZVI): aspects of the core-shell structure and reactions with inorganic species in water. Journal of contaminant hydrology *118*, 96-104.

Yang, C., Xie, H., Li, Q.C., Sun, E.J., and Su, B.L. (2015). Adherence and interaction of cationic quantum dots on bacterial surfaces. J Colloid Interface Sci *450*, 388-395.

Yang, Y.F., Chen, P.J., and Liao, V.H. (2016). Nanoscale zerovalent iron (nZVI) at environmentally relevant concentrations induced multigenerational reproductive toxicity in *Caenorhabditis elegans*. Chemosphere *150*, 615-623.

Yoon, R.Y., Yeom, S.J., Park, C.S., and Oh, D.K. (2009). Substrate specificity of a glucose-6-phosphate isomerase from Pyrococcus furiosus for monosaccharides. Appl Microbiol Biotechnol *83*, 295-303.

Zeyer, J., Wasserfallen, A., and Timmis, K.N. (1985). Microbial mineralization of ring-substituted anilines through an ortho-cleavage pathway. Applied and Environmental Microbiology *50*, 447-453.

Zhang, W.-x., and Elliott, D.W. (2006). Applications of iron nanoparticles for groundwater remediation. Remediation Journal *16*, 7-21.

Zhang, W., Hughes, J., and Chen, Y. (2012). Impacts of hematite nanoparticle exposure on biomechanical, adhesive, and surface electrical properties of Escherichia coli cells. Appl Environ Microbiol *78*, 3905-3915.

Zhang, W.X. (2003). Nanoscale iron particles for environmental remediation: An overview. J Nanopart Res *5*, 323-332.

Zhang, W.X., Wang, C.B., and Lien, H.L. (1998). Treatment of chlorinated organic contaminants with nanoscale bimetallic particles. Catalysis Today *40*, 387-395.

Zhang, Y.M., and Rock, C.O. (2008). Membrane lipid homeostasis in bacteria. Nat Rev Microbiol *6*, 222-233.

Zhou, L., Thanh, T.L., Gong, J., Kim, J.H., Kim, E.J., and Chang, Y.S. (2014). Carboxymethyl cellulose coating decreases toxicity and oxidizing capacity of nanoscale zerovalent iron. Chemosphere *104*, 155-161.

APPENDIX

Appendix A

To assess the relationship between the emergent smaller colony phenotype (SCV phenotype) and repetitive nZVI exposure, the frequency of the SCV phenotype in each cycle of repetitive nZVI exposure was investigated. By using the colony size as a criteria, it is difficult to determine the number of small-colony phenotype occurred at the low frequency/abundance in a large number of normal phenotype. Hence, the susceptibility to antibiotic was used to distinguish the SCV phenotype from the normal phenotype. Cells were grown overnight in TSB medium. The grown bacterial were inoculated (1% v/v) to fresh TSB medium and one-ml aliquots of cell culture were transferred to 24-well polystyrene plate. Gentamicin were added to obtain various final concentrations. Cell culture were cultivated at shaking condition 175 rpm, 30°C for 24 hours. Bacterial growth in the presence of gentamicin was determined by measuring OD600. The small colony phenotype (MIC = 6 µg/ml) was slightly more tolerance to gentamicin than the normal phenotype (MIC = 4 µg/ml), therefore, TSB agar plate containing 4 µg/ml gentamicin was further used to estimate the occurrence of the SCV phenotype. Without nZVI exposure, a small fraction of *P. putida* F1 (approximately 10^{-5}) are able to grow on TSB agar plate containing 4 µg/ml gentamicin.

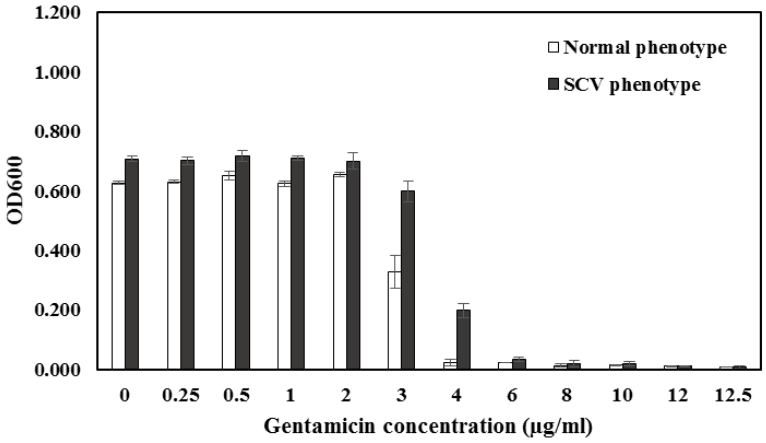

Figure A Bacterial growth in the presence of gentamicin.

Appendix B

For intracellular oxidative stress measurement, *P. putida* F1 cells from mid-exponential phase were collected, washed and resuspended in M9G medium (initial cell concentration ≈ 10^8 CFU/ml). Stock solution of CM-H_2DCFDA was added to cell suspension to obtain final concentration of 1 μM of CM- H_2DCFDA. Cell suspension was incubated in dark condition, 30°C for 30 minutes. After that, stock solution of nZVI was added to obtain final nZVI concentration of 0.5 g/L and incubated at shaking condition 200 rpm, 30°C for one hour. Two hundred μL of nZVI-treated sample were transferred to 96-wll black plate; Fluoresencence signal of CM-H_2DCFDA were detected using Biotex microplate reader (Biotek Instruments, Inc) with excitation/ emission wavelengths of 492/517 nm. The nZVI-induced intracellular stress was determined by comparing with the standard curve of H_2O_2 (Figure B). The fluorescence signal of nZVI-induced intracellular stress was 217 ± 14 which corresponds to the intracellular oxidative stress induced by 0.5 mM of H_2O_2.

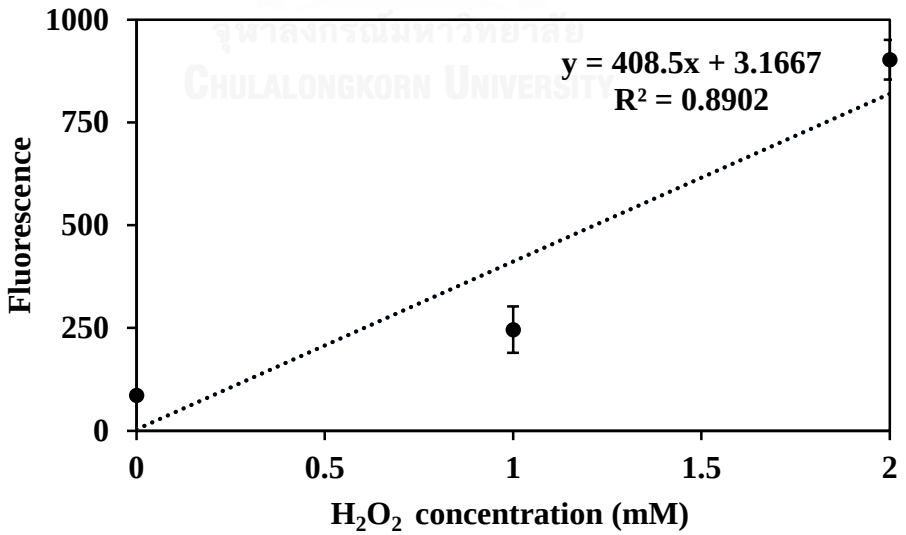

Figure B Standard curve of intracellular oxidative stress.

VITA

Miss Panaya Kotchaplai was born on 10th May, 1987 in Nakhon Sri Thammarat, Thailand. She completed high school at Benjamarachutit School in 2005. Panaya then entered Chulalongkorn University (CU) where she obtained her B.Sc. in Biochemistry with First Class Honors in 2009. After that, she entered a graduate program in Environmental Management at the International Program in Hazardous Substance and Environmental Management, CU and received a scholarship from the Royal Golden Jubilee PhD, Thailand Research Fund. Panaya also received the 90th Anniversary of Chulalongkorn University Fund (Ratchadaphiseksomphot Endowment Fund) for her dissertation. During her study, Panaya had an opportunity to conduct part of her research at North Dakota State University in Fargo, ND, USA. Her Ph.D. research resulted in several conference presentations including the International Conference of Asian Environmental Chemistry (ICAEC2014) which was awarded the Outstanding Student Research.